ELASTO-HYDRODYNAMIC STABILITY OF A TOWED SLENDER BODY

by

BYUNG-KUN, YU

Under the supervision of PROF. M.P. PAIDOUSSIS

A thesis submitted to the Faculty of Graduate Studies and Research in partial fulfillment of the requirements for the degree of Master of Engineering

Department of Mechanical Engineering
McGill University
Montreal, Canada

May, 1975

SYNOPSIS

A general theory is presented to account for the dynamics and stability of a slender, towed body with tapered ends, totally submerged in water, as it undergoes small, free, lateral motions. Stability conditions and modal shapes are found based on solutions to linearized equations resulting from small deflection assumptions.

It is found that the system may be subject to rigid-body type instabilities at low towing speeds, and to flexural instabilities at higher towing speeds. The rigid-body instabilities, occurring in the so-called zeroth and first mode of the flexible body, are shown to correspond to the instabilities of a rigid body of the same shape and gravimetric properties.

Particular attention is focused on the effects on stability of (a) the ratio of the length of tow-rope to the length of main body and (b) the bluntness of tail portion. The former affects the stability of a rigid or flexible system only in terms of oscillatory instabilities, but does not affect yawing; on the other hand, a sufficiently blunt tail may stabilize the system over the full flow-range in all its modes. It can be said that the stability of a slender body is virtually controlled by the shape of the tail portion of the body.

STABILITE ELASTO-HYDRODYNAMIQUE D'UN CORPS ALLONGE PRIS EN REMORQUE

SOMMAIRE

Cette thèse présente une étude de la dynamique et de la stabilité d'un corps allongé, aux extrémités coniques, complètement immergé dans un fluide visqueux dans lequel on le remorque. En se déplaçant ce corps subit de faibles déplacements latéraux. Si l'on suppose que ces déflexions sont de faible amplitude on peut utiliser des équations linéarisées qui permettent de déterminer les conditions de stabilité et les formes modales.

On constate que le système subit des instabilités de corps rigides lorsque la vitesse de remorquage est faible, tandis qu'à de plus grandes vitesses, on obtient des instabilités de flexion. Les instabilités se produisant dans le premier et le second modes du corps flexible, correspondent à des instabilités d'un corps rigide de même forme et de mêmes propriétés gravimétriques.

Deux paramètres, en particulier, semblent avoir un effet déterminant sur la stabilité du corps, il s'agit

a) du rapport de la longueur du filin à la longueur du corps

remorqué,

b) de la forme plus ou moins obtuse de la queue.

Le premier de ces deux paramétres peut causer des instabités oscillatoires, que le système soit rigide ou flexible mais n'a pas d'effet sur l'angle de lacet. Quant au second, si la queue est suffisamment obtuse, le système peut être stable dans tous ses modes quelle que soit la vitesse du remorquage. On peut même dire que la stabilité d'un corps allongé dépend virtuellement de la forme de sa queue.

ACKNOWLEDGEMENTS

The author wishes to take this opportunity to express his very sincere appreciation to Professor M.P. Païdoussis, who directed the research, for his kind patience, guidance and encouragement throughout this investigation.

Thanks are also due to Messrs. C. Guernier, M. Hannoyer and B. Laithier for discussion and helpful suggestions.

Appreciation is expressed to Ms. V.M. Jackson for typing the manuscript.

The research was sponsored by the Defence Research Board of Canada (Grant No. 9550-47). This financial assistance is gratefully acknowledged.

TABLE OF CONTENTS

NOMENCLATURE

a	defined by equation (17)
b	defined by equation (15)
C_{DB}	Base drag coefficient
C_D, C_f	friction drag coefficients defined by equations (10-12)
C_{fB}	friction drag coefficient on the forebody
c, c_f	equal to $(4/\pi)C_D$ and $(4/\pi)C_f$, respectively
c_o	equal to $cL(M/EI)^{\frac{1}{2}}$
D	diameter of cylinder
D_{Base}	diameter of base of cylinder
EI	flexural rigidity of cylinder
e	eccentricity of ellipsoid
F_n	normal viscous force on cylinder, per unit length
F_ℓ	longitudinal viscous force on cylinder, per unit length
f_1, f_2	slenderness coefficients for hydrodynamic forces at free ends
i	angle of inclination of cylinder to flow
I_n	normal inviscid hydrodynamic force on cylinder, per unit length
I_ℓ	longitudinal inviscid hydrodynamic force on cylinder, per unit length
L	length of main body
m	mass of cylinder per unit length
M	virtual mass of cylinder per unit length

P, P_n, P_ℓ	tow-rope forces defined by Figure 4b
Q	shear force at a cross-section of the cylinder
S_{Base}	surface area of base of cylinder
s	length of tow-rope
T	tension
t	time
U	mean flow velocity
u	dimensionless flow velocity = $(M/EI)^{\frac{1}{2}}UL$
u_c	critical dimensionless flow velocity
x	axial co-ordinate
y	lateral displacement of cylinder
α	bluntness of tail portion
β	equal to $M/(m+M)$
γ, δ	angles defined by Figure 4b
ε	equal to L/D
η	equal to y/L
Θ_1, Θ_2	defined by equation (2) and (5)
Λ	equal to s/L
$\mathcal{M}$	moment on a cross-section of the cylinder
μ	interal damping coefficient
ν	dimensionless interal damping coefficient = $\{I/[E(M+m)]\}^{\frac{1}{2}}\mu/L^2$
ξ	equal to x/L

ρ	fluid density
σ	equal to m/M
τ, τ'	equal to $\frac{Ut}{L}$ and $\{EI/(m+M)\}^{\frac{1}{2}}\frac{t}{L^2}$, respectively
Ω	circular natural frequency
ω	dimensionless natural frequency = $\{(m+M)/EI\}^{\frac{1}{2}}\Omega L^2$
ω_b, ω_f	dimensionless natural frequencies of rigid and flexible cylinders, respectively
ω_c	critical dimensionless natural frequency

1. INTRODUCTION

1.1 General

There are many problems in the operation of marine vehicle systems, associated with the dynamical stability and control of towed systems. By towed systems we understand the complete system comprising the towed body, the towing body and the tow-rope. The performance of each element of the system contributes to the stability and motion response of the system as a whole. In general, the three elements are intercoupled, one element of the system can destabilize the inherent stability of the other elements, or can stabilize an inherent instability of another element.

The analysis of the stability and small linear motion response of towed systems commences with a perturbation of an original condition or position of equilibrium--where the system (or body) moves at constant speed in an equilibrium configuration. For several types of towing situations, especially where the towing vehicle is a surface craft and the towed body is submerged at depth, it is essential to establish the equilibrium shape of the cable configuration and position and attitude of the towed body. This equilibrium condition depends on the speed of the system; the size, length, cross-sectional shape, weight and elasticity of the cable; and the size, geometry, weight and point of attachment of the towed body. Also, in establishing this condition, it must be ensured that the system remain intact; i.e., the amount of tension in the cable at all points must be below the breaking load, and the cable force at the points of attachment to the bodies must be below the tearing load of the attachment mechanism and supporting structure.

The behaviour of the towed body is important. Minimum resistance is experienced when the body is towed in a straight line. On the other hand, when the towed body has lateral motion about the tow-point on the towing vessel, resistance is increased and the speed of the whole towed system is reduced commensurately.

As was mentioned, in considering the stability of the towed system, we assume some kind of perturbation to the equilibrium state; here we shall consider this disturbance to be applied to the towed body. We are not concerned with the nature of this disturbance, but merely with its effects. The usual effect is a small sidewise translation of body as well as a rotation about its center of mass. The latter is the more important of the two, since the symmetry of the streamline flow is thereby disturbed and a lateral hydrodynamic force and a moment on the body are produced. This induced force and its moment are in most cases many times greater than the initial disturbing force and its moment. Besides this force and moment, another previously non-existant lateral force and turning moment arise from the tow rope force, if the tow rope is attached at the bow of the body, which usually is the case. Finally, translation and rotational inertia reactions come into play due to the fact that the lateral motion is an accelerated or decelerated motion superimposed on the steady forward motion of the towed body.

Finally, it should be mentioned that most solutions to instability of towed system involve design changes which either limit speed or result in increased drag (and hence power consumption). It is, therefore, of considerable practical interest:

a) to know accurately the limits of stability of a given system, and

b) to make design changes to an unstable system, so as to regain stability, which would not seriously affect its efficiency.

1.2 Outline of Previous Work

Interest in the dynamic stability of towed ships dates back to the halcyon-days when solutions to engineering problems could still be obtained by experience, without the aid of sophisticated analysis. Substantive work on the methods for mooring airships in the air by means of cable systems began early this century, as reported for instance by Krell [1], using the three wire "pyramid" system. This type of mooring apparently originated with Crocco [2], but received more extended use in England. Frazer [3] undertook laboratory experiments with this and other forms of "free" wire system, whose dynamics are essentially the same as with a solid mast but for the increased elasticity. A more complicated dynamical problem is offered when a ship is moored by one cable only, like a kite balloon, which was discussed by Bairstow, Relf and Jones [4]. Later, Munk [5], Glauert [6], and Bryant, Brown and Sweeting [7] contributed to the study of this problem.

In 1950 Strandhagen et al. [8], carefully discussed the dynamic stability of the course of towed ships, using the following assumptions:

i) the motion is steady along a straight line where the yaw angle of both the towing and towed ship is zero, which is referred to as "steady course conditions";

ii) the towing ship remains on this course and maintains a steady velocity even after the towed vessel has begun to yaw;

iii) the motion takes place in a horizontal plane;

iv) yawing angles and velocities are small and the tow line is massless and inextensible and lies in the plane of the motion.

They show that, when the towed ship is disturbed from its steady straight course, it experiences no change in velocity along the x-axis. The analysis also indicates that a dynamically stable ship when towed might become unstable when the tow line is long and that a dynamically unstable ship may become stable if towed with a short tow line.

The first analysis of stability of a flexible towed body was done by Hawthorne [9], for the case of the Dracone flexible barge. He laid down the following requirements for the directional stability of such a towed ship:

i) the point of attachment of the tow-line should be located forward of both the center of gravity and the center of pressure of the static lateral force;

ii) the ship should be dynamically stable when moving untowed;

iii) when condition (ii) is not fulfilled, it is possible to achieve directional stability either with a long enough or short enough tow-line.

The critical lengths depend upon the degree of the dynamical instability.

Recently many applications have arisen for underwater towed systems in oceanography, fishing, and maritime warfare. The recent development of faired towing cables has opened up new possibilities of higher speeds and depths, which call for a refined design approach. Jeffrey [10] conducted a parametric study on stability which demonstrated some fundamental effects of cable and body design and their interactions on body behaviour. A more complicated study of the three-dimensional motion of a cable-body towing system was undertaken by Schram and Reyle [11]. Many papers have been published in this field, e.g., by Eames [12], Reber [13], Parson and Casarella [14], Strandhagen and Thomson [15], Richardson [16], Patton and Schram [17] and Laitinen [18].

Païdoussis [19, 20] proposed a general theory to account for the small, free, lateral motions of a flexible, slender, cylindrical body immersed in fluid flowing parallel to the position of the rest of its axis. Later, Païdoussis [21, 22] extended his previous study of the dynamics of flexible cylinder in axial flow to deal with a towed system, which was studied both analytically and experimentally. In this work he confirmed that there exists two main factors for optimum stability of the system;

i) the tail must be as blunt as possible;

ii) the tow-rope as short as possible.

Also he found that the experiments do not show any advantage in making the nose particularly well streamlined, which does not entirely agree with theory. Ortloff and Ives [23] examined the stability and time-dependent deflections of a thin flexible cylinder with zero bending rigidity set in a viscous stream. Later Païdoussis [24] re-examined the dynamics of flexible towed bodies of revolution and determined the relation in dynamical behaviour between rigid and flexible bodies. It was found that the system may be subject to rigid-body type instabilities at low towing speeds; and to flexural instabilities at higher towing speeds.

The conditions of stability have been investigated by calculating systematically the critical flow velocities for neutral stability and their associated frequencies by Pao [25]. He estimated that for $L/D > 30$, the critical velocity and the associated frequency are $U_c\,[(4/T)(c_T/E)^{\frac{1}{2}}] \sim 6$ and $\Omega_c\,[(4D/c_T^{\,2})(\phi/\beta E)^{\frac{1}{2}}] \sim 12$. Pao and Tran [26] discussed the forced oscillations of a thin flexible cylinder towed in a viscous fluid. It was shown that the forcing frequency had a dominating influence on the modal-shape amplitude of the towed cylinder.

Yoder and Païdoussis [25] have formulated the equations for the dynamics of body towed in axial flow, focusing their attention to the various hydrodynamic forces arising near the nose and tail sections of body, which were not previously defined by Païdoussis [24]. The work presented in this Thesis is based on the formulation of the problem as developed by Yoder and Paidoussis, particularly the work of Appendix A.

1.3 Scope of Present Work

The present study is concerned with the extension of the theoretical analysis made by Hawthorne [9] and Païdoussis [24], of the small, lateral motions of slender bodies towed through incompressible fluid. The author's interest in this thesis is to examine carefully the various hydrodynamic forces arising near the nose and tail of the body which had been inadequately accounted for in the previous treatments. Accordingly, an extensive survey of the pertinent literature was undertaken, out of which has grown a drastic reformulation of the inviscid-flow forces acting near the ends of the body.

This theoretical development has entailed a substantial amount of effort, as evidenced by the fact that it comprises the latter half of Chapter 2, while at the same time drawing upon the results obtained in Appendix A. In Chapter 3, we have derived the equations of small, lateral motion; also, the tensile force, shear force and moment which are exerted by the tail and nose section. The complete equation of motion is constructed and four boundary conditions are formulated in Chapter 4. To compare the new theory with Païdoussis' [24] systematically, we modified the tow-rope force and the coordinate system of [24]. These are surveyed briefly in Chapter 5. Equations of motion of a rigid, towed body are discussed in Chapter 6. Instead of deriving the equations of force and moment balance independently of the previous work, we make use of the work of Chapter 4. Chapter 7 presents the theoretical results obtained for flexible cylinders. The instability regions are determined, and the effect of the different parameters on the behaviour of the system is discussed. Finally we consider the theoretical analysis of rigid cylinders in Chapter 8.

2. FORCES ACTING ON A SLENDER, TOWED BODY

Consider a slender body of revolution immersed in an incompressible fluid of density ρ, flowing with uniform velocity U parallel to the x-axis, which coincides with the position of rest of the body and of the "tow-rope", as shown in Figure 1. It is noted that this system is exactly equivalent to a slender body being towed with velocity U in still water. The body is presumed to be flexible or rigid and to be supported somehow at the other extremity of the tow-rope so that it is not washed away downstream. The x- and y-axes lie in a horizontal plane wherein all motions, $y(x,t)$, are supposed to be confined. At its two ends, the body is tapered over a short length, compared with its overall length; but the tapered sections are presumed to be sufficiently long so as to admit no discontinuities in the flow past the body. We denote the body diameter by $D(x)$, its cross-sectional area by $S(x)$, and its mass per unit length by $m(x)$. It is assumed to be of null buoyancy and uniform density, so that neither a lateral force nor a moment is necessary to keep it lying along the x-axis, at least at zero flow velocity.

2.1 Modification of Coordinates

Before proceeding with the analysis, it is desirable to express the problem in dimensionless terms and accordingly we put

$$\xi = \frac{x}{L}, \qquad \eta = \frac{y}{L}, \qquad \tau = \frac{Ut}{L}, \tag{1}$$

where L is the length of main portion of body and U is the flow velocity of the fluid in the x-direction.

We begin by dividing the body, for the sake of analysis, into three parts, as indicated in Figure 2 and take the origin of the x-axis to coincide with the equilibrium position of its midpoint. The lengths of the nose and tail sections, ℓ_1 and ℓ_2, respectively, need not at this stage be precisely specified. We do require, though, that $\lambda_1 = \ell_1/L$ and $\lambda_2 = \ell_2/L$ be of the order of $[\eta]^{\frac{1}{2}}$, so that $[\lambda_1]^2$ and $[\lambda_2]^2$ can be treated as small quantities.

These assumptions lead to significant mathematical simplifications over the nose and tail sections, as can be appreciated by expanding $\eta(\xi, \tau)$ in a Taylor series in ξ about the $\xi = -\frac{1}{2}$;

$$\eta(\xi,\tau) = \eta(-\tfrac{1}{2},\tau) + \frac{\partial\eta}{\partial\xi}(-\tfrac{1}{2},\tau)\{\xi + \tfrac{1}{2}\} + \frac{1}{2!}\frac{\partial^2\eta}{\partial\xi^2}(-\tfrac{1}{2},\tau)\{\xi + \tfrac{1}{2}\}^2 + \frac{1}{3!}\frac{\partial^3\eta}{\partial\xi^3}(-\tfrac{1}{2},\tau)(\xi + \tfrac{1}{2})^3 + \cdots$$

Over the nose, i.e., in the interval $-\frac{1}{2}-\lambda_1 \leq \xi \leq -\frac{1}{2}$, the quantity $(\xi + \frac{1}{2})$ is of the order of λ_1. Recalling that $[\lambda_1]^2$, $\frac{\partial^2\eta}{\partial\xi^2}$ and $\frac{\partial^3\eta}{\partial\xi^3}$ are very small quantities, we conclude that along the nose section $\eta(\xi,\tau)$ can be adequately represented by

$$\eta(\xi,\tau) \doteq \eta(-\frac{1}{2},\tau) + \frac{\partial\eta}{\partial\xi}(-\frac{1}{2},\tau) \{\xi+\frac{1}{2}\} .$$

Introducing the notation

$$\eta_1(\tau) = \eta(-\frac{1}{2},\tau) , \tag{2}$$

$$\Theta_1(\tau) = \frac{\partial\eta}{\partial\xi}(-\frac{1}{2},\tau) ,$$

displacements over the nose section may now be written as

$$\eta(\xi,\tau) = \eta_1(\tau) + \Theta_1(\tau)\{\xi + \frac{1}{2}\} . \tag{3}$$

It is clear from the form of equation (3) that, in physical terms, we have simply taken the nose section to be short enough to allow us to treat it as rigid; although it is, in fact, flexible. By the same process, $\eta(\xi,\tau)$ over the tail section may be written as

$$\eta(\xi,\tau) \doteq \eta_2(\tau) + \Theta_2(\tau) \{\xi - \frac{1}{2}\} , \tag{4}$$

where

$$\eta_2(\tau) = \eta(\frac{1}{2},\tau) ,$$

$$\Theta_2(\tau) = \frac{\partial\eta}{\partial\xi}(\frac{1}{2},\tau) . \tag{5}$$

The tail, thus, can also be treated as rigid without loss of generality.

2.2 Base Drag Force

Considering viscous flow past a rigid, blunt-based body of revolution at a large angle of attack, Kelly [28] has shown by means of semi-empirical arguments that the force arising from boundary-layer buildup along the leeward side of the body is of the order α^3, where α is the angle of attack. Since we are treating $\frac{\partial\eta}{\partial\xi}$ as a small quantity, this force can clearly be neglected. There will, on the other hand, inevitably arise flow separation at the tail. Accordingly, we shall follow Kelly [28] and assume the tail to be truncated upstream of the point where flow separation would otherwise take place. In this way we can assure that only the blunt base itself is in contact with the wake and that the form drag at the tail acts in the lateral direction. Thus we express the base drag as follows:

$$C_{DB} = D_{Base}/\tfrac{1}{2}\rho U^2 S_{Base} \tag{6}$$

Hoerner [29] describes the so-called "jet-pump" mechanism by which the pressure in the wake of a blunt-based body is reduced as a result of the tubular "jet" around it. He also describes the "insulating" effect of the separated boundary layer, tending to diminish the jet-pump effect.

It is clear that the drag in equation (6) will be inversely proportional to some measure of the boundary-layer thickness at the base, which can be characterized by the drag on the fore-body. Accordingly, he proposed that

$$C_{DB} = 0.029/(C_{fB})^{\frac{1}{2}} \qquad (7\text{-a})$$

where C_{fB}, the skin friction drag on the forebody, is given by

$$C_{fB} = D_{fore}/\tfrac{1}{2}\rho U^2 S_{Base} \quad . \qquad (8)$$

This is applicable to cases where the base area is essentially equal to the maximum cross-sectional area. Otherwise, if the body is tapered ahead of the base, then referring the drag to the maximum cross-sectional area of such bodies, Hoerner proposes

$$C_{DB} = 0.029 \cdot \left(\frac{D_{Base}}{D_{max}}\right)^3 / \sqrt{C_{Df}} \quad , \qquad (7\text{-b})$$

where the forebody drag C_{Df} is

$$C_{Df} = \left(\frac{D_{Base}}{D_{max}}\right)^2 C_{fB} \quad .$$

Hence the base drag coefficients C_{DB}'s are, respectively,

$$C_{DB} = 0.029\left(\frac{\frac{1}{2}\rho U^2 S_{Base}}{D_{fore}}\right)^{\frac{1}{2}} \quad , \qquad (9\text{-a})$$

and

$$C_{DB} = 0.029\left(\frac{D_{Base}}{D_{max}}\right)^2\left(\frac{\frac{1}{2}\rho U^2 S_{Base}}{D_{fore}}\right)^{\frac{1}{2}} \qquad (9\text{-b})$$

2.3 Skin Friction Forces

The viscous forces acting on long inclined cylinders have been discussed by Taylor [30]. For rough cylinders and turbulent boundary layers, Taylor proposed the following expressions:

$$F_n = \frac{1}{2}\rho D U^2 (C_{Dp}\mathrm{Sin}^2 i + C_f \mathrm{Sin}\, i) \quad , \qquad (10)$$

$$F_\ell = \frac{1}{2}\rho D U^2 C_f \mathrm{Cos}\, i \quad ,$$

where $i = \tan^{-1}(\frac{\partial\eta}{\partial\tau}) + \tan^{-1}(\frac{\partial\eta}{\partial\xi})$. Hoerner [29] compiled data on the viscous forces on inclined cylinders and obtained the expressions for the forces acting in the ξ-and η-directions;

$$F_\xi = \frac{1}{2}\rho D(\xi) U^2 (C_{DP}\, \mathrm{Sin}^3 i + C_f)$$

and

$$F_\eta = \frac{1}{2}\rho\, D(\xi) U^2 C_{DP} \mathrm{Sin}^2 i \mathrm{Cos}\, i \quad .$$

Upon being transformed to the directions used here, these reduce identically to equation (10). It is of interest that C_f is given by

$$C_f = \lim_{i\to 0} \pi\left[\frac{(\text{Drag force})_\xi}{\frac{1}{2}\rho U^2 \pi D(\xi)}\right] \quad , \qquad (11)$$

the π factor appearing since the skin friction coefficient is based on the surface area. It is recognized that, at best, equations (10) give mean values since, strictly speaking, the coefficients vary from point to point with the developing boundary layer. Typically, $C_f = 0.01$ to 0.03 for $Re_D > 10^4$. For small $\frac{\partial \eta}{\partial \xi}$ and $\frac{\partial \eta}{\partial \tau}$ equations (10) reduce to

$$F_n = \tfrac{1}{2}\rho U^2 c_f \frac{S(\xi)}{D(\xi)}\left(\frac{\partial \eta}{\partial \tau} + \frac{\partial \eta}{\partial \xi}\right) + \tfrac{1}{2}\rho U c \frac{S(\xi)}{D(\xi)} \frac{\partial \eta}{\partial \tau} , \qquad (12)$$

$$F_\ell = \tfrac{1}{2}\rho U^2 c_f \frac{S(\xi)}{D(\xi)} ,$$

where the second term in F_n represents a linearization of the quadratic viscous force at zero flow velocity, $\frac{1}{2}\rho U^2 C_{DP} \left|\frac{\partial \eta}{\partial \tau}\right|\left(\frac{\partial \eta}{\partial \tau}\right)$; this was retained since all other terms vanish at $U = 0$.

2.4 Inviscid Hydrodynamic Forces

2.4.1 Main Portion of Body

Lighthill [31, 32], has investigated the potential flow pattern arising near a slender, flexible body undergoing small scale deflections $y(x,t)$ while subjected to nominally longitudinal flow and has shown, on the basis of the first perturbation to the undisturbed flow field, that the body experiences a force per unit length normal to its axis of symmetry and acting in what is roughly the negative y-direction;

$$I_n = [\frac{\partial}{\partial t} + U\frac{\partial}{\partial x}](Mv) \quad , \tag{13}$$

where v is the lateral relative velocity between the body and the fluid flowing past it, and M is the virtual mass of the fluid. Here the effects of sideslip have been neglected, effectively assuming that each cross-section of the body is part of an infinite cylinder; boundary layer effects have also been neglected. The virtual mass $M(x)$, is equal to $\rho S(x)$ for unconfined flow, and $v(x,t) = [(\partial/\partial t) + U(\partial/\partial x)]\ [y(x,t)]$, which when substituted into equation (13) yield

$$I_n = [(\frac{\partial}{\partial t}) + U(\frac{\partial}{\partial x})]\rho S(x)\ [(\frac{\partial y}{\partial t}) + U(\frac{\partial y}{\partial x})]$$

$$= \frac{\rho U^2 S(\xi)}{L}[\frac{\partial}{\partial \tau} + \frac{\partial}{\partial \xi}]^2 \eta + \frac{\rho U^2}{L}\frac{dS(\xi)}{d\xi}[\frac{\partial \eta}{\partial \tau} + \frac{\partial \eta}{\partial \xi}] \tag{14-a}$$

According to Lighthill's work, there exists no corresponding force in the longitudinal direction; thus,

$$I_\ell = 0. \tag{14-b}$$

2.4.2 <u>Tapered Ends</u>

Unfortunately, the above expressions are valid only over those portions of the body for which $dD(\xi)/d\xi$ can be considered small. This clearly is not the case near the nose or the tail; indeed, in the vicinity of a rounded nose $dD(\xi)/d\xi$

can be expected to approach infinity. Païdoussis [22, 24], was obviously aware of this problem, as evidenced by the fact that he multiplied the expression given in equation (14-a) by a correction factor f before applying it near the nose or tail.

For this present investigation a better formulation has been sought. General expressions which are analogous to those obtained by Lighthill but uniformly valid over the whole length of the body have been derived- the derivation being presented in Appendix A- for the distribution of force and moment along a prolate ellipsoid of revolution as it undergoes general plane motion through an infinite medium of ideal fluid. These expressions will ultimately be used to test out the corrected Lighthill formulation when it becomes available. In the interim we shall apply the expressions worked out in Appendix A somewhat more directly.

To examine the end sections more carefully, we now introduce a procedure which has been shown by Upson and Klikoff [33] to produce a fairly accurate approximation to the inviscid pressure forces arising along a typical, rigid airship hull. We fit to each cross-sectional element of the nose and tail sections an element from an axisymmetric ellipsoid which has, as nearly as possible, the same geometric characteristics. Then we take the potential flow forces acting on the element from the nose or tail to equal the corresponding forces which arise on the ellipsoidal element while, as part of the total ellipsoid, it undergoes translation and rotation equivalent to that of the nose or tail element to which it is fitted.

The criteria for fitting are as follows:

i) the ellipsoid fitted to any element of the nose or of the tail be concentric to that end section or, in other words, have the same longitudinal axis;

ii) the maximum diameter of the ellipsoid be equal to the maximum diameter of the flexible body, D_{max}; in terms of the notation of Appendix A, this can equivalently be stated as follows:

$$b = \tfrac{1}{2}D_{max} ; \tag{15}$$

iii) the local diameter of the ellipsoid match the local diameter of the nose or tail at the point of fit; in view of equations (A19), (A20), and (A21) of Appendix A, this implies that

$$2\,b(1-[x^2]^2)^{\frac{1}{2}} = D(\xi) ,$$

so that

$$x^2 = \{1 - (\frac{D(\xi)}{D_{max}})^2\}^{\frac{1}{2}} \quad . \tag{16}$$

iv) the product of the first and second derivatives of local diameter with respect to longitudinal distance be the same for the ellipsoid as for the body at the point of fit;

$$\frac{dD(x)}{dx} \cdot \frac{d^2D(x)}{dx^2} = \frac{dD(z^1)}{dz^1} \cdot \frac{d^2D(z^1)}{d[z^1]^2}$$

$$= \frac{d}{dz^1}\{2b(1-\frac{[z^1]^2}{a^2})^{1/2}\} \cdot \frac{d^2}{d[z^1]^2} \times$$

$$\times \{2b(1-\frac{(z^1)^2}{a^2})^{1/2}\}$$

$$= \frac{\frac{1}{a^3} D_{max}^5 \{D_{max}^2 - D^2(\xi)\}^{1/2}}{D^4(\xi)} \quad .$$

Finally we get

$$a = \{\frac{D_{max}^5 L^3 [D_{max}^2 - D^2(\xi)]^{1/2}}{D^4(\xi) \frac{dD(\xi)}{d\xi} \cdot \frac{d^2D(\xi)}{d\xi^2}}\}^{1/3} \quad . \tag{17}$$

Using the z^i co-ordinate system of Appendix A, we must relate the velocity and notation of each cross-sectional element of the nose and tail sections.

a) Nose Section

From the Figure 3a, we can easily find the longitudinal velocity component

$$v^1 = U\{\frac{d\eta_1}{d\tau} + (\xi+\frac{1}{2})\frac{d\theta_1}{d\tau}\} \sin\theta_1 - U\cos\theta_1,$$

and a lateral component

$$v^2 = U\{\frac{d\eta_1}{d\tau} + (\xi+\frac{1}{2})\frac{d\theta_1}{d\tau}\} \cos\theta_1 + U\sin\theta_1,$$

and the angular velocity

$$\omega^3 = \frac{U}{L}\frac{d\theta_1}{d\tau} \quad .$$

Actually the motion is very small, and we can drop the second order terms to obtain,

$$v^1 = -U$$

$$\dot{v}^1 = 0$$

$$v^2 = U\{\frac{d\eta_1}{d\tau} + (\xi+\frac{1}{2})\ \frac{d\theta_1}{d\tau}\} + \dot{U}\theta_1,$$

$$\dot{v}^2 = \frac{U^2}{L}\{\frac{d^2\eta_1}{d\tau^2} + (\xi+\frac{1}{2})\ \frac{d^2\theta_1}{d\tau^2}\} + \frac{U^2}{L}\ \frac{d\theta_1}{d\tau} \tag{18}$$

$$\omega^3 = \frac{U}{L}\ \frac{d\Theta_1}{d\tau}$$

$$\dot{\omega}^3 = \frac{U^2}{L^2}\ \frac{d^2\Theta_1}{d\tau^2}\ .$$

To follow Upson and Klikoff's procedure, we substitute the above relations into equation (A37) of Appendix A, we obtain expressions for the transverse and longitudinal inviscid forces acting per unit length along the nose;

$$\begin{aligned} I_n = -\frac{\rho U^2 S(\xi)}{L}\ [\{\frac{d^2\eta_1}{d\tau^2} + (\xi+\frac{1}{2})\ \frac{d^2\Theta_1}{d\tau^2} + \frac{d\Theta_1}{d\tau}\}\ k_2 \\ - \{\frac{d\eta_1}{d\tau} + (\xi+\frac{1}{2})\ \frac{d\Theta_1}{d\tau} + \Theta_1\}\frac{L}{a}(1+k_1)(1+k_2)\ \frac{x^2}{1-e^2[x^2]^2} \\ + \frac{d^2\Theta_1}{d\tau^2}\frac{a}{L}\ \ell_3\ x^2 - \frac{d\Theta_1}{d\tau}\ \{\frac{(1+k_1)(1+\ell_3(2[x^2]^2-1))}{1-e^2[x^2]^2} - 1\}], \end{aligned} \tag{19-a}$$

$$I_\ell = \rho U^2 S_{max}\ \frac{x^2}{a}\ [\frac{(1+k_1)^2(1-[x^2]^2)}{1-e^2[x^2]^2} - 1]\ . \tag{19-b}$$

b) Tail Section

Similarly, applying the Upson and Klikoff scheme to the tail section, we have

$$V' = -U$$

$$\dot{V}' = 0$$

$$V^2 = U\{\frac{d\eta_2}{d\tau} + (\xi-\frac{1}{2})\frac{d\theta_2}{d\tau}\} + U\theta_2$$

$$\dot{V}^2 = \frac{U^2}{L}\{\frac{d^2\eta_2}{d\tau^2} + (\xi-\frac{1}{2})\frac{d^2\theta_2}{d\tau^2}\} + \frac{U^2}{L}\frac{d\theta_2}{d\tau}$$

$$\omega^3 = \frac{U}{L}\frac{d\theta_2}{d\tau}$$

$$\dot{\omega}^3 = \frac{U^2}{L^2}\frac{d^2\theta_2}{d\tau^2}$$

and

$$I_n = \frac{\rho U^2 S(\xi)}{L}[\{\frac{d^2\eta_2}{d\tau^2} + (\xi-\frac{1}{2})\frac{d^2\theta_2}{d\tau^2} + \frac{d\theta_2}{d\tau}\}k_2$$

$$-\{\frac{d\eta_2}{d\tau} + (\xi-\frac{1}{2})\frac{d\theta_2}{d\tau} + \theta_2\}\frac{L}{a}(1+k_1)(1+k_2)\frac{x^2}{1-e^2[x^2]^2}$$

$$+\frac{d^2\theta_2}{d\tau^2}\frac{a}{L}\ell_3 x^2 - \frac{d\theta_2}{d\tau}\{\frac{(1+k_1)(1+\ell_3(2[x^2]^2-1))}{1-e^2[x^2]^2} - 1\}] \quad , (20\text{-a})$$

$$I_\ell = \rho U^2 S_{max} \frac{x^2}{a} \left[\frac{(1+k_1)^2 (1-[x^2]^2)}{1-e^2 [x^2]^2} - 1 \right] \tag{20-b}$$

where $S_{max} = \frac{1}{4}\pi D^2_{max}$, the maximum cross-sectional area of the body.

It is important to realize, and can be readily appreciated by examining equations (15), (16), (17), (A20) and (A31), that the quantities x^2, a, e, k_1, k_2 and ℓ_3 are all functions of ξ.

3. EQUATIONS OF SMALL LATERAL MOTIONS

We shall devote this chapter to a discussion of free motions of a slender body. In section 3.1, we shall restrict our attention to the main portion of the body, that is, the part along which we can apply Lighthill's formulation (14) of the inviscid-flow forces. In section 3.2 and 3.3, we derive the tensile force, shear force and moment exerted by the tail and nose sections based on the work of Chapter 2.

3.1 Equations of Motion Governing the Main Portion of the Body

Consider now a small element $\delta\xi$ of the cylinder undergoing small free lateral motions $\eta(\xi,\tau)$. The cylinder is subjected to a lateral force due to inviscid flow around it, $I_n\delta\xi$, and to viscous forces $F_n\delta\xi$ and $I_\ell\delta\xi$, in the lateral and longitudinal directions respectively. We also assume that it is subjected to a tension $T(\xi)$. We consider the cylinder as an Euler-Bernoulli beam subject to lateral shear forces $Q(\xi)$ and to bending moments $\mathcal{M}(\xi)$, as shown in Figure 3c.

Now taking force balances in the ξ- and η-directions and a moment balance, we obtain

$$\frac{\partial T}{\partial \xi} + F_\ell L + (F_n + I_n) L \left(\frac{\partial \eta}{\partial \xi} + \frac{\partial \eta}{\partial \tau}\right) = 0 \quad , \qquad (21)$$

$$\frac{\partial Q}{\partial \xi} - (F_n + I_n)L + \frac{\partial}{\partial \xi}\left(T\frac{\partial \eta}{\partial \xi}\right) + F_\ell L\,\frac{\partial \eta}{\partial \xi} - mU^2\,\frac{\partial^2 \eta}{\partial \tau^2} = 0, \tag{22}$$

$$QL + \frac{\partial \mathcal{M}}{\partial \xi} = 0, \tag{23}$$

where we have dropped terms of second and higher order of magnitude in $\frac{\partial \eta}{\partial \xi}$.

Now, substituting equations (12) and (14-a) into (21), neglecting terms of second order in small quantities, and integrating from some arbitrary value of ξ out to the point where the tail section begins, we obtain

$$T(\xi) = T_2 + \frac{1}{2}\,\rho U^2 L c_f \int_{\xi}^{\frac{1}{2}} \frac{S(\zeta)}{D(\zeta)}\,d\zeta\,, \tag{24}$$

where T_2 is the axial force exerted by the tail on the main portion of the body.

If in turn we substitute equation (24), along with (12) and (14-a), into (22) and make use of equation (21), we obtain, upon dropping terms of second order in η and its derivatives,

$$- \frac{\partial Q}{\partial \xi} + \rho U^2 S(\xi)\left[\frac{\partial}{\partial \tau} + \frac{\partial}{\partial \xi}\right]^2 \eta + \rho U^2\,\frac{dS(\xi)}{d\xi}\left[\frac{\partial \eta}{\partial \tau} + \frac{\partial \eta}{\partial \xi}\right]$$

$$+ \frac{1}{2}\rho U^2 c_f\,\frac{S(\xi)}{D(\xi)} L \left(\frac{\partial \eta}{\partial \tau} + \frac{\partial \eta}{\partial \xi}\right) + \frac{1}{2}\rho U c\,\frac{S(\xi)}{D(\xi)} L\,\frac{\partial \eta}{\partial \xi}$$

$$- \left[T_2 + \frac{1}{2}\rho U^2 c_f L \int_{\xi}^{\frac{1}{2}} \frac{S(\zeta)}{D(\zeta)}\, d\zeta \right] \frac{\partial^2 \eta}{\partial \xi^2} + m(\xi) U^2 \frac{\partial^2 \eta}{\partial \tau^2} = 0, \quad (25)$$

which is the equation of small lateral motions valid only over the major part of the body. If, as a special case, we take this major portion to be a uniform cylinder, the above equation becomes

$$- \frac{\partial Q}{\partial \xi} + \rho U^2 S \left[\frac{\partial}{\partial \tau} + \frac{\partial}{\partial \xi}\right]^2 \eta + \frac{1}{2}\rho U^2 c_f \frac{S}{D} L \left(\frac{\partial \eta}{\partial \tau} + \frac{\partial \eta}{\partial \xi}\right)$$

$$+ \frac{1}{2} Uc \frac{S}{D} L \frac{\partial \eta}{\partial \xi} - \left[T_2 + \frac{1}{2}\rho U^2 c_f \frac{S}{D} L \left(\frac{1}{2} - \xi\right)\right] \frac{\partial^2 \eta}{\partial \xi^2} \quad (26)$$

$$+ mU^2 \frac{\partial^2 \eta}{\partial \tau^2} = 0 ,$$

where D and m are now constant.

Equations (25) and (26) are actually identical in form to equations (9) and (10) derived by Paidoussis [24]. But it should be realized, though, that Païdoussis construed these equations as being valid over the entire length of the body, we here claim them to be applicable only over the main section of body.

3.2 The Tail Section

We try to develop expressions for the tensile and shear force and for the moment exerted by the tail on the main part of the body, starting with the evaluation of the tensile force T_2. Referring to Figure 4a, we take a force balance in the longitudinal direction to get

$$T_2 = \int_{\frac{1}{2}}^{\frac{1}{2}+\lambda_2} (F_\ell + I_\ell) L d\xi + \frac{1}{2}\rho U^2 S_{Base} C_{DB} \tag{27}$$

$$= \frac{1}{2}\rho U^2 S_{max} \varepsilon c_f i_{120} + \rho U^2 S_{max} i_{720} + \frac{1}{2}\rho U^2 S_{Base} C_{DB}$$

where we have made use of equations (12) and (20-b) and have introduced

$$\varepsilon \equiv \frac{L}{D_{max}} \tag{28}$$

along with a couple of the quantities defined in Appendix B. Recalling that C_{DB} depends upon the forebody drag, we now set out to find an expression for it.

$$D_{fore} = \int_{-\frac{1}{2}-\lambda_1}^{\frac{1}{2}+\lambda_2} (F_\ell + I_\ell) L d\xi$$

$$= \frac{1}{2}\rho U^2 S_{max} \varepsilon c_f (i_{110} + i_{120} + \frac{D_{max}}{S_{max}} \int_{-\frac{1}{2}}^{\frac{1}{2}} \frac{S(\zeta)}{D(\zeta)} d\zeta)$$

$$+ \rho U^2 S_{max} (i_{710} + i_{720})$$

making use of equations (12), (19-b), and (20-b).

In view of equation (9), it follows that

$$C_{DB} = 0.029\left(\frac{D_{Base}}{D_{max}}\right)^3 \{\varepsilon c_f(i_{110} + i_{120} + \frac{D_{max}}{S_{max}} \times$$

$$\times \int_{-\frac{1}{2}}^{\frac{1}{2}} \frac{S(\xi)}{D(\xi)}\, d\xi) + 2(i_{710} + i_{720})\}^{-\frac{1}{2}} \qquad (29)$$

If the major portion of the body is a uniform cylinder, this equation leads to

$$C_{DB} = 0.029\left(\frac{D_{Base}}{D_{max}}\right)^3 \{\varepsilon\, c_f(1+i_{110}+i_{120}) + 2(i_{710}+i_{720})\}^{-1/2} \qquad (30)$$

In order to find a shear ~~force~~ force Q_2, we take a force balance in the lateral direction, dropping terms of second order in small quantities.

$$Q_2 = -\int_{\frac{1}{2}}^{\frac{1}{2}+\lambda_2} (F_\eta + I_\eta + \frac{m(\xi)U^2}{L}\frac{\partial^2\eta}{\partial\tau^2})L\, d\xi$$

$$= -\tfrac{1}{2}\rho U^2 S_{max}\, \varepsilon c_f i_{120}\left(\frac{d\eta_2}{d\tau} + \theta_2\right) - \tfrac{1}{2}\rho U S_{max} \varepsilon c i_{120}[\theta_2]$$

$$- \rho U^2 S_{max} i_{320}\left(\frac{d^2\eta_2}{d\tau^2} + \frac{d\theta_2}{d\tau}\right) + \rho U^2 S_{max} i_{420}\left(\frac{d\eta_2}{d\tau} + \theta_2\right)$$

$$- \rho U^2 S_{max} i_{520}\left(\frac{d^2\theta_2}{d\tau^2}\right) + \rho U^2 S_{max} i_{620}\left(\frac{d\theta_2}{d\tau}\right)$$

$$- m_{max} U^2 i_{220}\left(\frac{d^2\eta_2}{d\tau^2}\right), \qquad (31)$$

where we have used equations (4) and (12) in evaluating the skin friction forces and (20-a) in treating the inviscid forces. In dealing with the inertial force, we have set the mass per unit length of the body (equal to displaced fluid for neutral buoyancy)

$$m(\xi) = \rho S(\xi) \tag{32}$$

and

$$m_{max} = \rho S_{max} \tag{33}$$

Finally, we seek an expression for the moment $\mathcal{M}_2$. Accordingly, we take a moment balance about the point B as shown in Figure 4a. Before proceeding , though, we should note that the longitudinal component of inviscid-flow force arising along an ellipsoid of revolution gives rise to a distributed moment acting in the plane of motion which has magnitude $(b^2/a)x^2I_n$ and is opposed in sense to the moment arising equation (A38) of Appendix A. In any case, this moment is of negligible magnitude since (b/a) is presumably of the same order as D_{max}/L, which is a small quantity.

In fact, it can readily be seen that

$$\mathcal{M}_2 = - \int_{\frac{1}{2}}^{\frac{1}{2}+\lambda_2} L(\xi-\tfrac{1}{2})(F_n + I_n + \frac{m(\xi)U^2}{L} \frac{\partial^2\eta}{\partial\tau^2})L\, d\xi$$

$$+\int_{\frac{1}{2}}^{\frac{1}{2}+\lambda_2} \frac{b^2}{a} x^2 I_n L d\xi = 0 . \qquad (34)$$

to first order in small quantities.

3.3 The Nose Section

In this section we turn our attention to developing expressions for the shear force and moment exerted by the nose on the main portion of the body. Upon glancing at Figure 4b, we see that before proceeding we must consider the functional form of the tow rope force . Accordingly, we tackle that problem first.

Substituting equation (27) into equation (24), setting $\xi = -\frac{1}{2}$ and employing equations (12) and (19-b) in evaluating integral, we find T_1

$$T_1 = T_2 + \tfrac{1}{2}\rho U^2 L c_f \int_{-\frac{1}{2}}^{\frac{1}{2}} \frac{S(\zeta)}{D(\zeta)} d\zeta$$

$$= \tfrac{1}{2}\rho U^2 S_{max} \varepsilon c_f \left(i_{120} + \frac{D_{max}}{S_{max}} \int_{-\frac{1}{2}}^{\frac{1}{2}} \frac{S(\zeta)}{D(\zeta)} d\zeta\right)$$

$$+ \rho U^2 S_{max}\, i_{720} + \tfrac{1}{2}\rho U^2\, S_{Base}\, C_{DB} . \qquad (35)$$

Thus,

$$P_\ell = T_1 + \int_{-\frac{1}{2}-\lambda_1}^{-\frac{1}{2}} (F_\ell + I_\ell)\, L d\xi$$

$$= \rho U^2 S_{max}\, \varepsilon c_f (i_{110} + i_{120} + \frac{D_{max}}{S_{max}} \int_{-\frac{1}{2}}^{\frac{1}{2}} \frac{S(\xi)}{D(\xi)}\, d\xi)$$

$$+ \rho U^2 S_{max} (i_{710} + i_{720}) + \frac{1}{2}\rho\, U^2\, S_{Base}\, C_{DB} \quad . \qquad (36)$$

Now, the total force P must clearly act in the direction of the tow-line. Taking the length of the tow-rope to be s and letting $\Lambda = s/L$ serve as its non-dimensional analogue, we conclude that the normal component P_n is equal to the total tow-rope force, P, times the tangent of the angle that the tow-rope makes with the position of rest. For small motions this is linearized (Durand [34] and Strandhagen [8]).

$$P_n = P_\ell \tan (\gamma - \delta) \; .$$

where

$$\text{Cos}\gamma = \frac{\eta}{\Lambda}\Big|_{\xi = -\frac{1}{2}-\lambda_1} ,$$

and

$$\cot \delta = \frac{\partial\eta}{\partial\xi}\Big|_{\xi = -\frac{1}{2}\lambda_1}$$

as shown in Figure 4b.

Using familiar trigonometric identities and the binomial expansion for the expressions for $(\partial\eta/\partial\xi)$ and (η/Λ), and neglecting terms of second order of magnitude,

$$\tan(\gamma-\delta) = \frac{\partial\eta}{\partial\xi} - \frac{\eta}{\Lambda}\Big|^{*}_{\xi = -\frac{1}{2}\lambda_1} .$$

It follows, then, that the normal component of the tow-rope pull,

$$P_n = P_\ell\left(\frac{\partial\eta}{\partial\xi} - \frac{\eta}{\Lambda}\right)\Big|_{\xi = -\frac{1}{2}\lambda_1}$$

$$= P_\ell\left(\Theta_1 - \frac{\eta_1 - \Theta_1\lambda_1}{\Lambda}\right) , \qquad (37)$$

making use of equation (3).

It is informative and intuitively reassuring as well to note that when the slope of the nose, Θ_1 (to first order), equals the inclination of the tow-rope, $(\eta_1-\Theta_1\lambda_1)/\Lambda$, then the normal component of tow-line pull vanishes.

Returning to Figure 4a, we now balance forces in the transverse directions in order to obtain an expression for the shear force.

$$Q_1 = -P_n + \int_{-\frac{1}{2}\lambda_1}^{-\frac{1}{2}} \left(F_n+I_n+\frac{m(\xi)U^2}{L}\frac{\partial^2\eta}{\partial\tau^2}\right) L\,d\xi$$

$$= \frac{1}{2}\rho U^2 S_{max} \left\{\varepsilon c_f(i_{110}+i_{120}+\frac{D_{max}}{S_{max}}\int_{-\frac{1}{2}}^{\frac{1}{2}} \frac{S(\zeta)}{D(\zeta)}\,d\zeta\right)$$

* this equation is not valid as $\Lambda\to 0$. Λ must be greater than $O(\eta^{\frac{1}{2}})$. In this thesis, calculations are conducted when $\Lambda \geq 0.5$.

$$+ 2(i_{710}+i_{720}) + \frac{S_{Base}}{S_{max}} C_{DB} \} (\frac{\eta_1 - \theta_1\lambda_1}{\Lambda} - \theta_1)$$

$$+ \frac{1}{2}\rho U^2 S_{max}\ \epsilon c_f\ i_{110}(\frac{d\eta_1}{d\tau}+\theta_1)$$

$$+ \frac{1}{2}\rho U S_{max}\epsilon c\ i_{110}\ \dot{\theta}_1$$

$$- \rho U^2 S_{max}\ i_{310}\ (\frac{d^2\eta_1}{d\tau^2} + \frac{d\theta_1}{d\tau})$$

$$+ \rho U^2 S_{max}\ i_{410}\ (\frac{d\eta_1}{d\tau} + \theta_1) - \rho U^2 S_{max}\ i_{510}\ \frac{d^2\theta_1}{d\tau^2}$$

$$+ \rho U^2 S_{max}\ i_{610}\ \frac{d\theta_1}{d\tau} + m_{max}\ U^2\ i_{210}\ \frac{d^2\eta_1}{d\tau^2}\ , \qquad (38)$$

where we have substituted equation (36) into (37) to obtain P_n, invoked equation (12) and (3) to evaluate the frictional forces, made use of equation (19a) in treating the inviscid forces, and employed equations (32) and (33) in dealing with the inertial force. As usual, we have dropped terms of second order in small quantities. Finally, we must obtain an expression for the moment $\mathcal{M}_1$. Accordingly, we take a moment balance about the point A shown in Figure 4a. Proceeding much as we did in Section 3.2 we get

$$\mathcal{M}_1 = L\lambda_1 P_n + \int_{-\frac{1}{2}-\lambda_1}^{-\frac{1}{2}} L(\xi+\tfrac{1}{2})(F_n+I_n + \frac{m(\xi)U^2}{L}\frac{\partial^2\eta}{\partial\tau^2})\ Ld\xi$$

$$- \int_{-\frac{1}{2}\lambda_1}^{-\frac{1}{2}} \frac{b^2}{a} x^2 I_n L d\xi$$

$$= L\lambda_1 \cdot \frac{1}{2}\rho U^2 S_{max} \{\epsilon c_f (i_{110}+i_{120}+ \frac{D_{max}}{S_{max}} \int_{-\frac{1}{2}}^{\frac{1}{2}} \frac{S(\zeta)}{D(\zeta)} d\zeta)$$

$$+ 2(i_{710}+i_{720}) + \frac{S_{Base}}{S_{max}} C_{DB} \}(\theta_1 - \frac{\eta_1-\theta_1\lambda_1}{\Lambda}) , \quad (39)$$

since all terms except those associated with the tow-rope force are negligibly small.

4. EQUATIONS OF MOTION AND BOUNDARY CONDITIONS OF OF A FLEXIBLE TOWED BODY

4.1 Equations of Motion

We shall assume the flexural rigidity, EI, to be constant along the cylindrical segment of the body, though it may vary appreciably over the end sections or even be infinite there. It has been assumed that the Euler-Bernoulli beam theory is adequate to describe the motions along the body's uniform middle section; moveover, a Kelvin-Voigt type of damping in the material of the cylinder has been assumed to apply. Thus,

$$\mathcal{M} = \frac{EI}{L}\frac{\partial^2\eta}{\partial\xi^2} + \mu I\frac{U}{L^2}\frac{\partial^3\eta}{\partial\tau\partial\xi^2}\,, \tag{40}$$

where $\mathcal{M}$ is the bending moment shown in Figure 3c. Invoking equation (23), the shear force Q is

$$Q = -\frac{EI}{L^2}\frac{\partial^3\eta}{\partial\xi^3} - \frac{\mu IU}{L^3}\frac{\partial^4\eta}{\partial\tau\partial\xi^3}\,. \tag{41}$$

Substituting now equation (41) into (26) and making use of (27), we obtain

$$\frac{\mu IU}{L^3}\frac{\partial^5\eta}{\partial\tau\partial\xi^4} + \frac{EI}{L^2}\frac{\partial^4\eta}{\partial\xi^4} + \rho U^2 S\left(\frac{\partial}{\partial\tau} + \frac{\partial}{\partial\xi}\right)^2\eta$$

$$+ \frac{1}{2}\rho U^2 S\varepsilon c_f\left(\frac{\partial\eta}{\partial\tau} + \frac{\partial\eta}{\partial\xi}\right) + \frac{1}{2}\rho US\varepsilon c\left(\frac{\partial\eta}{\partial\xi}\right)$$

$$- \frac{1}{2}\rho U^2 S \; \{\varepsilon c_f (\tfrac{1}{2}+i_{120}-\xi) + 2i_{720} + \frac{S_{Base}}{S} C_{DB}\} \frac{\partial^2\eta}{\partial\xi^2}$$

$$+ mU^2 \frac{\partial^2\eta}{\partial\tau^2} = 0 \, , \qquad (42)$$

where $S = S_{max}$.

4.2 Boundary Conditions

Consider the towed flexible cylindrical body depicted in Figure 1. The body consists of a uniform cylinder terminated by a rounded nose and a truncated, streamlined tail, incorporated to provide reasonable axial flow conditions over the body. It has been assumed that the towing craft moves horizontally in a straight course with uniform velocity U, so that the tow-rope in its undisturbed state lies along the x-axis.

The two boundary conditions at $\xi = -\frac{1}{2}$ are obtained by substituting equation (41) and (2) into (38) and then similarly applying (40) and (2) in conjunction with (39).

$$\frac{\mu I U}{L^3} \frac{\partial^4\eta}{\partial\tau\partial\xi^3} + \frac{EI}{L^2}\frac{\partial^3\eta}{\partial\xi^3} + \frac{1}{2}\rho U^2 S \; \{\varepsilon c_f (1+i_{110}+i_{120}) + 2(i_{710}+i_{720})$$

$$+ \frac{S_{Base}}{S} C_{DB}\} \cdot \left(\frac{\eta - \frac{\partial\eta}{\partial\xi}\lambda 1}{\Lambda} - \frac{\partial\eta}{\partial\xi}\right) + \frac{1}{2}\rho U^2 S \; \varepsilon c_f i_{110} \left(\frac{\partial\eta}{\partial\tau} + \frac{\partial\eta}{\partial\xi}\right)$$

$$+ \frac{1}{2} US\varepsilon c \; i_{110}\left(\frac{\partial\eta}{\partial\xi}\right) - \rho U^2 S \; i_{310}\left(\frac{\partial^2\eta}{\partial\tau^2} + \frac{\partial^2\eta}{\partial\tau\partial\xi}\right)$$

$$+ \rho U^2 S\, i_{410} \left(\frac{\partial\eta}{\partial\tau} + \frac{\partial\eta}{\partial\xi}\right) - \rho U^2 S\, i_{510} \left(\frac{\partial^3\eta}{\partial\tau^2\partial\xi}\right)$$

$$+ \rho U^2 S\, i_{610} \left(\frac{\partial^2\eta}{\partial\tau\partial\xi}\right) + mU^2\, i_{210} \left(\frac{\partial^2\eta}{\partial\tau^2}\right) = 0\ , \tag{43}$$

and

$$\frac{\mu IU}{L^3} \frac{\partial^3\eta}{\partial\tau\partial\xi^2} + \frac{EI}{L^2} \frac{\partial^2\eta}{\partial\xi^2} + \frac{1}{2}\rho U^2 S\, \lambda_1 \{\varepsilon c_f (1+i_{110} + i_{120})$$

$$+ 2(i_{710} + i_{720}) + \frac{S_{Base}}{S}\, C_{DB}\} \left(\frac{\eta - \frac{\partial\eta}{\partial\xi}\,\lambda_1}{\Lambda} - \frac{\partial\eta}{\partial\xi}\right) = 0\ . \tag{44}$$

The other two boundary conditions required at $\xi = \frac{1}{2}$ are obtained by using equations (40), (41), (5), (31) and (34) analogously;

$$\frac{\mu IU}{L^3} \frac{\partial^4\eta}{\partial\tau\partial\xi^3} + \frac{EI}{L^2} \frac{\partial^3\eta}{\partial\xi^3} - \frac{1}{2}\, \rho U^2 S\varepsilon c_f\, i_{120} \left(\frac{d\eta}{d\tau} + \frac{\partial\eta}{\partial\xi}\right) - \frac{1}{2}\rho US\varepsilon c\, i_{120}\left(\frac{\partial\eta}{\partial\xi}\right)$$

$$- \rho U^2 S i_{320} \left(\frac{d^2\eta}{d\tau^2} + \frac{\partial^2\eta}{\partial\tau\partial\xi}\right) + \rho U^2 S i_{420} \left(\frac{d\eta}{d\tau} + \frac{\partial\eta}{\partial\xi}\right)$$

$$- \rho U^2 S i_{520} \left(\frac{\partial^3\eta}{\partial\tau^2\partial\xi}\right) + \rho U^2 S i_{620} \left(\frac{\partial^2\eta}{\partial\tau\partial\xi}\right) - mU^2\, i_{220} \left(\frac{\partial^2\eta}{\partial\tau^2}\right) = 0\ , \tag{45}$$

and

$$\frac{\mu IU}{L^3} \frac{\partial^3\eta}{\partial\tau\partial\xi^2} + \frac{EI}{L^2} \frac{\partial^2\eta}{\partial\xi^2} = 0\ . \tag{46}$$

5. EQUATIONS OF MOTION AND BOUNDARY CONDITIONS OF THE MODIFIED OLD THEORY

The equations of motion and boundary conditions of Reference [24] are given by

$$-\frac{\partial Q}{\partial x} + M\left[\left(\frac{\partial}{\partial t}\right) + U\left(\frac{\partial}{\partial x}\right)\right]^2 y + \frac{1}{2}C_N\left(\frac{\rho S}{D}\right)U\left[\left(\frac{\partial}{\partial t}\right) + U\left(\frac{\partial}{\partial x}\right)\right]y$$

$$- T\frac{\partial^2 y}{\partial x^2} + m\frac{\partial^2 y}{\partial t^2} = 0 , \qquad (47)$$

and

$$-Q + f_1 MU\left(\frac{\partial y}{\partial t} + U\frac{\partial y}{\partial x}\right) + \frac{1}{2}MU^2(C_1 + C_2 + \varepsilon C_T)\left(\frac{\partial y}{\partial x} - \frac{y}{s}\right)$$

$$+ (m + f_1 M)X_1\frac{\partial^2 y}{\partial t^2} = 0 , \qquad \text{at } x = 0 \qquad (48)$$

$$Q - f_2 MU\left(\frac{\partial y}{\partial t} + U\frac{\partial y}{\partial x}\right) + (m + f_2 M)X_2\frac{\partial^2 y}{\partial t^2} = 0 , \text{ at } x = L \qquad (49)$$

where $X_1 = \frac{1}{S}\int_0^{\ell_1} S(x)dx$ and $X_2 = \frac{1}{S}\int_{L-\ell_2}^{L} S(x)dx$

the other two boundary conditions are

$$\mathcal{M} = 0 \qquad \text{at} \qquad x = 0 \qquad (50)$$

$$\mathcal{M} = 0 \qquad \text{at} \qquad x = L \qquad (51)$$

In order to transform these equations to a similar form as that used in the theory presented in this thesis, we must transform the coordinates, since in the theory of Reference [24] the origin of the axes was taken at the nose. We divide the body into three sections, as shown in Figure 2b. It is recalled that the main portion of the body is of length L and the lengths of the nose and tail sections are ℓ_1 and ℓ_2, respectively. For the sake of simplicity, we assume that the center of mass of the main portion coincides with the geometric center of body. For convenience we now measure x from the center of mass, so that the main portion of the body extends from $x = -L/2$ to $x = L/2$.

Hence, the modified equations of Reference [24] may be obtained by applying equations (41), (24), (27) and (28) to (47) in conjunction with (1); yielding

$$\begin{aligned}
&\frac{\mu I U}{L^3}\frac{\partial^5 \eta}{\partial\tau\partial\xi^4} + \frac{EI}{L^2}\frac{\partial^4\eta}{\partial\xi^4} + \rho U^2 S\left(\frac{\partial}{\partial\tau} + \frac{\partial}{\partial\xi}\right)^2 \eta \\
&+ \frac{1}{2}\rho U^2 S\varepsilon c_f\left(\frac{\partial\eta}{\partial\tau} + \frac{\partial\eta}{\partial\xi}\right) \\
&- \frac{1}{2}\rho U^2 S\left\{\varepsilon c_f\left(\frac{1}{2} - \xi\right) + \frac{S_{Base}}{S} C_2\right\}\frac{\partial^2\eta}{\partial\xi^2} \qquad (47a)\\
&+ mU^2\frac{\partial^2\eta}{\partial\tau^2} = 0 ,
\end{aligned}$$

where $c_f = C_N = C_T$, $C_2 = C_{DB}$

This equation is almost the same as equation (42).

Substituting equation (41) into (48) and also making use of (1), we obtain the boundary condition at $\xi = -\frac{1}{2}$

$$\frac{\mu IU}{L^3}\frac{\partial^4\eta}{\partial\tau\partial\xi^3} + \frac{EI}{L^2}\frac{\partial^3\eta}{\partial\xi^3} + f_1MU^2\left(\frac{\partial\eta}{\partial\tau}+\frac{\partial\eta}{\partial\xi}\right) - \frac{1}{2}MU^2[C_1+C_2+\varepsilon c_f] \times$$

$$\times\left(\frac{\partial\eta}{\partial\xi} - \frac{\eta-\lambda_1\Theta_1}{\Lambda}\right) + U^2 i_{210}(m+Mf_1)\frac{\partial^2\eta}{\partial\tau^2} = 0\ . \qquad (48a)$$

Similarly applying equations (1) and (41) to (49)

$$\frac{\mu IU}{L^3}\frac{\partial^4\eta}{\partial\tau\partial\xi^3} + \frac{EI}{L^2}\frac{\partial^3\eta}{\partial\xi^3} + f_2MU^2\left(\frac{\partial\eta}{\partial\tau}+\frac{\partial\eta}{\partial\xi}\right) - U^2(m+Mf_2)i_{220}\frac{\partial^2\eta}{\partial\tau^2}$$

$$= 0\ , \qquad \text{at } \xi = \frac{1}{2} \qquad (49a)$$

where we introduce $i_{210} = X_1/L$ and $i_{220} = X_2/L$.

The other two boundary conditions at $\xi = \pm\frac{1}{2}$ are obtained directly from equations (34) and (39) respectively, using (40),

$$\frac{\mu IU}{L^2}\frac{\partial^3\eta}{\partial\tau\partial\xi^2} + \frac{EI}{L}\frac{\partial^2\eta}{\partial\xi^2} + \frac{1}{2}\rho U^2 S\lambda_1(C_1+C_2+\varepsilon c_f)\left(\frac{\eta-\lambda_1\frac{\partial\eta}{\partial\xi}}{\Lambda} - \frac{\partial\eta}{\partial\xi}\right) = 0\ ,$$

$$\text{at } \xi = -\tfrac{1}{2} \qquad (50a)$$

$$\frac{\mu IU}{L^2}\frac{\partial^3\eta}{\partial\tau\partial\xi^2} + \frac{EI}{L}\frac{\partial^2\eta}{\partial\xi^2} = 0 \ . \qquad \text{at } \xi = \tfrac{1}{2} \qquad (51a)$$

The parameters f_1 and f_2, which are equal to unity for slender-body, inviscid flow theory, are introduced to account for the theoretical lateral forces at the free ends not being fully realized because of (a) the lateral flow not being truly two-dimensional, since the fluid has opportunity to pass around (sideslip) rather than over the tapered ends (Munk [5]), and (b) boundary-layer effects (Hawthorne [9]). Accordingly, f_1 and f_2 will normally be less than unity.

Comparing the above boundary conditions with equations (43), (44), (45), and (46), we can get the values of f_1 and f_2 theoretically.

6. EQUATIONS OF MOTION OF A RIGID, TOWED BODY

6.1 Mathematical Model

Consider the equation of motion for exactly the same configuration as in Figure 1, but impose the restriction that the body is rigid, having a streamlined nose and a truncated tail. In this case, the system can be completely described by just two generalized co-ordinates. Accordingly, we define $\eta(\xi,\tau)$ to be the non-dimensionalized displacement of the centre of the cylindrical portion of the body, η_c to be the lateral displacement of the center of mass, and take ϕ to be the angle that the axis of symmetry makes with the x-axis.

Thus the displacement at any point along the body is given by

$$\eta(\xi,\tau) = \eta_c(\tau) + \phi(\tau)\xi \quad . \tag{52}$$

6.2 Equation of Motion Based on the Present Theory

Instead of deriving the equations of force and moment balance independently of the previous work, we shall first integrate equation (26) along the cylindrical region to obtain

$$Q_1 - Q_2 + \rho U^2 S \left[\frac{d^2\eta_c}{d\tau^2} + 2\,\frac{d\phi}{d\tau} \right]$$

$$+ \frac{1}{2}\rho U^2 S\varepsilon c_f \left(\frac{d\eta_c}{d\tau} + \phi\right) + \frac{1}{2}\rho U S\varepsilon c\phi \tag{53}$$

$$+ mU^2 \frac{d^2\eta_c}{d\tau^2} = 0 \ .$$

Similarly we shall integrate the product of the forces in equation (26) by ξ in order to obtain the equation of moment balance.

Consequently the equation leads to

$$- [L\xi Q]_{\xi=-\frac{1}{2}}^{\frac{1}{2}} + \int_{-\frac{1}{2}}^{\frac{1}{2}} LQd\xi + \rho U^2 SL \left(\frac{1}{12}\frac{d^2\phi}{d\tau^2}\right)$$

$$+ \frac{1}{2}\rho U^2 SL\varepsilon c_f \left(\frac{1}{12}\frac{d\phi}{d\tau}\right)$$

$$+ mU^2 L \left(\frac{1}{12}\frac{d^2\phi}{d\tau^2}\right) = 0 \ .$$

Using equation (23), we see that the above is equivalent to

$$- \frac{L}{2}Q_1 - \frac{L}{2}Q_2 + \mathcal{M}_1 - \mathcal{M}_2 + \frac{1}{12}\rho U^2 SL \left(\frac{d^2\phi}{d\tau^2}\right)$$

$$+ \frac{1}{24}\rho U^2 S \ \varepsilon c_f L \left(\frac{d\phi}{d\tau}\right) + \frac{1}{12} mU^2 L \left(\frac{d^2\phi}{d\tau^2}\right) = 0 \ . \tag{54}$$

The following relations are used to perform the integrations:

$$\int_{-\frac{1}{2}}^{\frac{1}{2}} \eta(\xi,\tau)d\xi = \eta_c(\tau) \ ,$$

$$\int_{-\frac{1}{2}}^{\frac{1}{2}} \frac{\partial\eta}{\partial\xi}(\xi,\tau)d\xi = \phi(\tau) \ ,$$

$$\int_{-\frac{1}{2}}^{\frac{1}{2}} \frac{\partial^2\eta}{\partial\xi^2}(\xi,\tau)d\xi = 0 \ ,$$

and

$$\int_{-\frac{1}{2}}^{\frac{1}{2}} \xi\,\eta(\xi,\tau)d\xi = \frac{\phi}{12} \ ,$$

$$\int_{-\frac{1}{2}}^{\frac{1}{2}} \xi\,\frac{\partial\eta}{\partial\xi}(\xi,\tau)d\xi = 0 \ ,$$

$$\int_{-\frac{1}{2}}^{\frac{1}{2}} \xi\,\frac{\partial^2\eta}{\partial\xi^2}(\xi,\tau)d\xi = 0 \ .$$

The shear forces Q_1 and Q_2 and moments $\mathcal{M}_1$ and $\mathcal{M}_2$ which the end sections exert upon the cylindrical part of the body have already been found. Now comparing equation (52) with (3) and (4) we see that

$$\eta_1 = \eta_c - \tfrac{1}{2}\phi \ ,$$

$$\eta_2 = \eta_c + \tfrac{1}{2}\phi \ , \tag{55}$$

$$\Theta_1 = \Theta_2 = \phi \,.$$

Substituting these relations into equations (31), (34), (38) and (39), and then substituting in turn the results into equations (53) and (54), we obtain after collecting terms,

$$[2 + i_{210} + i_{220} - i_{310} + i_{320}] \frac{d^2\eta_c}{d\tau^2}$$

$$+ [\tfrac{1}{2}\varepsilon c_f (1 + i_{110} + i_{120}) + i_{410} - i_{420}] \frac{d\eta_c}{d\tau}$$

$$+ [\frac{1}{2\Lambda}\{\varepsilon c_f (1 + i_{110} + i_{120}) + 2(i_{710} + i_{720}) + \frac{S_{Base}}{S} C_{DB}\}]\eta_c$$

$$+ [\tfrac{1}{2}(-i_{210} + i_{220} + i_{310} + i_{320}) - i_{510} + i_{520}] \frac{d^2\phi}{d\tau^2}$$

$$+ [2 - i_{310} + i_{320} + i_{610} - i_{620} - \tfrac{1}{2}(i_{410} + i_{420}) + \tfrac{1}{4}\varepsilon c_f(-i_{110} + i_{120})] \frac{d\phi}{d\tau}$$

$$+ [\tfrac{1}{2}\varepsilon c_f (1 + i_{110} + i_{120}) + i_{410} - i_{420} \tag{56a}$$

$$- \frac{1}{2\Lambda}\{\varepsilon c_f (1 + i_{110} + i_{120}) + 2(i_{710} + i_{720}) + \frac{S_{Base}}{S} C_{DB}\}(\tfrac{1}{2} + \lambda_1 +$$

$$+ \Lambda)] \phi = 0 \,,$$

$$[\tfrac{1}{2}(-i_{210} + i_{220} + i_{310} + i_{320})] \frac{d^2\eta_c}{d\tau^2}$$

$$+ [\tfrac{1}{2}(-i_{410} - i_{420}) + \tfrac{1}{4}\varepsilon c_f (-i_{110} + i_{120})] \frac{d\eta_c}{d\tau}$$

$$+ \left[\frac{1}{2\Lambda} \{\varepsilon c_f (1 + i_{110} + i_{120}) + 2(i_{710} + i_{720}) + \frac{S_{Base}}{S} C_{DB}\}\{-\frac{1}{2}\lambda_1\}\right] \eta_c$$

$$+ \left[\frac{1}{6} + \frac{1}{4}(i_{210}+i_{220}-i_{310}+i_{320}) + \frac{1}{2}(i_{510}+i_{520}) \right] \frac{d^2\phi}{d\tau^2}$$

$$+ \left[\frac{1}{2}(i_{310} + i_{320} - i_{610} - i_{620}) + \frac{1}{4}(i_{410} - i_{420}) \right.$$

$$\left. + \frac{1}{8}\varepsilon c_f (\frac{1}{3} + i_{110} + i_{120}) \right] \frac{d\phi}{d\tau} \tag{56b}$$

$$+ \left[\frac{1}{4}\varepsilon c_f (-i_{110} + i_{120}) - \frac{1}{2}(i_{410} + i_{420}) \right.$$

$$+ \frac{1}{2\Lambda} \{\varepsilon c_f (1 + i_{110} + i_{120}) + 2(i_{710} + i_{720})$$

$$\left. + \frac{S_{Base}}{S} C_{DB}\} (\frac{1}{2} + \lambda_1)(\frac{1}{2}+\lambda_1+\Lambda) \right] \phi = 0 ,$$

where we have set $c = 0$.

6.3 Equation of Motion Based on the Modified Old Theory

In this case boundary conditions (48a-51a) are incorporated through the integral of the first term of these equations; alternatively, the shear forces at $\xi = \pm \frac{1}{2}$ may be viewed as forces replacing the effect of nose and tail on the main part of the body. Similarly, as we did in Section 6.2, we shall use equation (53) with the boundary conditions (48a), (49a) to get the force balance equation,

$$[2 + (1 + f_1)i_{210} + (1 + f_2)i_{220}]\,\frac{d^2\eta_c}{d\tau^2}$$

$$+ [\tfrac{1}{2}\varepsilon c_f + f_1 - f_2]\,\frac{d\eta_c}{d\tau} + \frac{1}{2\Lambda}[C_1 + C_2 + \varepsilon c_f]\,\eta_c$$

$$+ [-\tfrac{1}{2}\{(1 + f_1)i_{210} - (1 + f_2)i_{220}\}]\,\frac{d^2\phi}{d\tau^2} + [\,2 - \tfrac{1}{2}(f_1 + f_2)]\,\frac{d\phi}{d\tau}$$

$$+ [\tfrac{1}{2}\varepsilon c_f\,\{1 - (C_1 + C_2 + \varepsilon c_f)(\frac{\lambda_1 + \frac{1}{2} + \Lambda}{\Lambda})\} + f_1 - f_2]\,\phi = 0\,, \tag{57a}$$

In order to obtain the moment balance equation we shall apply the boundary conditions (50a) and (51a) to equation (54), and this yields

$$[-\tfrac{1}{2}(1 + f_1)i_{210} + \tfrac{1}{2}(1 + f_2)i_{220}]\,\frac{d^2\eta_c}{d\tau^2}$$

$$+ [-\tfrac{1}{2}(f_1 + f_2)]\,\frac{d\eta_c}{d\tau} + [\,\{C_1 + C_2 + \varepsilon c_f\,(-\frac{1}{2\Lambda})(\tfrac{1}{2} + \lambda_1)]\,\eta_c$$

$$+ [\tfrac{1}{6} + \tfrac{1}{4}(1 + f_1)\,i_{210} + \tfrac{1}{4}(1 + f_2)\,i_{220}]\,\frac{d^2\phi}{d\tau^2}$$

$$+ [\tfrac{1}{24}\varepsilon c_f + \tfrac{1}{4}(f_1 - f_2)]\,\frac{d\phi}{d\tau} \tag{57b}$$

$$+ \;[-\tfrac{1}{2}(f_1 + f_2) + \frac{1}{2\Lambda}\,(\lambda_1 + \tfrac{1}{2} + \Lambda)(\lambda_1 + \tfrac{1}{2})(C_1 + C_2 + \varepsilon c_f)]\,\phi = 0\,,$$

where we have set c = 0.

7. DYNAMICS OF FLEXIBLE, TOWED CYLINDERS

Before proceeding with the analysis, it is desirable to express the problem in dimensionless terms and accordingly we put

$$\xi = x/L \,, \quad \eta = y/L \,, \quad \tau' = \left(\frac{EI}{m+M}\right)^{\frac{1}{2}} \frac{t}{L^2} \,, \tag{58}$$

$$\beta = \frac{M}{m+M} \,,$$

comparing these relations with equation (1), we find τ' to be modified as

$$\tau' = \left\{\frac{EI}{m+M}\right\}^{\frac{1}{2}} \frac{t}{L^2} = \left\{\frac{EI}{m+M}\right\}^{\frac{1}{2}} \frac{\tau}{UL}$$

$$= \beta^{\frac{1}{2}} \frac{\tau}{u} \,, \tag{59}$$

$$\text{where } u = \left(\frac{M}{EI}\right)^{\frac{1}{2}} UL \,. \tag{60}$$

The reason for using τ' in preference to τ is that with this definition the dimensionless frequencies of the flexural modes then become identical to those of a free-free beam at zero towing speed.

Now substituting equations (59) and (60) into (42), and dropping the prime on τ, for simplicity, we obtain

$$\nu \frac{\partial^5 \eta}{\partial\tau\partial\xi^4} + \frac{\partial^4 \eta}{\partial\xi^4} + u^2 \left[1 - \frac{1}{2}\varepsilon c_f\left(\frac{1}{2} + i_{120} - \xi\right) + 2i_{720} + \frac{S_{Base}}{S} C_{DB}\right]\frac{\partial^2\eta}{\partial\xi^2}$$

$$+ [2\beta^{1/2} u] \frac{\partial^2\eta}{\partial\tau\partial\xi} + \frac{1}{2} u^2 \varepsilon [c_f + c_o] \frac{\partial\eta}{\partial\xi}$$

$$+ \frac{\partial^2\eta}{\partial\tau^2} + \frac{1}{2}\beta^{1/2} u \varepsilon c_f \frac{\partial\eta}{\partial\tau} = 0 . \qquad (61)$$

Similarly, the boundary conditions can be expressed dimensionlessly by substituting equations (59) and (60) into (43), (44), (45) and (46), yielding

$$\nu \frac{\partial^4 \eta}{\partial\tau\partial\xi^3} + \frac{\partial^3\eta}{\partial\xi^3} - \beta i_{510} \frac{\partial^3\eta}{\partial\tau^2\partial\xi} + \beta^{\frac{1}{2}} u \left[-i_{310} + i_{610}\right] \frac{\partial^2\eta}{\partial\tau\partial\xi}$$

$$+ \frac{u^2}{2}\left[\varepsilon i_{110} (c_f + c_o) + 2 i_{410} - \left(\frac{\lambda_{1+\Lambda}}{\Lambda}\right) \{\varepsilon c_f (1 + i_{110} + i_{120})\right.$$

$$\left. + 2(i_{710} + i_{720}) + \frac{S_{Base}}{S} C_{DB}\}\right] \frac{\partial\eta}{\partial\xi}$$

$$+ \frac{u^2}{2\Lambda}\left[\varepsilon c_f (1 + i_{110} + i_{120}) + 2(i_{710} + i_{720}) + \frac{S_{Base}}{S} C_{DB}\right]\eta \qquad (62)$$

$$+ \beta[i_{210} - i_{310}] \frac{\partial^2\eta}{\partial\tau^2} + u\beta^{1/2} \left(\frac{1}{2}\varepsilon c_f\, i_{110} + i_{410}\right)\frac{\partial\eta}{\partial\tau} = 0 ,$$

$$\text{at } \xi = -\frac{1}{2}$$

and

$$\nu \frac{\partial^3 \eta}{\partial \tau \partial \xi^2} + \frac{\partial^2 \eta}{\partial \xi^2} - \frac{\lambda_1(\lambda_1+\Lambda)}{2\Lambda} u^2 [\epsilon c_f(1 + i_{110} + i_{120}) + 2(i_{710} + i_{720}) + \frac{S_{Base}}{S} C_{DB}] \frac{\partial \eta}{\partial \xi}$$

$$+ \frac{\lambda_1}{2\Lambda} u^2 [\epsilon c_f (1 + i_{110} + i_{120}) + 2(i_{710} + i_{720}) + \frac{S_{Base}}{S} C_{DB}] \eta = 0, \text{ at } \xi = -\frac{1}{2} \tag{63}$$

and

$$\nu \frac{\partial^4 \eta}{\partial \tau \partial \xi^3} + \frac{\partial^3 \eta}{\partial \xi^3} - \beta i_{520} \frac{\partial^3 \eta}{\partial \tau^2 \partial \xi} + \beta^{\frac{1}{2}} u [-i_{320} + i_{620}] \frac{\partial^2 \eta}{\partial \tau \partial \xi}$$

$$+ \frac{u^2}{2} [-\epsilon i_{120} (c_f + c_o) + 2 i_{420}] \frac{\partial \eta}{\partial \xi} - \beta [i_{220} + i_{320}] \frac{\partial^2 \eta}{\partial \tau^2} \tag{64}$$

$$+ u\beta^{\frac{1}{2}} [-\frac{1}{2} \epsilon c_f i_{120} + i_{420}] \frac{\partial \eta}{\partial \tau} = 0 , \quad \text{at } \xi = \frac{1}{2}$$

and

$$\nu \frac{\partial^3 \eta}{\partial \tau \partial \xi^2} + \frac{\partial^2 \eta}{\partial \xi^2} = 0 . \quad \text{at } \xi = \frac{1}{2} \tag{65}$$

Similarly, the equation of motion of the modified old theory of Reference [24] can be expressed as follows:

$$\nu \frac{\partial^5 \eta}{\partial \tau \partial \xi^4} + \frac{\partial^4 \eta}{\partial \xi^4} + u^2 [1 - \frac{1}{2}\{\epsilon c_f (\frac{1}{2} - \xi) + \frac{S_{Base}}{S} C_2\}] \frac{\partial^2 \eta}{\partial \xi^2}$$

$$+ [2 \beta^{\frac{1}{2}} u] \frac{\partial^2 \eta}{\partial \tau \partial \xi} + \frac{1}{2} u^2 \epsilon c_f \frac{\partial \eta}{\partial \xi} + \frac{\partial^2 \eta}{\partial \tau^2} + \frac{1}{2} \beta^{\frac{1}{2}} u \epsilon c_f \frac{\partial \eta}{\partial \tau} = 0 . \tag{61a}$$

The boundary conditions are given by

$$\nu \frac{\partial^4\eta}{\partial\tau\partial\xi^3} + \frac{\partial^3\eta}{\partial\xi^3} + u^2 [f_1 - \frac{(\lambda_1+\Lambda)}{2\Lambda} (C_1 + C_2 + \varepsilon c_f)] \frac{\partial\eta}{\partial\xi}$$

$$+ \frac{u^2}{2\Lambda} [C_1 + C_2 + \varepsilon c_f] \eta \qquad (62a)$$

$$+ \beta i_{210} [1 + f_1] \frac{\partial^2\eta}{\partial\tau^2} + u\beta^{\frac{1}{2}} f_1 \frac{\partial\eta}{\partial\tau} = 0 , \qquad \text{at } \xi = -\tfrac{1}{2}$$

$$\nu \frac{\partial^3\eta}{\partial\tau\partial\xi^2} + \frac{\partial^2\eta}{\partial\xi^2} - \frac{\lambda_1(\lambda_1+\Lambda)}{2\Lambda} u^2 [C_1 + C_2 + \varepsilon c_f] \frac{\partial\eta}{\partial\xi} \qquad (63a)$$

$$+ \frac{\lambda_1 u^2}{2\Lambda} [C_1 + C_2 + \varepsilon c_f] \eta = 0 , \qquad \text{at } \xi = -\tfrac{1}{2}$$

and

$$\nu \frac{\partial^4\eta}{\partial\tau\partial\xi^3} + \frac{\partial^3\eta}{\partial\xi^3} + f_2 u^2 \frac{\partial\eta}{\partial\xi} - \beta[1 + f_2] i_{220} \frac{\partial^2\eta}{\partial\tau^2} \qquad (64a)$$

$$+ f_2 \beta u \frac{\partial\eta}{\partial\tau} = 0 \qquad \text{at } \xi = \tfrac{1}{2}$$

$$\nu \frac{\partial^3\eta}{\partial\tau\partial\xi^2} + \frac{\partial^2\eta}{\partial\xi^2} = 0 . \qquad \text{at } \xi = \tfrac{1}{2} \qquad (65a)$$

7.1 Method of Analysis

Let us consider motions of the cylinder of the form

$$\eta = Y(\xi)e^{i\omega\tau} , \qquad (66)$$

where ω is a dimensionless frequency defined by

$\omega = [(m+M)/EI]^{1/2} \, \Omega L^2$, in which Ω is the circular frequency of motion. In general Ω will be complex and the system will be stable or unstable accordingly as the imaginary part of ω is positive or negative; in the case of neutral stability $Im(\omega) = 0$.

The system under consideration has an infinite number of degrees of freedom. The complete solution of the dynamical problem therefore involves the determination of the infinite set of frequencies of the normal modes of oscillation of the system, as continuous functions of the dimensionless velocity u and the system parameters i_{110}, i_{120}, . . . , i_{720}, λ_1, λ_2, f_1, f_2, α, β, . . . , ε, c, c_f, etc.

Applying Equation (66) to the new theory we obtain the main equation and four boundary conditions which are written conveniently in the form

$$g_o \frac{d^4Y}{d\xi^4} + g_1 \frac{d^2Y}{d\xi^2} + g_2 \xi \frac{d^2Y}{d\xi^2} + g_3 \frac{dY}{d\xi} + g_4 Y = 0 , \tag{67}$$

and at $\xi = -\frac{1}{2}$

$$g_o \frac{d^3Y}{d\xi^3} + g_5 \frac{dY}{d\xi} + g_6 Y = 0 , \tag{68}$$

$$g_o \frac{d^2Y}{d\xi^2} + g_7 \frac{dY}{d\xi} + g_8 Y = 0 , \tag{69}$$

and at $\xi = \frac{1}{2}$

$$g_o \frac{d^2Y}{d\xi^2} + g_9 \frac{dY}{d\xi} + g_{10}Y = 0 \tag{70}$$

$$g_o \frac{d^2Y}{d\xi^2} = 0 \quad . \tag{71}$$

Similar equations can be obtained by substituting equation (66) into the modified old theory of Reference [24],

$$h_o \frac{d^4Y}{d\xi^4} + h_1 \frac{d^2Y}{d\xi^2} + h_2\xi \frac{d^2Y}{d\xi^2} + h_3 \frac{dY}{d\xi} + h_4Y = 0, \tag{67a}$$

The boundary conditions at $\xi = -\frac{1}{2}$

$$h_o \frac{d^3Y}{d\xi^3} + h_5 \frac{dY}{d\xi} + h_6Y = 0, \tag{68a}$$

$$h_o \frac{d^2Y}{d\xi^3} + h_7 \frac{dY}{d\xi} + h_8Y = 0, \tag{69a}$$

and at $\xi = \frac{1}{2}$

$$h_o \frac{h^3Y}{d\xi^3} + h_9 \frac{dY}{d\xi} + h_{10}Y = 0, \tag{70a}$$

$$h_o \frac{d^2Y}{d\xi^2} = 0, \tag{71a}$$

where the coefficients g_i and h_i are given in Appendix C and D respectively.

Let us try the solution

$$Y(\xi) = \Sigma_{r=0}^{\infty} A_r (\xi + \tfrac{1}{2})^r , \tag{72}$$

where A_r are generally complex quantities to be determined. It is assumed that the motion of the cylinder may be described adequately by a sufficient number of terms in power series to approximate the shape of the body.

Substituting equation (72) into (68), (69), (70) and (71)

$$g_6 A_o + g_5 A_1 + 6 g_o A_3 = 0$$

$$g_8 A_o + g_7 A_1 + 2 g_o A_2 = 0$$

$$2A_2 + 6A_3 + \Sigma_{r=4}^{\infty} [r(r-1)] A_r = 0$$

$$g_{10} A_o + (g_9 + g_{10}) A_1 + (2g_9 + g_{10}) A_2 + (6g_o + 3g_9 + g_{10}) A_3$$

$$+ \Sigma_{r=4}^{\infty} [g_o r(r-1)(r-2) + r g_9 + g_{10}] A_r = 0 \tag{73}$$

and substituting equation (72) into (67) and collecting terms, we obtain

$$24 g_o A_4 + 2 g_1 A_2 + g_3 A_1 + g_4 A_o = 0$$

$$120g_oA_5 + 6g_1A_3 + 2(g_2+g_3)A_2 + g_4A_1 = 0$$

$$360g_oA_6 + 12g_1A_4 + (6g_2 + 3g_3)A_3 + g_4A_2 = 0 \qquad (74)$$

$$n(n-1)(n-2)(n-3)g_oA_n + (g_1-\frac{g_2}{2})(n-2)(n-3)A_{n-2}$$

$$+ (n-3)\,[\,g_2(n-4) + g_3\,]\,A_{n-3} + g_4A_{n-4} = 0\,.$$

From the first three equations in (74), it is evident that all the A_r may be expressed as linear combinations of A_o, A_1, A_2 and A_3 alone. Consequently equation (73) can be expressed as a 4 x 4 determinant which must vanish for non-trivial solution. Hence this provides an implicit relation between ω on the one hand, and u and the system parameters on the other.

The modified old theory may be analyzed in much the same manner.

In general, ω will be complex. Clearly, we have an infinite set of frequencies, ω_i, as the system has an infinite number of degrees of freedom. If the imaginary components of the frequencies, $Im(\omega_i)$, are all positive, then the system will be stable. If on the other hand, for the jth mode we have $Im(\omega_j) < 0$, then the system will be unstable in that mode; now if the corresponding real component of the frequency, $Re(\omega_j)$, is zero this will represent a divergent motion without oscillations, which we shall call yawing; $\mathrm{Re}(\omega_j) \neq 0$, then the instability will be oscillatory.

The calculation procedure is as follows:

(a) a set of values of λ_1, ϵ, α, β, f_1, f_2, c_1, c_2 and Λ are selected;

(b) the complex frequencies of the lowest five modes of the system are traced as functions of u, starting with u = 0 and increasing the flow velocity in small steps. The results demonstrate the general character of the dynamical behaviour of the system for varying u, illustrating some of the modes of instability to which it may be subjected.

7.2 Theoretical Results

7.2.1 The Modified Old Theory

Typical results of the modified old theory are displayed as an Argand diagram in Figure 6, obtained by using equations (61a) to (65a). In this case we only consider the second mode to compare the modified old theory with the present theory. Figure 6 shows the loci of the so-called second mode of the system of the present theory and that of the modified old theory as functions of towing speed. The frequency of this mode at zero towing speed corresponds to the second-mode frequency of the flexible body treated as a free-free beam; accordingly, this is flexural in character.

The form drag coefficient at the tail for this theory, c_2', is arbitrarily taken to have a numerical value

$$c_2' = (1 - f_2)/2 ,$$

on the reasonable assumption that, as the tail becomes blunter, f_2 is reduced and the form drag coefficient increases.

We see that the coefficient f_2 can be found approximately, on comparing g_9 of Equation (70) with h_9 of Equation (70a); on the other hand, f_1 is determined from other coefficients. A systematic comparison was made between the old theory and the present one to determine the values of f_1 and f_2 in a rational manner, at least for ellipsoidal ends. This was done by comparing equivalent terms in the boundary conditions. In some cases the comparison was made by equating the magnitude of the whole coefficients of u^2 in g_5 and g_9 with those of h_5 and h_9; in such cases the results clearly depend on the particular values of some parameters, e.g., Λ. In other cases the coefficients of u^2 in the terms g_5 and g_9, i.e., f_1 or f_2, were compared with the corresponding dominant coefficients in h_5

and h_9 in the old theory which depend only on shape, i.e., i_{410} or i_{420}. The results are shown in Figure 7, where λ_1 (or λ_2, as the case may be) are compared with f_1 and f_2.

Returning now to the discussion of Figure 6, it is noted that small flow velocities act to damp free oscillations of the system. As the flow velocity increases, however, the system becomes unstable. We observe that for $8.7 < u < 10.7$, the system of the present theory loses stability. On the other hand, the system analysed by the modified old theory is unstable in the range $8 < u < 10.8$ for $f_1 = 0.56$ and $8.6 < u < 10.6$ for $f_1 = 0.62$.

It is seen that the behaviour of the system in this mode is very sensitive to the values of f_1 and, of course, to the values of α. Other similar second modes corresponding to systems with $\alpha = 0.9$ and various f_1 and $f_2 = 0.57$, are shown in Figure 6b. Comparing the present theory with the old one in this case, it is observed that the systems lose stability for $u \approx 5.9$ and $u \approx 5.8$, respectively. Another notable feature of this system is that the second mode goes back to the stable region after it first crosses over to the unstable one.

In short, these particular diagrams lead to the following conclusions:

a) the parameters f_1 and f_2, which are less than unity, may be approximately estimated by comparing the coefficients g's and h's numerically,

b) for optimal stability, the tail should be blunt (f_2 small, c_2 large).

7.2.2 The Present Theory

Figures 8 to 15 illustrate the results obtained by the present theory, using the equations (61) to (65).

Figures 8 and 9 show the dynamical behaviour, with increasing towing speed, of the zeroth, first, second, third and fourth modes of a system with well streamlined nose and tail.

The nose and tail sections consist of originally identical half ellipsoids whose diameter is a minor axis. The nose section is always streamlined. On the other hand, the tail section becomes blunt by cutting it at the end; α is the ratio of the cut length to the original length. Therefore, as α decreases the tail becomes blunter. Hence, α is equivalent to f_2 in the modified old theory. It is also noted here that Λ is taken as the ratio of tow rope length/length of the main body.

The 'zeroth' and 'first' mode (Figure 8) correspond to essentially rigid-body motions, at least for very low values of u. At $u = 0$, the frequency $\omega = 0$ corresponds to rigid-body rotation about the point where the tow-rope is attached to the towing vessel; for $u > 0$, however, evidently two distinct modes emanate from this point, one oscillatory and the other non-oscillatory. The zeroth mode generally remains on the $[\mathrm{Im}(\omega)]$-axis and the instability associated with this mode will be called 'yawing'. At low flow the system is evidently stable in the zeroth, first, second, third and fourth modes. The loci of the zeroth mode initially recede from the origin but eventually double back, and the negative branch eventually crosses the origin. It is seen that the zeroth mode of the system with $\Lambda = 1$ leads to stability for $u \approx 3.38$. At higher u the loci reunite and leave the $\mathrm{Im}(\omega)$-axis and then again rejoin it, bifurcating at $u \approx 6.625$.

The first mode with $\Lambda = 1$ is unstable, in the range $4.15 < u < 6.81$. Similarly, the system loses stability in its second, third and fourth mode at respectively higher towing speeds.

Further calculations were conducted for the same system as above, but with other values of α and Λ, to show the effect on stability, as shown in Figures 8 and 9 (dashed lines). It is found that the zeroth and first modes are stabilized with decreasing α. The ranges of instability of the first mode, for various values of Λ are found to be as follows: $4.30 < u < 6.95$ for $\Lambda = 0.5$; $4.15 < u < 6.81$ for $\Lambda = 1$; $4.28 < u < 6.20$ for $\Lambda = 5$; $4.38 < u < 6.05$ for $\Lambda = 10$ (Cf. Figures 10 and 11). Thus, the effect of Λ is not uniform insofar as stability in this mode is concerned. On the other hand, the other modes are stabilized uniformly with decreasing α and increasing Λ, as shown numerically in Table 1 (Cf. Figure 12).

Λ's / Modes	0.5	1.0	5.0	10.0
	Values of u_c			
Zeroth	3.328 7.950	3.381 7.935	3.343	3.378
First	4.298 6.951	4.150 6.806	4.276 6.206 7.935	4.381 6.045 7.935
Second	3.776	4.592	5.562	5.674
Third	6.299	7.102	7.799	7.897
Fourth	8.793	9.608	10.305	10.400

TABLE I. Critical velocities of a flexible cylinder with various Λ's. Other parameters: $\alpha=1$, $\beta=0.5$, $\varepsilon c_o=0$, $\varepsilon c_f=1$, $\lambda_1=0.015$.

Figure 13 shows the effect of the tow-rope length on the frequency associated with neutral stability for a system with $\varepsilon c_f = 1$, $\alpha = 1$, and $\lambda_1 = 0.015$. Here λ_1, which is the value of ℓ_1/L, is taken based on modified old theory. Païdoussis [24] set $\chi_1 = \chi_2 = 0.01$, which correspond to i_{210} and i_{220} respectively for a cylinder with streamlined nose and tail sections. From Appendix B, we get $i_{210} = 2\lambda_1/3 = 0.01$. Finally we have $\lambda_1 = 0.015$. It is also seen that ω_c becomes larger for higher modes, with decreasing Λ.

Figure 14 shows the effect of the tow-rope length on a system with $\varepsilon c_f = 1$, $\lambda_1 = 0.015$ and perfectly streamlined nose and tail sections. The upper regions marked 'first-mode oscillatory instability' corresponds to the second unstable loop of the first mode. We see that reducing the tow-rope length does not enlarge the stable region, contrary to Païdoussis' [24] results. For $\Lambda = 0.5$, for instance, there appears to be a region of yawing $0 < u < 3.3$; the system is stable for $3.3 < u < 3.8$, approximately, $u \approx 3.8$ being the threshold of second-mode oscillatory instability. It is seen that for $\Lambda < 0.7$, the stable region is reduced; for $\Lambda > 0.7$, this region is independent of Λ.

Figure 15a shows the effect on stability of the shape of the tail of a cylinder with $\varepsilon c_f = 1$, $\lambda_1 = 0.015$ and $\Lambda = 1$, and a perfectly streamlined nose. We see that the range of u over which the system is stable is enlarged as the tail becomes blunter. For $\alpha < 0.5$ approximately, the system is stable over the whole range of flow velocities in all modes. It is also noted that the system is always stable for $3.6 < u < 4.2$.

Another attempt was made to check the stability for a higher value of λ_1, i.e., for more elongated end sections. The effect on stability of the shape of the tail of a cylinder with $\varepsilon c_f = 1$, $\lambda_1 = 0.05$ and Λ with a streamlined nose is shown in Figure 15b. As was expected, the region of stability is enlarged tremendously, comparing with Figure 15a, presumably because the stabilizing effect of streamlining the nose section overcomes the destabilizing effect of streamlining the tail. It is noted that the threshold of the second mode oscillatory instability appears over the range of $u = 12$. It is seen that the system is always stable for $\alpha < 0.57$. Thus we have concluded the system becomes more stable by making both nose and tail more elongated.

Finally, the following general conclusions may be drawn:

a) the tail should be blunt (α small) for optimal stability,

b) a system that is unstable by yawing, within a range of towing speeds, can be stablized by blunting the tail, but not by manipulating the length of the tow-rope,

c) in some cases, it is possible to stabilize a system which is unstable at low towing speeds, by towing it faster, within a specified range of towing speeds,

d) Tow-rope length does not enlarge the stable towing speed range if $\lambda > 0.7$.

8. DYNAMICS OF RIGID, TOWED CYLINDERS

8.1 Method of Analysis

Let us consider motions of the cylinder of the form

$$\eta = He^{i\omega\tau} \quad \text{and} \quad \phi = \Phi e^{i\omega\tau}$$

where ω is a dimensionless frequency defined as $\omega = \Omega/U$, Ω being the complex circular frequency of oscillation.

Substituting η and ϕ into the Equation (56) we obtain

$$
\begin{aligned}
&[\{2+i_{210}+i_{220}-i_{310}+i_{320}\}(-\omega^2) + \{\tfrac{1}{2}\epsilon c_f(1+i_{110}+i_{120}) \\
&\qquad + i_{410} - i_{420}\}(i\omega) \\
&+ \frac{1}{2\Lambda}\{\epsilon c_f(1+i_{110}+i_{120}) + 2(i_{710}+i_{720}) + \frac{S_{Base}}{S} C_{DB}\}]\, H \\
&+ [\{\tfrac{1}{2}(-i_{210}+i_{220}+i_{310}+i_{320}) - i_{510}+i_{520}\}(-\omega^2) \qquad (75) \\
&+ \{2-i_{310}+i_{320}+i_{610}-i_{620} - \tfrac{1}{2}(i_{410}+i_{420}) + \tfrac{1}{4}\epsilon c_f(i_{110}+i_{120})\}(i\omega) \\
&\qquad + \tfrac{1}{2}\epsilon c_f(1+i_{110}+i_{120}) + i_{410}-i_{420} \\
&- \frac{1}{2\Lambda}(\epsilon c_f(1+i_{110}+i_{120}) + 2(i_{710}+i_{720}) + \frac{S_{Base}}{S} C_{DB})(\tfrac{1}{2}+\lambda_1+\Lambda)]\, \Phi = 0 \,,
\end{aligned}
$$

and

$$[\{\frac{1}{2}(-i_{210}+i_{220}+i_{310}+i_{320})\}(-\omega^2) + \{\frac{1}{2}(-i_{410}-i_{420}) + \frac{1}{4}\varepsilon c_f(-i_{110}+i_{120})\}(i\omega)$$

$$+ \frac{1}{2\Lambda}\{\varepsilon c_f(1+i_{110}+i_{120}) + 2(i_{710}+i_{720}) + \frac{S_{Base}}{S}C_{DB}\}(-\frac{1}{2}-\lambda_1)]\ H$$

$$+ \{\{\frac{1}{6}+\frac{1}{4}(i_{210}+i_{220}-i_{310}+i_{320}) + \frac{1}{2}(i_{510}+i_{520})\}\ (-\omega^2)$$

$$+ \{\frac{1}{2}(i_{310}+i_{320}-i_{610}-i_{620}) + \frac{1}{4}(i_{410}-i_{420}) + \frac{1}{8}\varepsilon c_f(\frac{1}{3}+i_{110}+i_{120}\}\ (i\omega)$$

$$+ \{\frac{1}{4}\varepsilon c_f(i_{110}+i_{120}) - \frac{1}{2}(i_{410}+i_{420})$$

$$+ \frac{1}{2\Lambda}(\varepsilon c_f(1+i_{110}+i_{120}) + 2(i_{710}+i_{720}) + \frac{S_{Base}}{S}C_{DB})\ \times$$

$$\times\quad (\frac{1}{2}+\lambda_1)(\frac{1}{2}+\lambda_1+\Lambda)\}]\ \Phi = 0\ ,$$

where we have set $c = 0$.

Similar equations are obtained when using the modified old theory, i.e., Equation (57), namely

$$[\{2 + (1+f_1)i_{210} + (1+f_2)i_{220}\}(-\omega^2) + \{\frac{1}{2}\varepsilon c_f + f_1 - f_2\}\ (i\omega)$$

$$+ \frac{1}{2\Lambda}\{c_1+c_2+\varepsilon c_f\}]\ H \tag{75a}$$

$$+ [-\frac{1}{2}\{(1+f_1)i_{210} - (1+f_2)i_{220}\}(-\omega^2) + \{2 - \frac{1}{2}(f_1+f_2)\}\quad (i\omega)$$

$$+ \{\frac{1}{2}\varepsilon c_f(1 + (c_1+c_2+\varepsilon c_f)(\frac{\lambda_1+\frac{1}{2}+\Lambda}{\Lambda})) + f_1 - f_2\}] \Phi = 0 ,$$

and

$$[\frac{1}{2}\{-(1+f_1)i_{210} + (1+f_2)i_{220}\} (-\omega^2) + \{-\frac{1}{2}(f_1+f_2)\} (i\omega)$$

$$+ \{-\frac{1}{2\Lambda} (\frac{1}{2}+\lambda_1)(c_1+c_2+\varepsilon c_f)\}] H$$

$$+ [\{ \frac{1}{6} + \frac{1}{4}(1+f_1)i_{210} + \frac{1}{4}(1+f_2)i_{220}\} (-\omega^2) + \{\frac{1}{24}\varepsilon c_f + \frac{1}{4}(f_1-f_2)\} (i\omega)$$

$$+ \{-\frac{1}{2}(f_1+f_2) + \frac{1}{2\Lambda}(\lambda_1+\frac{1}{2}+\Lambda)(\lambda_1+\frac{1}{2})(c_1+c_2+\varepsilon c_f)\}] \Phi = 0 . \tag{76a}$$

For nontrivial solutions, the determinant of the coefficients of H and Φ in Equations (75) and (76), or in (75a) and (76a), must vanish, yielding a quartic in ω

$$\omega^4 + A\omega^3 + B\omega^2 + C\omega + E = 0 , \tag{77}$$

where A, B, C, and E are complex.

8.2 Theoretical Results

8.2.1 The Modified Old Theory

Calculations were conducted to compare the dynamical behaviour of the rigid body to that of a flexible body; as the rigid body may be regarded as a flexible one of very large flexural rigidity, it would be reasonable to expect correspondence of the dynamical behaviour of the rigid body to the 'rigid-body' modes of the flexural one, i.e., the zeroth and first modes. Recalling that the dimensionless flow velocity in the case of a flexural body was defined as $u = (M/EI)^{1/2}UL$, the dynamical behaviour of the rigid body should approach that of the flexible one as $u \to 0$. So the system is independent of flow velocity u.

We define the dimensionless complex frequency of the rigid body $\omega_r = \Omega L/U$ in 8.1. On the other hand, the dimensionless complex frequency of the flexible body is defined as $\omega_f = [(M+m)/EI]^{1/2}\Omega L^2$, which may be rewritten as $\omega_f = [(M+m)/M]^{1/2}u\Omega L/U$, where u is dimensionless flow velocity. Since m = M, we have $\omega_f = \sqrt{2}u\Omega L/U$. Now if the dimensionless frequency, Ω, of the rigid body and of the flexible body are identical, we may rewrite this as $\omega_f = \sqrt{2}u\omega_r$, and we can see that identity of dimensionless frequency will occur when $u = \frac{1}{\sqrt{2}}$.

8.2.2 <u>The Present Theory</u>

Making use of Equation (77), the four rigid body frequencies are computed for various Λ's. It is found that, in the case also, the dynamical behaviour of the rigid body corresponds to that of the zeroth and first modes of the flexible one at low towing speeds- quantitative correspondence of frequencies occurring at $u = 1/\sqrt{2}$ (See Table 2).

	Rigid Body			Flexible body $(u=1/\sqrt{2})$		
Λ's \ ω's	ω_1	ω_2	ω_3	ω_1	ω_2	ω_3
0.5	-0.412i	0.822i	1.899+0.050i	-0.401i	0.818i	1.873+0.055i
1	-0.422i	0.641i	1.496+0.145i	-0.410i	0.640i	1.479+0.146i
5	-0.455i	0.202i	1.089+0.381i	-0.441i	0.203i	1.075+0.377i
10	-0.466i	0.102i	1.046+0.437i	-0.453i	0.102i	1.033+0.432i

TABLE 2. Rigid body and flexible-body frequencies compared. Other parameters: $\alpha = 1$, $\beta = 0.5$, $\varepsilon c = 0$, $\varepsilon c_f = 1$, $\lambda_1 = 0.015$.

From the results shown in Figures 8, 10 and 11, we have the four frequencies for the flexible body; two are associated with the zeroth mode, and the other two with the first mode for $u = 1/\sqrt{2}$. Table 2 shows that agreement in behaviour of the rigid body and the flexible body is good. It is observed that oscillatory instability never occurs, because the system is always stable in the first modes in range $0 \leqslant u \leqslant 1/\sqrt{2}$; the system is only subject to yawing instability for various Λ's.

Based on such complex-frequency calculations it is possible to construct stability diagrams illustrating the effect of various parameters on the system. An example is given in Figure 16 showing the effect of α and Λ on stability of a rigid cylinder. One noteworthy aspect of the analysis is that the existence of yawing instability is not affected by Λ, i.e., by altering the tow-rope length. In the case of the rigid body this becomes obvious upon considering Equation (77). Since the threshold for yawing instability implies $\omega = 0$, this threshold is established by the equation $E_0 = 0$.

It is shown that yawing instability is affected by various ε. The stable region becomes large as slenderness of cylinder increases.

The last criterion for stability is studied by elongating the nose section. Here we see that elongated streamlined nose has stabilized the system markedly. Accordingly, for optimum stability the nose shall be made as streamlined as possible.

9. CONCLUSIONS

The analysis presented in this thesis is appropriately characterized as an attempt to extend the theoretical studies of Hawthorne [9] and Païdoussis [24], concerned with the small, lateral motions of slender bodies towed through incompressible fluid.

Hydrodynamic forces arising near the nose and tail sections of the body had been inadequately accounted for in the previous treatments. Accordingly, an extensive survey of the pertinent literature has been untertaken, out of which has grown a reformulation of the inviscid-flow forces acting near the ends of the body. The other difference is associated with tow-rope force which is incorporated more correctly here. It is found that these modifications predict the system to be more stable in all its modes than does the previous work. Specially we should note that the first mode is stable at low towing speeds, which is contrary to Païdoussis' [24] previous findings.

A substantive analysis has been conducted to treat the forces on the non-cylindrical end sections, making use of Upson & Klikoff's [33] work. An ellipsoid whose minor axis is equal to the maximum diameter of the main body is divided into axisymmetric slices and fitted to nose and tail sections respectively. The nose section is always streamlined; on the other hand, the tail is manipulated to be blunt.

An attempt has been made to find the coefficients f_1 and f_2, which were used in Paidoussis [24] to express the hydrodynamic forces at nose and tail sections, respectively. First we have modified the coordinate systems and tow rope force of previous paper. For a given condition, comparing the boundary conditions of the present theory with those of modified [24], these processes have led to inter-relate the two theories. It is seen that coefficients f_1 and f_2 of the modified old theory agree well with i_{410} and i_{420} respectively for comparatively small values of λ_1 (or λ_2).

It is observed that the system of the flexible body is subject to rigid-body-type instabilities at low towing speeds, and to flexural instabilities at higher towing speeds. The rigid body instabilities, occurring in the so-called zeroth and first mode of the flexible body are shown to correspond to the instabilities of a rigid body of the same shape and gravimetric properties. Indeed, the study of the dynamics of towed flexible body yields sufficient information to establish the dynamical behaviour of the corresponding rigid body. It is also reviewed that, whereas the dynamical behaviour in the case of rigid body is independent of towing speed, in the case of flexible body the dynamic stability of the system is highly dependent on towing speed.

We first consider briefly the instabilities of rigid body. The behaviour of rigid body motion is equivalent to that of flexible body at low towing speed. It is observed that oscillatory instabilities do not occur. At the beginning (low towing speeds) the first mode is stable; this is caused by the modification in the formulation of the tow-rope in this theory. The yawing instabilities, which are associated with the zeroth mode, are diminished by manipulating some parameters, specially by making the tail section blunt. Strandhagen et al [8] proposed that a dynamically unstable ship may become directionally stable when towed with a short enough towline. But it is noted that yawing instabilities are independent of tow-rope length in this study. We have found that this agrees well with Païdoussis [14] in terms of tow-rope length effect. He had shown that the instabilities (yawing) are independent of tow-rope length. It is concluded that according to the present theory, where the tow-rope force was introduced in a more refined way, the system is generally more stable - and that stability is not affected by tow-rope length.

We next consider the flexural instabilities. As we have seen, the cylinder may be stable as a rigid body, yet for sufficiently high towing speeds it may be unstable in one of its flexural modes. Several attempts have been undertaken to check the stability. It is possible to make a number of recommendations regarding optimum stability of the system. The two main ones are the following: (a) the tail should be as blunt as possible, and (b) the tow-rope length does not enlarge the stability region. The former is the most effective way of stabilizing a towed system, which has the disadvantage of increasing the towing drag. Clearly, what is needed is a blunt tail without separated flow. The latter is contrary to Paidoussis'[24] work. He had proposed the tow-rope should be as short as possible for stability.

From Figure 15a (λ_1=0.015) it is seen that the system is unconditionally stable when α=0.5, while from Figure 15b (λ_1=0.05) it is seen that the same condition applies when α=0.57. Since the tail base area in the latter case is smaller, and hence the base drag is smaller, it is clearly preferable to use the more streamlined end (λ_1=0.05); besides being more stable, generally, it would require a small amount of power for towing. The experiments [22] do not show any advantage in making the nose particularly well streamlined. In practice, of course, the desire to minimize drag would dictate a well streamlined nose in any case.

In terms of application of this work, it has been shown that, provided that the tail is blunt, a system may be designed which would be stable to high towing speeds.

REFERENCES

1. KRELL, O., 1929 'Contribution to the Technique of Landing Large Airships', N.A.C.A. TM 512 and 513.

2. CROCCO, G.A., 1924 'Mooring Airships', N.A.C.A. TM 283.

3. FRAZER, R.A., Feb. 1921 'Note on the mooring of Airships by Free Wire Systems', J. Royal Aero. Soc.

4. BAIRSTOW, L., RELF, E.F., JONES, R., 1915 'The Stability of Kite-Balloons: Mathematical Investigation', A.R.C.R. and M208.

5. MUNK, M.M., 1924 'The Aerodynamic Forces on Airship Hulls', N.A.C.A. Report No. 184.

6. GLAUERT, H., 1930 'The Stability of a Body Towed by a Light Wire', A.R.C.R. and M 1312.

7. BRYANT, L.W., BROWN, W.S., SWEETING, N.E., 1942 'Collected Research on Stability of Kites and Towed Gliders', A.R.C.R. and M 2303.

8. STRANDHAGEN, A.G., SCHOENHERR, K.E., KOBAYASHI, F.M., 1950 'The Dynamic Stability Course of Towed Ships', Trans. Soc. Naval Arch. and Marine Eng., 58 pp. 32-66.

9. HAWTHORNE, W.R., 1961 'The Early Development of the Dracone Flexible Barge', Proc. Inst. Mech. Engrs., 175, pp. 52-83.

10. JEFFREY, N.E., 1968 'Influence of Design Features on Underwater Towed System Stability', J. Hydronautics, 2, pp. 205-213.

11. SCHRAM, J.W., REYLE, S.P., 1968 'A Three-Dimensional Dynamic Analysis of Towed Systems', J. Hydronautics, 2, pp. 213-220.

12. EAMES, M.C. 1968 'Steady-State Theory of Towing Cables', Quart. Trans. Royal-Inst. Naval Arch., 10, pp. 185-206.

13. REBER, R.K., Feb. 1944 'The Configuration and Towing Tension of Towed Sweep Cables Supported by Floats', Bureau of Ships, Rept. 75.

14. PARSONS, M.G., CASARELLA, M.J., 1959 'A Survey of Studies on the Configuration of Cable System under Hydrodynamic Loading', Dep't. of Mech. Eng., The Catholic Univ. of Washington, TR 69-1.

15. STRANDHAGEN, A.G., THOMAS, C.F., 1963 'Dynamics of Towed Underwater Vehicles', Rept. No. 219, U.S. Navy Mine Defence Lab., Panama City, Florida, U.S.A.

16. RICHARDSON, J.R., 1965 'The Dynamics of Towed Underwater Systems', Eng. Res. Associates Dept. No. 56-1, Toronto, CANADA.

17. PATTON, K.T., SCHRAM, J.W., 1966 'Equations of Motion of a Towed Body Moving in a Vertical Plane', Rept. No. 736, U.S. Navy Underwater Sound Lab., Fort Turnbull, Conn., U.S.A.

18. LAITINEN, P.O., 1967 'Cable-Towed Underwater Body Design', Rept. No. 1452, U.S. Navy Electronics Lab., San Diego, Calf., U.S.A.

19. PAIDOUSSIS, M.P., 1966 'Dynamics of Flexible Slender Cylinders in Axial Flow-Part I, Theory', J. Fluid Mech., 26, pp. 716-736.

20. PAIDOUSSIS, M.P., 1966 'Dynamics of Flexible Slender Cylinders in Axial Flow - Part 2, Experiments', J. Fluid Mech., 26, pp. 737-751.

21. PAIDOUSSIS, M.P., 1967 'Stability of Towed, Totally Submerged Flexible Cylinders', Rept. Eng. R-5, Atomic Energy of Canada, Chalk River, Ontario, Canada.

22. PAIDOUSSIS, M.P., 1968 'Stability of Towed, Totally Submerged Flexible Cylinders', J. Fluid Mech., 34, pp. 273-297.

23. ORTLOFF, C.R., IVES, J., 1969 'On the Dynamic Motion of a Thin Flexible Cylinder in a Viscous Stream', J. Fluid Mech., 38, pp. 713-720.

24. PAIDOUSSIS, M.P., 1970 'Dynamics of Submerged Towed Cylinders', Proc. 8th Symposium on Naval Hydrodynamics, A.R.C. No. 179, pp. 981-1016.

25. PAO, H.P., 1970 'Dynamical Stability of a Towed Thin Flexible Cylinder', J. Hydronautics, 4, pp. 145-150.

26. PAO, H.P., TRAN. Q., 1973 'Response of a Towed Thin Flexible Cylinder in a Viscous Fluid', J. Acoustical Soc. America, 53, No. 5, pp. 1441-1444.

27. YODER, P.J., PAIDOUSSIS,M.P.,1973 ' Equations Governing the Small Lateral Motions of a Slender Axysymmetric Body Towed through an Incompressible Fluid ', Undergraduate Thesis, Dep't of Mechanical Eng., McGill University, Montreal, Québec.

28. KELLY, H.R., 1954 'Estimation of Normal-force, Drag, and Pitching Moment Coefficients for Blunt-based Bodies of Revolution at Large Angles of Attack', J. Aero Science, pp. 549-565.

29. HOERNER, S.F., 1965 'Fluid Dynamic Drag', Washington: published by author.

30. TAYLOR, G.I., 1952 'Analysis of the Swimming of Long and Narrow Animals', Proc. Roy. Soc. (A), 214, pp. 158-183.

31. LIGHTHILL, M.J., 1960 'Mathematics and Aeronautics', J. Roy. Aero. Soc., 64, pp. 375-394.

32. LIGHTHILL, M.J., 1960 'Note on the Swimming of Slender Fish', J. Fluid Mech., 9, pp. 305-317.

33. UPSON, R.H., KLIKOFF, W.A., 1931 'Application of Practical Hydrodynamics to Airship Design', N.A.C.A. Report 405.

34. DURAND, W.F., 1934 'Aerodynamic Theory', Vol. 6, Division R, Chapt. 5.

35. LAMB, H., 1932 'Hydrodynamics' Cambridge University Press.

36. JONES, R., 1927 'Distribution of Normal Pressures on a Prolate Spheroid' A.R.C.R. and M. No. 1061.

FIGURES

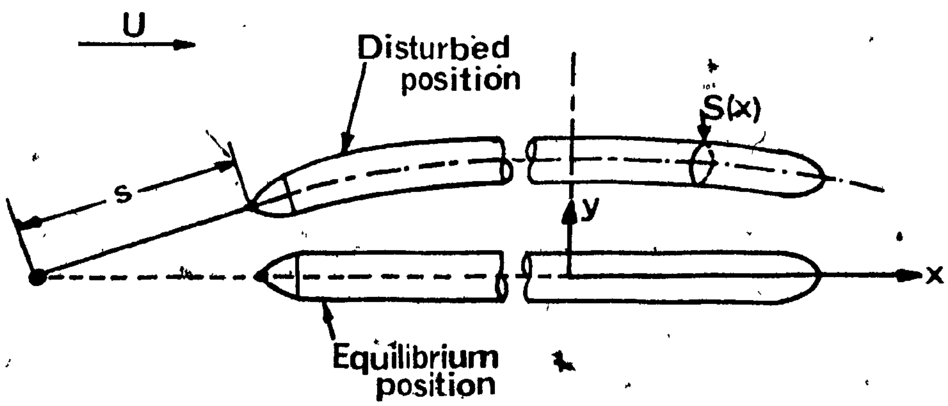

Figure 1. Diagram of a towed flexible, slender cylinder with streamlined "nose" and "tail" sections

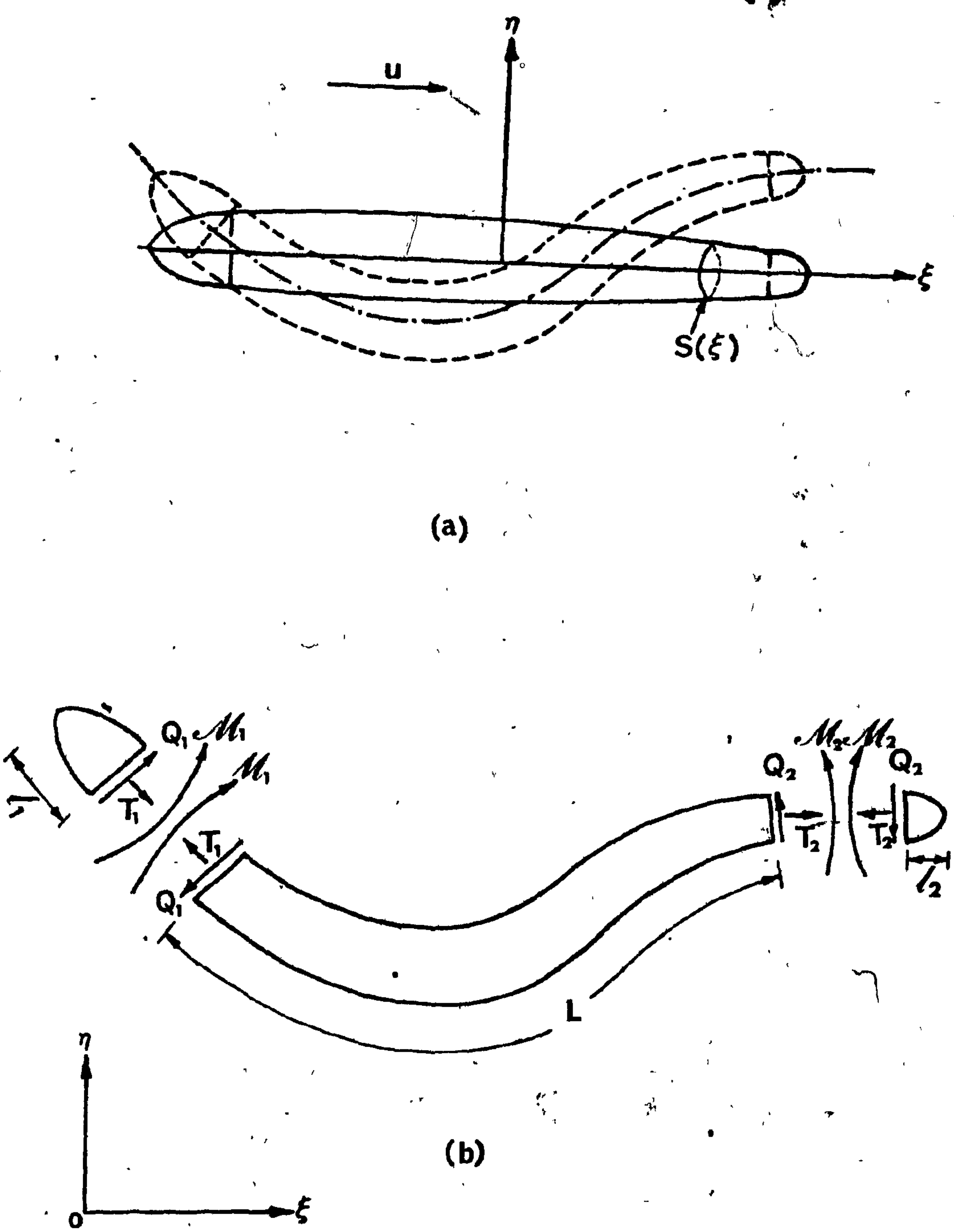

Figure 2. (a) Diagram of a flexible, slender body of revolution in axial flow

(b) the three parts of the body showing the shear forces, tensile forces and moments exerted by the nose and tail sections

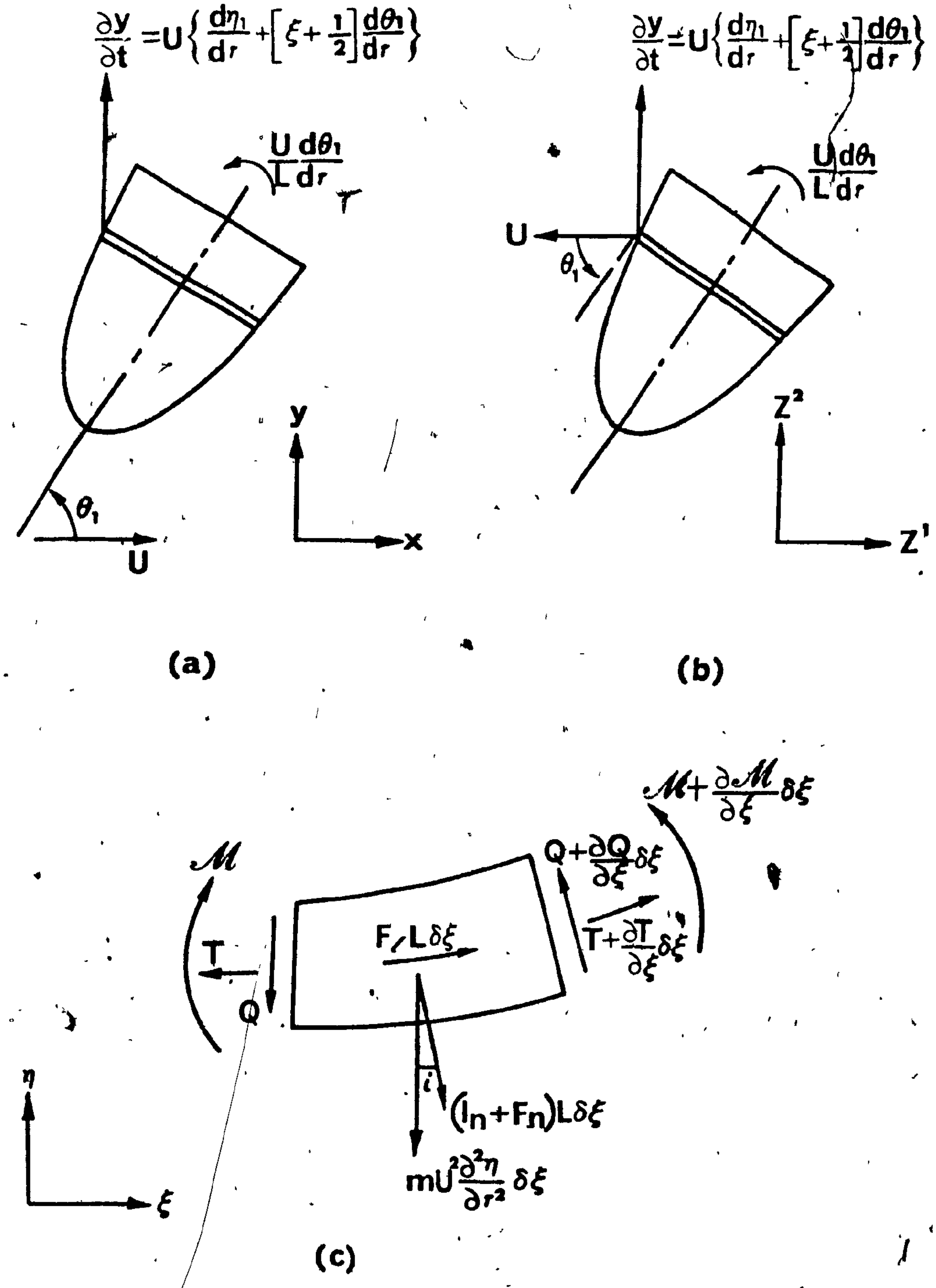

Figure 3. (a) Velocity and rotation of the nose section as seen by an observer fixed in the x-y coordinate system.

(b) Velocity and rotation of the nose section as seen by an observer fixed in space.

(c) Forces and moments acting on an element $\delta\xi$ of the main portion of the body.

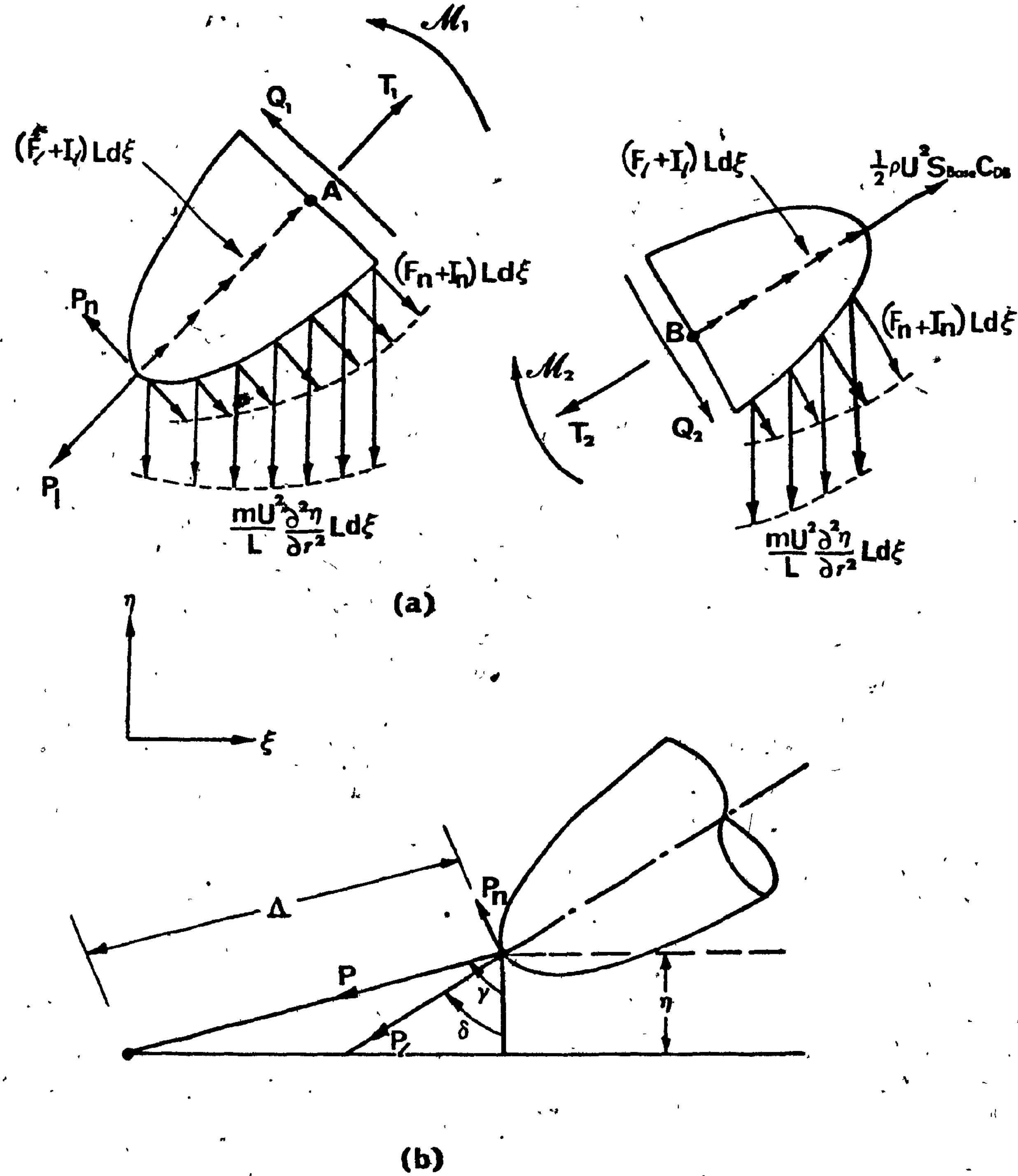

Figure 4. (a) Forces and moments acting on the nose and the tail sections.

(b) Normal and longitudinal components of tow-rope pull.

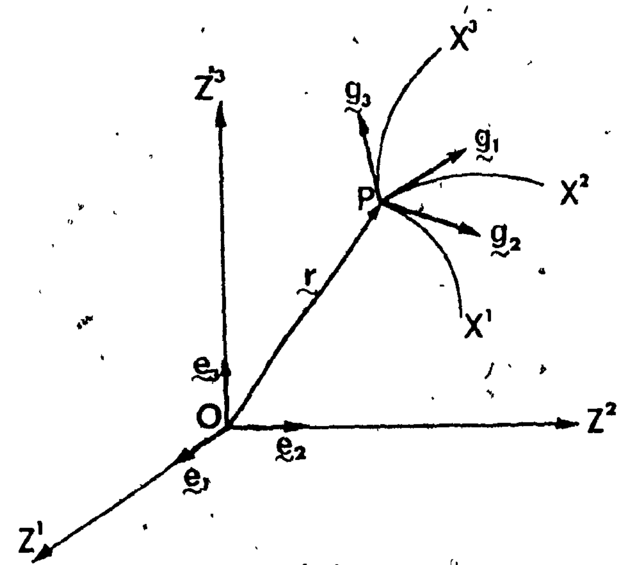

(a)

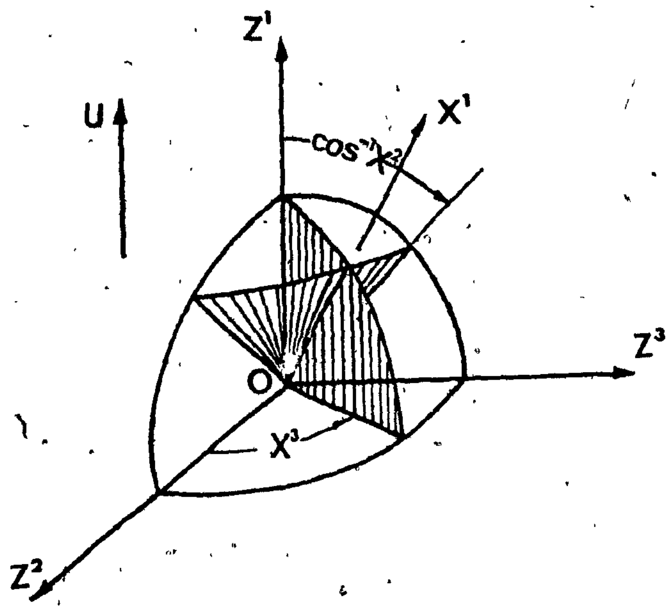

(b)

Figure 5, (a) Cartesian and curvilinear base vectors.

(b) Spheroidal co-ordinates.

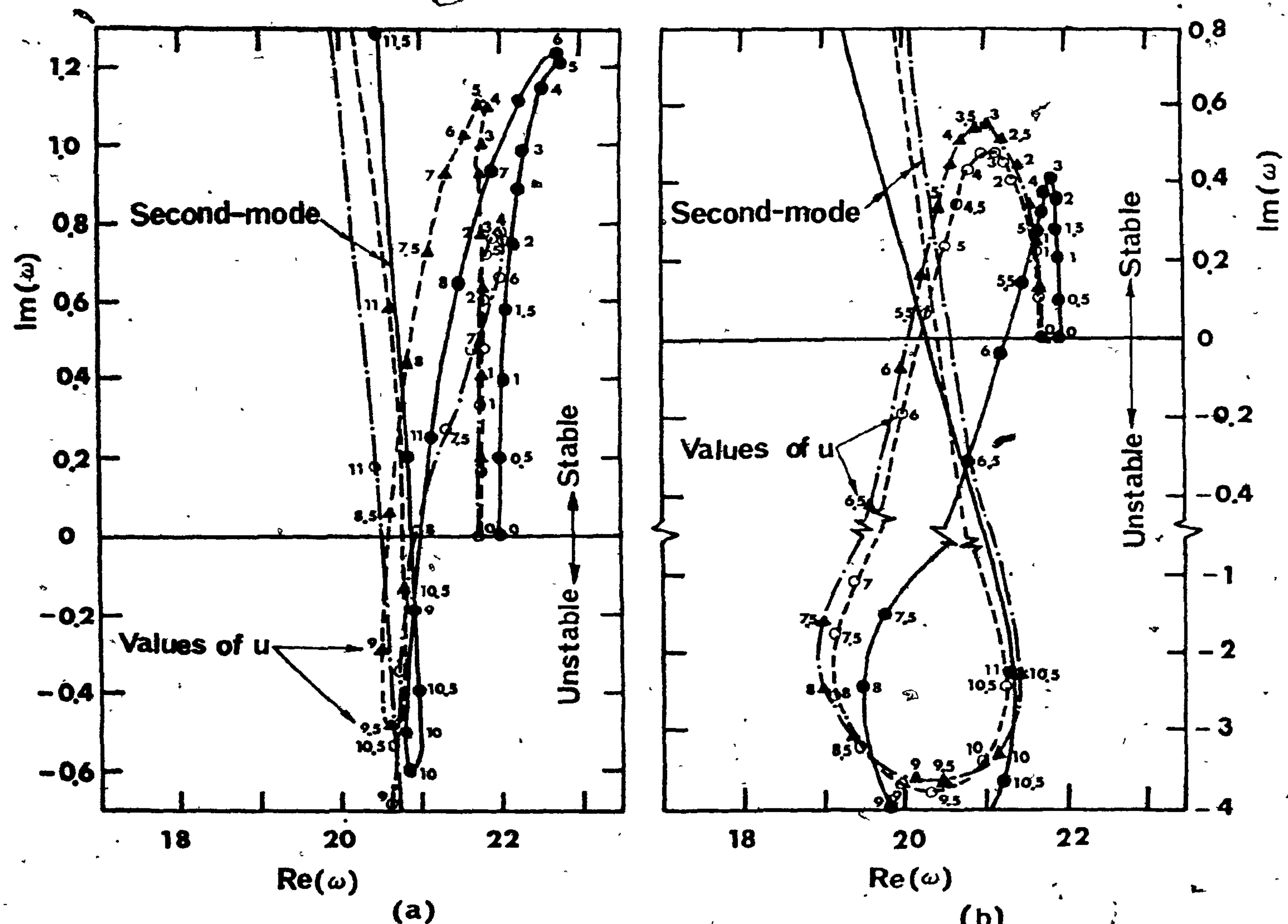

Figure 6. The dimensionless complex frequencies of the second mode of a flexible cylinder with $\beta=0.5$, $\varepsilon c_o=0$, $\varepsilon c_f=1$, $\lambda_1=0.015$, $\Lambda=1$, (a)—— new theory $\alpha=0.7$; —·— modified old theory $f_1=0.56$, $f_2=0.43$; --- modified old theory $f_1=0.62$, $f_2=0.43$ (b)—— new theory $\alpha=0.9$; —·— modified old theory $f_1=0.635$, $f_2=0.57$; --- modified old theory $f_1=0.62$, $f_2=0.57$.

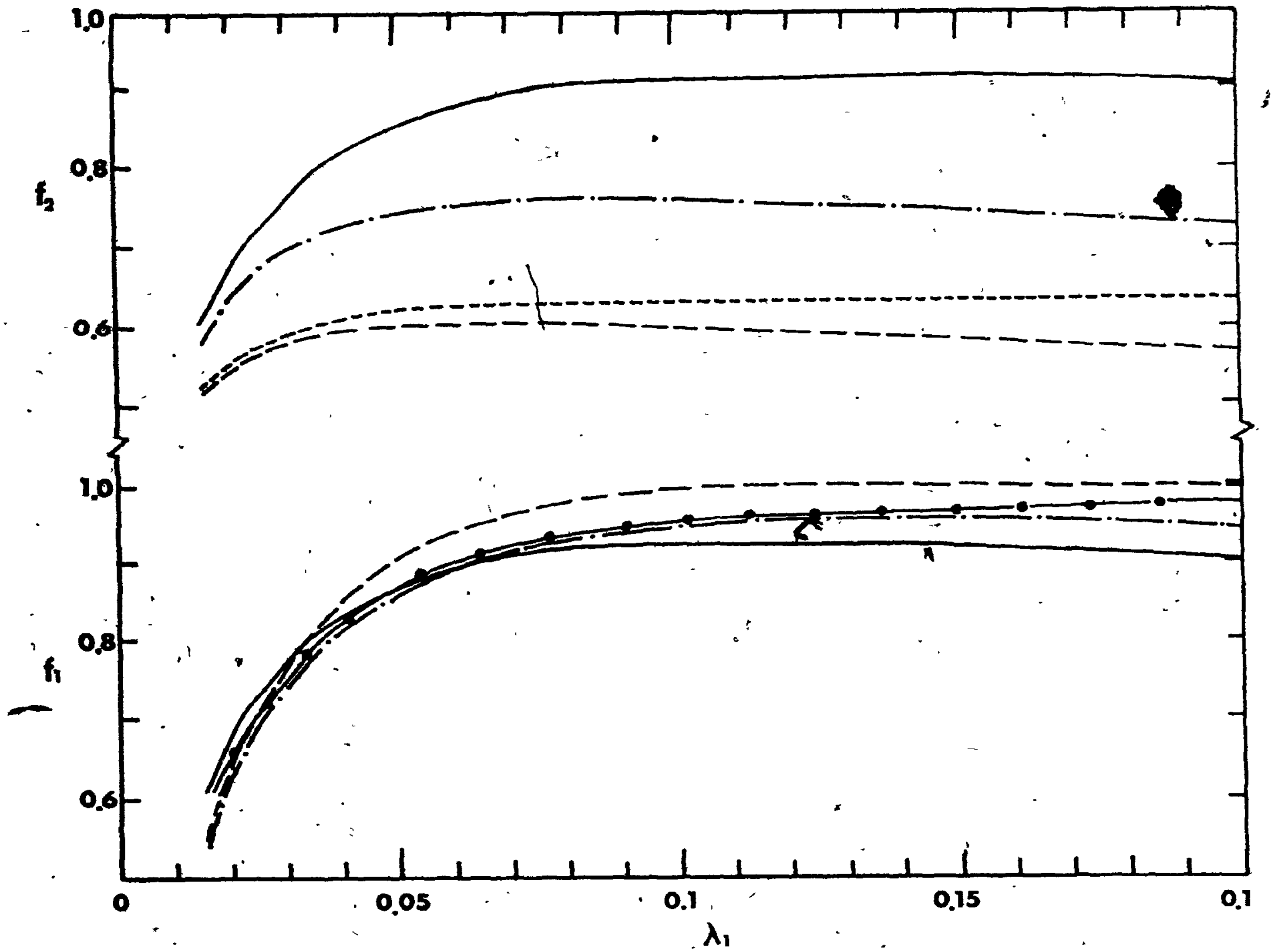

Figure 7. Comparison of the factors f_1 and f_2 of the modified old theory with λ_1 or λ_2 of this theory by comparing terms in the corresponding boundary conditions with $\beta=0.5$, $\varepsilon c_o=0$, $\varepsilon c_f=1$, $\Lambda=1$. (a) By comparing whole coefficient of u^2 in g_5 and g_9 with that in h_5 and h_9, with $\alpha=1$ —— ; $\alpha=0.9$ —·— ; $\alpha=0.8$ - - -
(b) By comparing f_1 and f_2 with i_{410} and i_{420} respectively; for nose ($\alpha=1$) —•—•— ; for tail ($\alpha=0.8$) ------

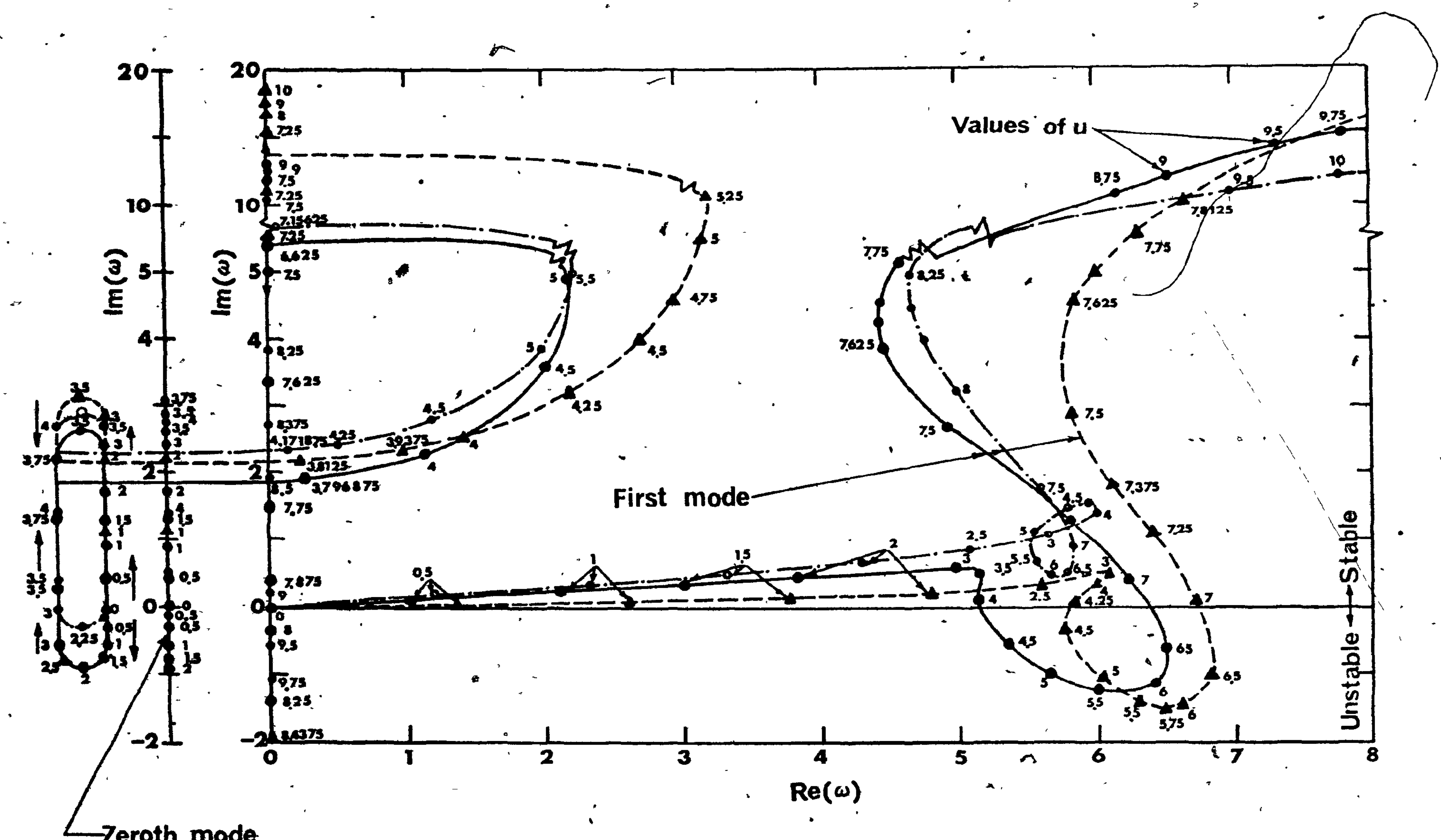

Figure 8. The dimensionless complex frequencies of the Zeroth and first modes of a flexible cylinder with $\beta=0.5$, $\varepsilon c_o=0$, $\varepsilon c_f=1$, $\lambda_1=0.015$; --- $\alpha=1$, $\Lambda=0.5$; —— $\alpha=1$, $\Lambda=1$; —·— $\alpha=0.7$, $\Lambda=1$.

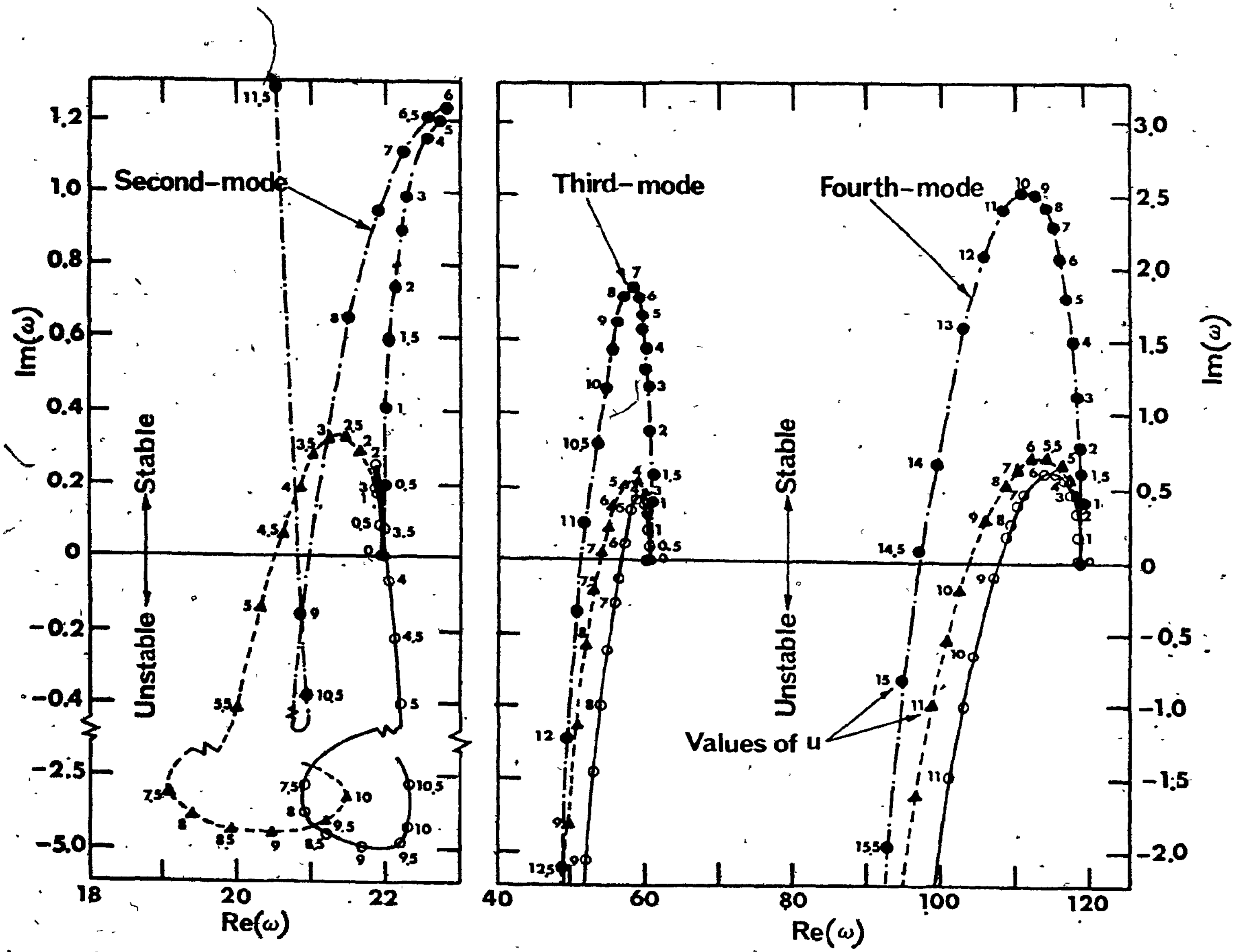

Figure 9. The dimensionless complex frequencies of the second, third and fourth modes of a flexible cylinder with $\beta=0.5$, $\varepsilon c_o=0$, $\varepsilon c_f=1$, $\lambda_1=0.015$; —— $\alpha=1$, $\Lambda=0.5$; --- $\alpha=1$, $\Lambda=1$; —·— $\alpha=0.7$, $\Lambda=1$

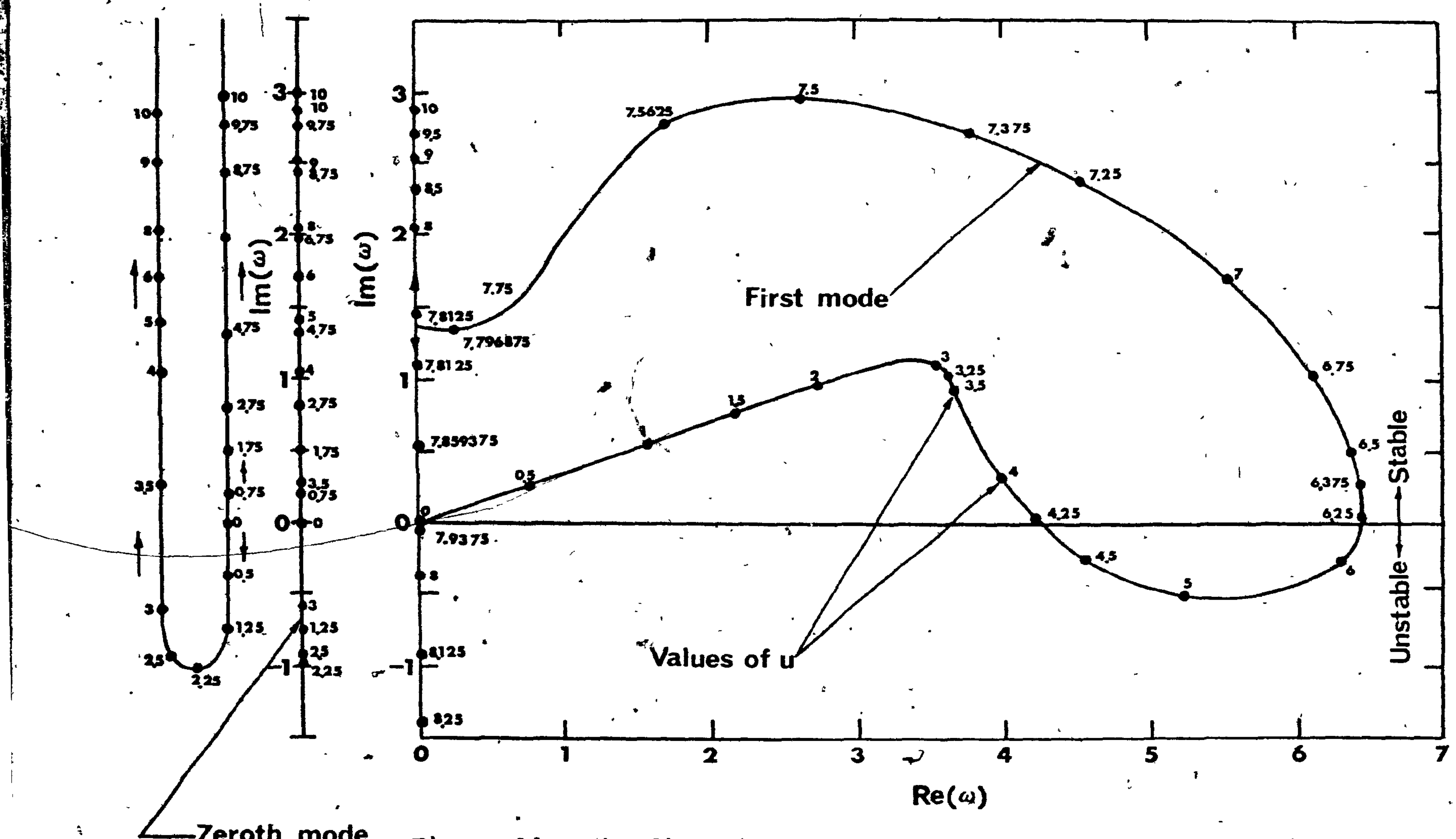

Figure 10. The dimensionless complex frequencies of the zeroth and the first modes of a flexible cylinder with $\alpha=1$, $\beta=0.5$, $\varepsilon c_o=0$, $\varepsilon c_f=1$, $\lambda_1=0.015$ and $\Lambda=5$

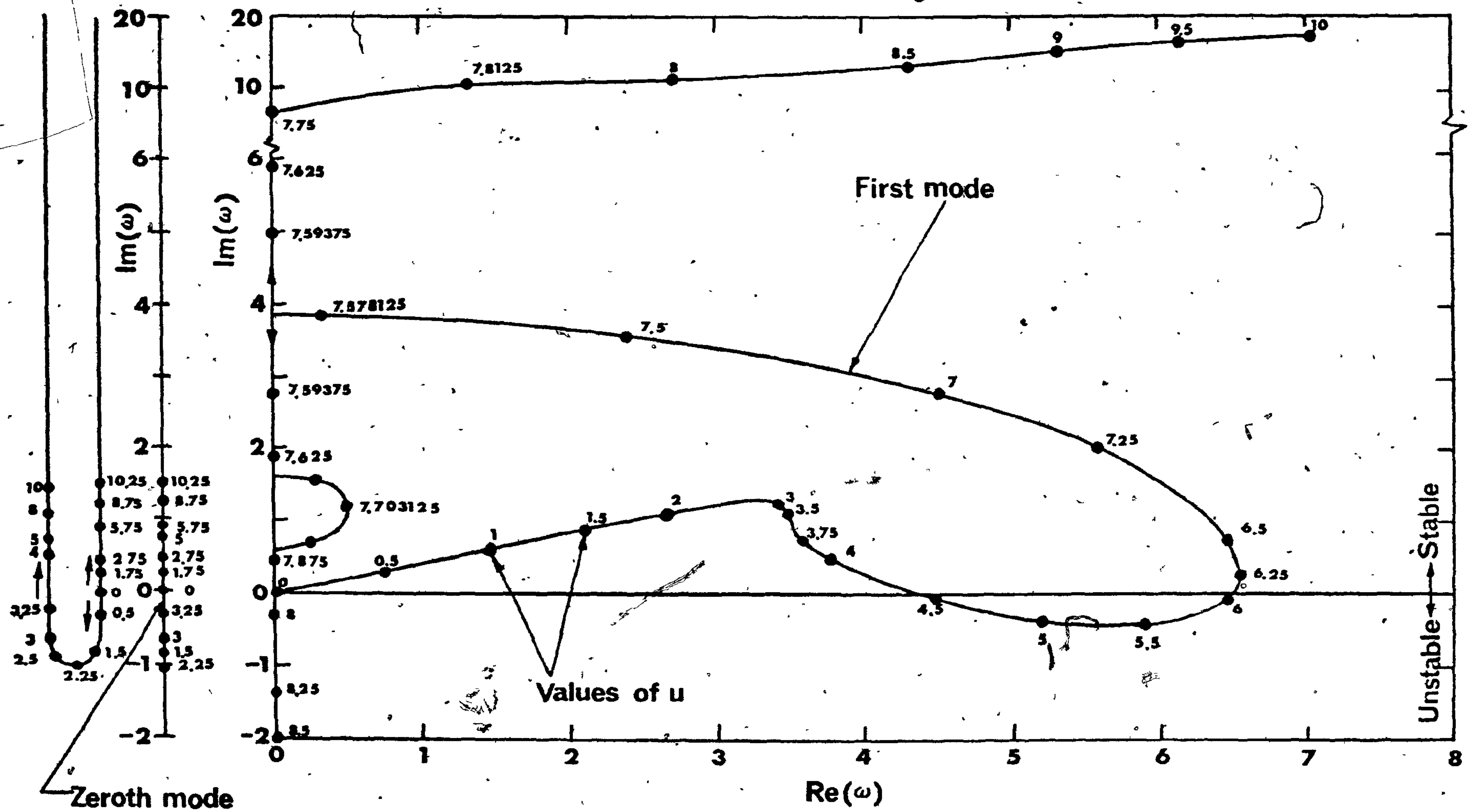

Figure 11. The dimensionless complex frequencies of the zeroth and the first modes of a flexible cylinder with $\alpha=1$, $\beta=0.5$, $\epsilon c_o=0$, $\epsilon c_f=1$, $\lambda_1=0.015$ and $\Lambda=10$

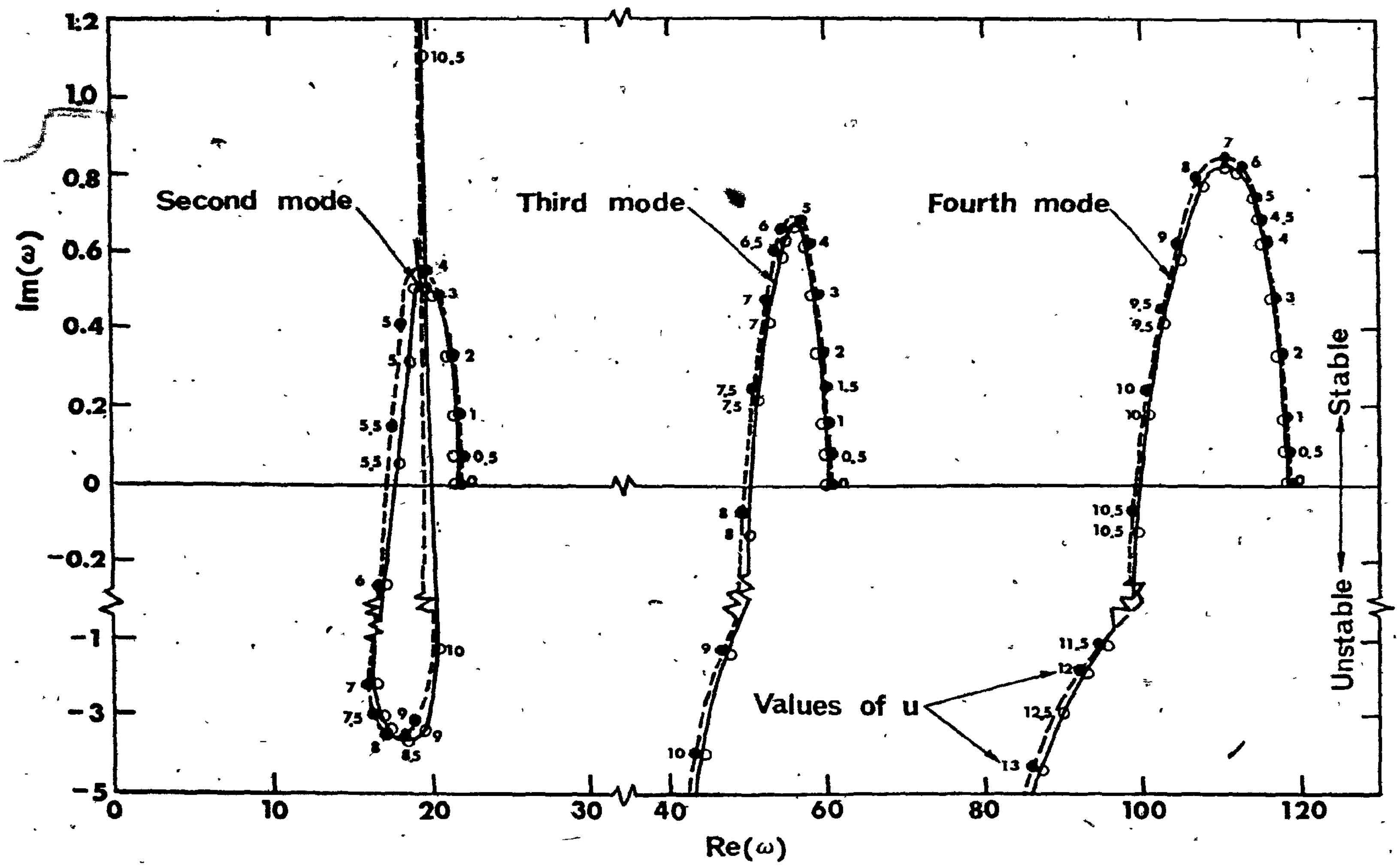

Figure 12. The dimensionless complex frequencies of the second, third and fourth modes of a flexible cylinder with $\alpha=1$, $\beta=0.5$, $\epsilon c_o=0$, $\epsilon c_f=1$, $\lambda_1=0.015$; —— $\Lambda=5$; --- $\Lambda=10$

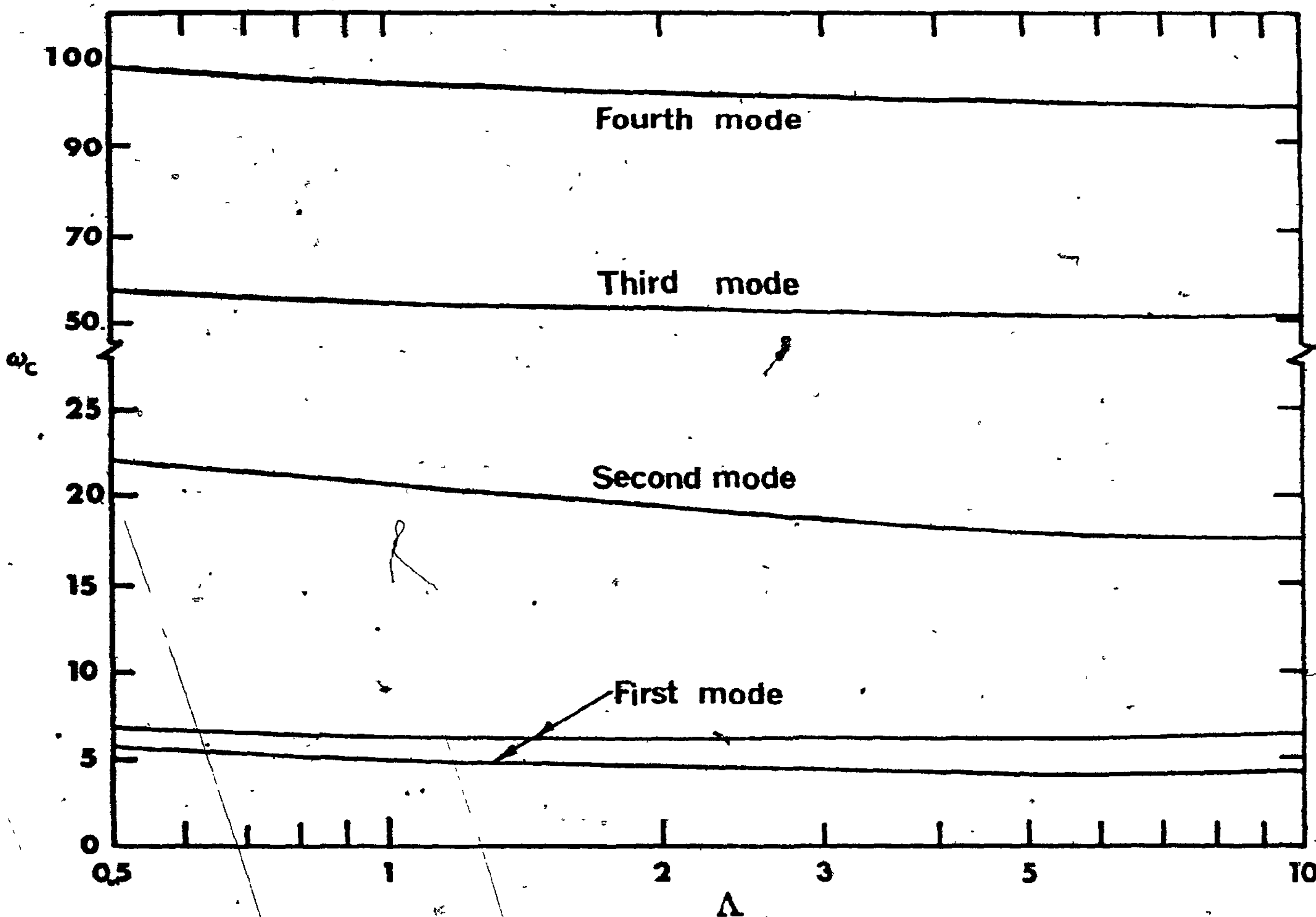

Figure 13. Corresponding complex frequency associated with neutral stability of a flexible cylinder with $\alpha=1$, $\beta=0.5$, $\varepsilon c_o=0$, $\varepsilon c_f=1$ and $\lambda_1=0.015$

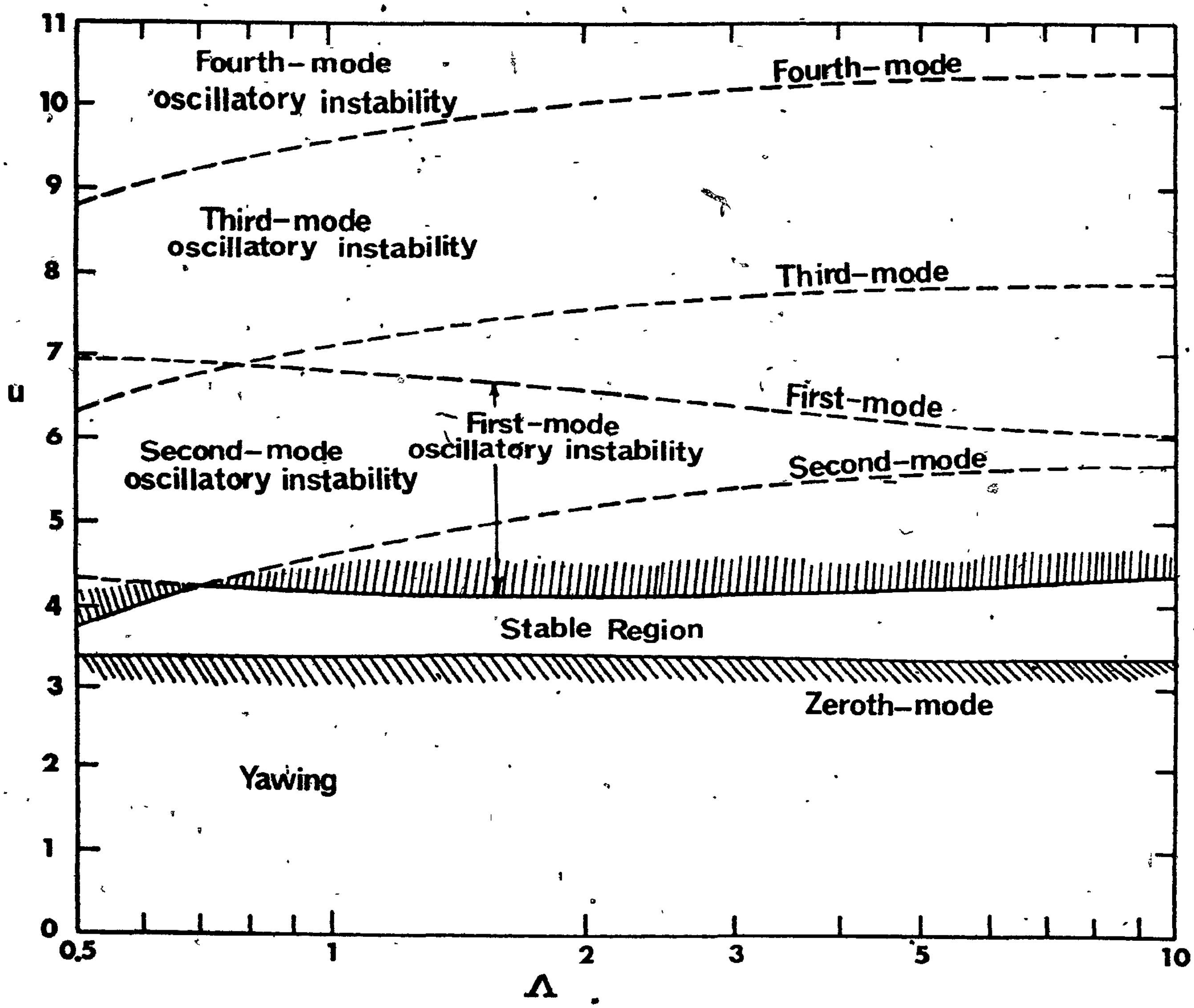

Figure 14. Stability map showing the effect of Λ for a flexible cylinder with $\alpha=1$, $\beta=0.5$, $\varepsilon c_o=0$, $\varepsilon c_f=1$ and $\lambda_1=0.015$

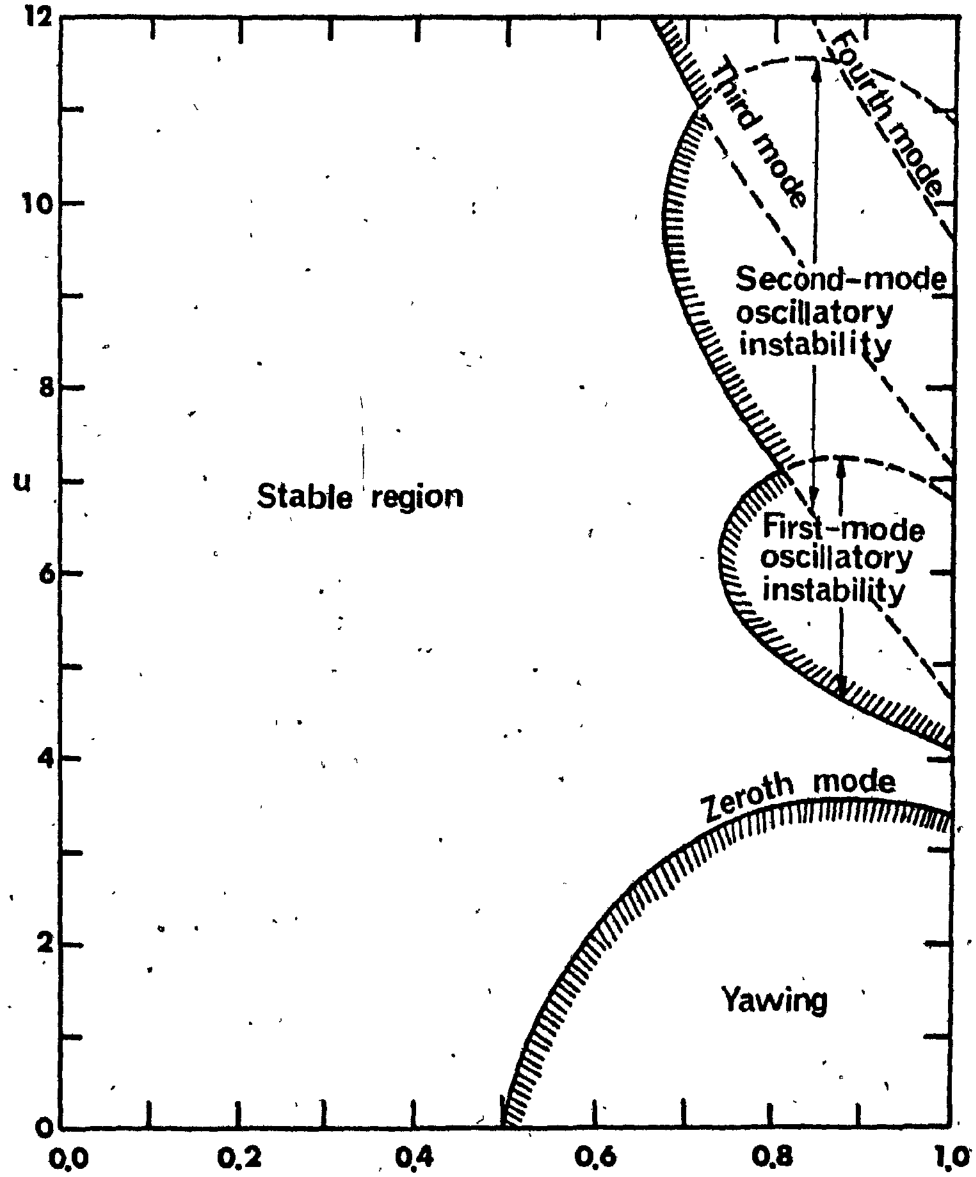

Blunt tail ← α → Elongated streamlined tail

Figure 15a. Stability map showing the effect of the tail shape for a flexible cylinder with $\beta=0.5$, $\varepsilon c_o=0$, $\varepsilon c_f=1$, $\lambda_1=0.015$ and $\Lambda=1$

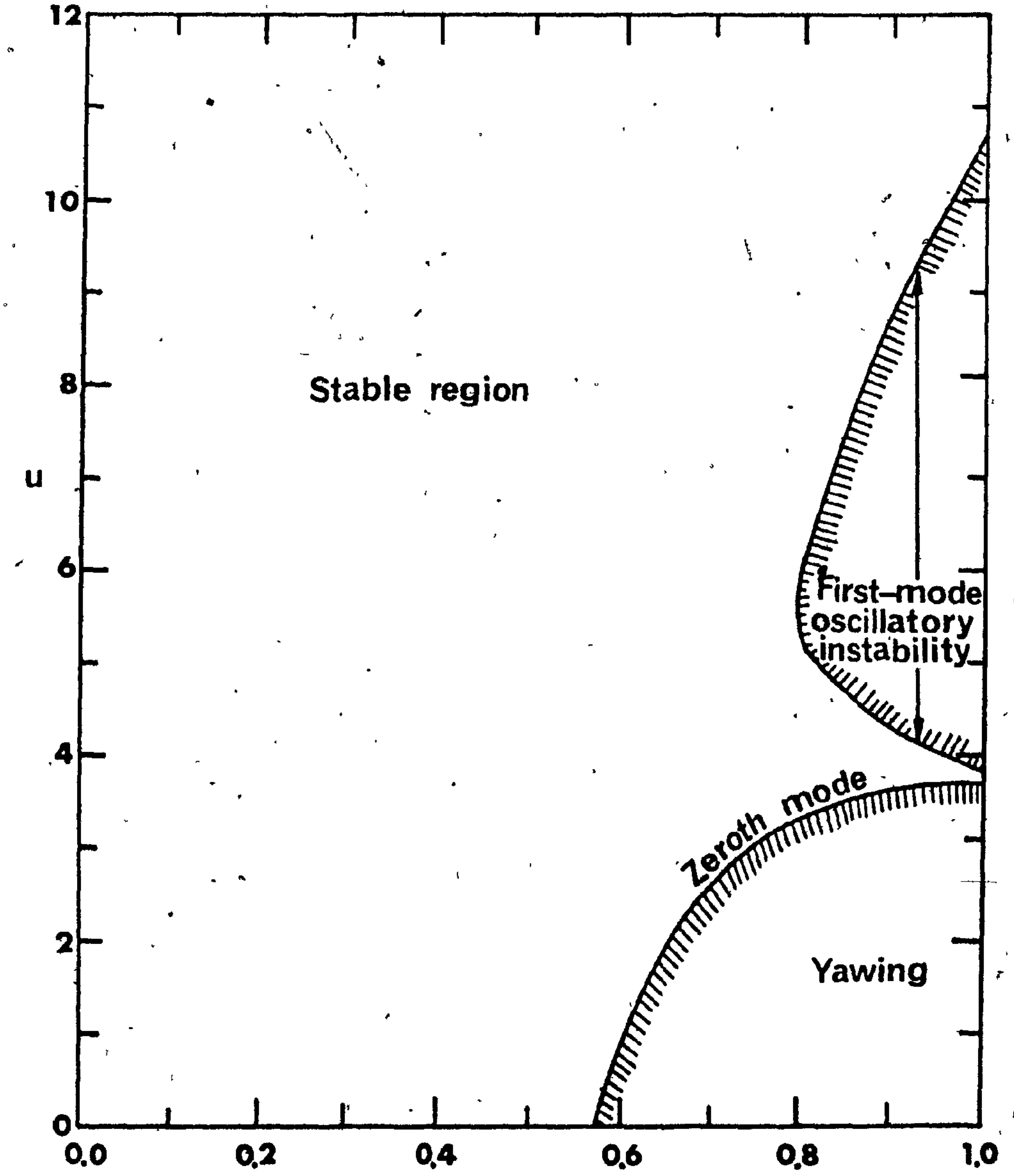

Blunt tail ⟵ α ⟶ Elongated streamlined tail

Figure 15b, Stability map showing the effect of the tail shape for a flexible cylinder with β=0.5, εc_o=0, εc_f=1, λ_1=0.05 and Λ=1

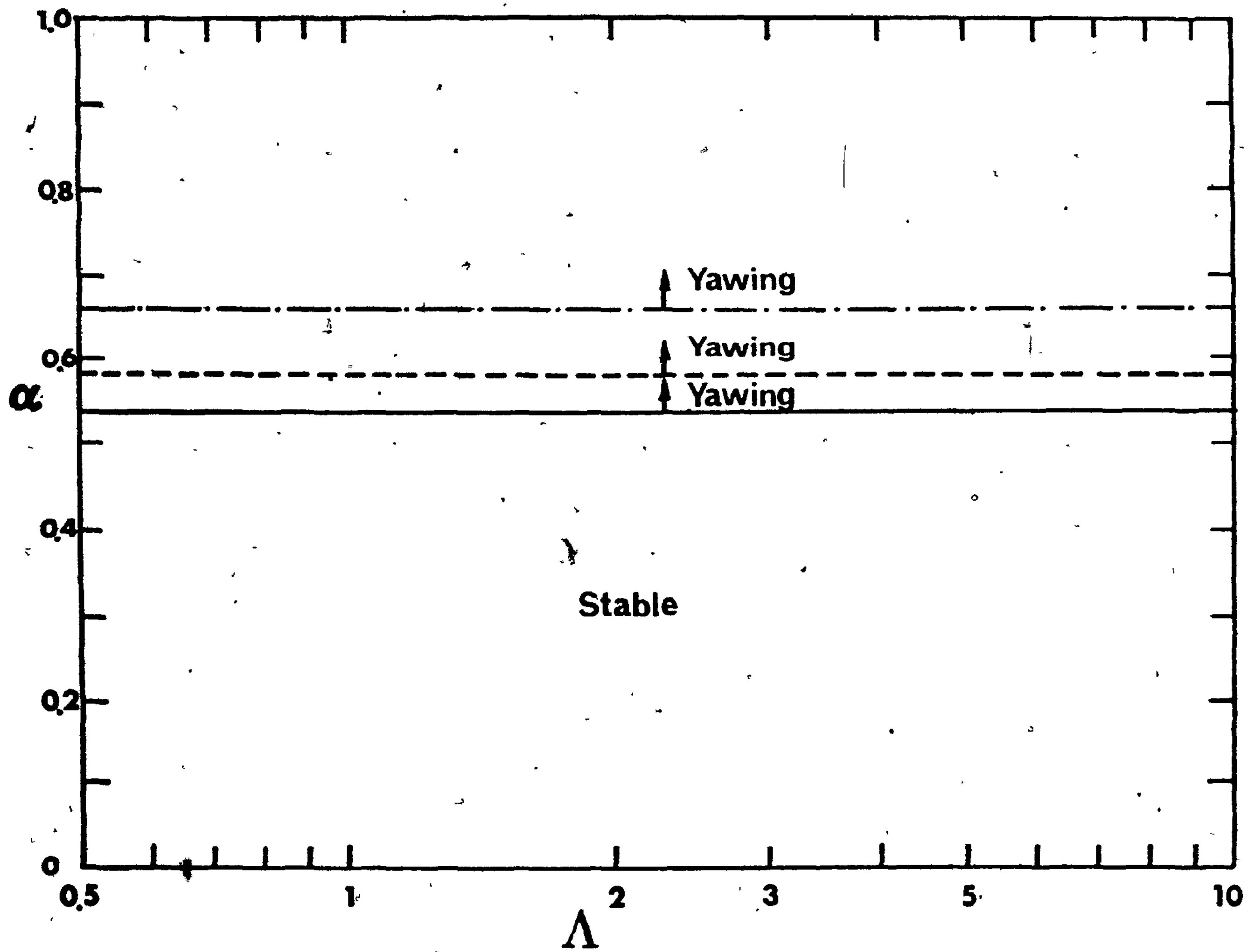

Figure 16. The effect of Λ on stability of a rigid cylinder; —— $\beta=0.5$, $\epsilon c_o=0$, $\epsilon c_f=1$, $\lambda_1=0.015$; – – – $\beta=0.5$, $\epsilon c_o=0$, $\epsilon c_f=1$, $\lambda_1=0.05$; —·— $\beta=0.5$, $\epsilon c_o=0$, $\epsilon c_f=1.5$, $\lambda_1=0.015$

APPENDICES

APPENDIX A: FORCE AND MOMENT DISTRIBUTION ALONG AN ELLIPSOID OF REVOLUTION

In this section we turn our attention to developing expressions for the force and moment acting per unit length along the axis of a prolate spheroid as it undergoes general plane motion through an infinite medium of ideal fluid. The fundamental problem of determining the flow pattern that arises under these conditions has been discussed by Lamb [35] in sections 103-106 of his classic volume, Hydrodynamics (1932). In that work Lamb investigates the net overall forces and moments exerted by the fluid on a translating and rotating spheroid, but, seeking to avoid the "troublesome calculation of the effect of the fluid pressures on the surface of the solids," (section 117) he refrains from exploring the distribution of these forces and moments. The troublesome calculations to which Lamb refers have been carried out by Jones [36] for the case of a spheroid undergoing steady-state motion confined to a plane. Regrettably, though, Jones' failure to account for the effects of linear and angular accelerations renders his findings inadequate for our purposes.

Given this situation, it would be tempting to provide here just a bare outline of how to generalize Jones' arguments, were it not for the age and the evident obscurity of his paper. In view of these latter considerations, though, and also of the fact that Jones and Lamb chose to work in terms of a notation which is now passing out of use, it has seemed appropriate to give a derivation from first principles of the expressions required. In the interest of making this appendix as self-sufficient as practicable, we include as Section A.1 a brief review of the theory of curvilinear tensors. Having laid these foundations, we shall then be ready to derive in Section A.2 expressions for the force and moment acting per unit length along the axis of a spheroid undergoing general plane motion.

A.1 An Aside on Curvilinear Tensors

We begin by setting forth the genometric basis of tensorial notation. Suppose, as indicated in Figure 5a , we are given Cartesian coordinates z^i and want to describe the location of any point in space also by use of the curvilinear coordinates x^i, where $z^i = z^i(x^j)$ and $x^i = x^i(z^j)$. Clearly, it is possible to express an arbitrary position vector $\underset{\sim}{r}$ in terms of the unit base vectors e_i corresponding to the Cartesian system:

$$\underset{\sim}{r} = z^i \underset{\sim}{e}_i \left(= z^1 \underset{\sim}{e}_1 + z^2 \underset{\sim}{e}_2 + z^3 \underset{\sim}{e}_3 \right) .$$

Alternatively, we can define curvilinear base vectors $\underset{\sim}{g}_i$, whose magnitude and direction are, in general, position dependent, such that

$$\underset{\sim}{r} = x^i \underset{\sim}{g}_i$$

It follows that

$$\mathbf{g}_i = \frac{\partial \mathbf{r}}{\partial x^i} = \frac{\partial z^j}{\partial x^i}\,\mathbf{e}_j \,, \tag{A1}$$

and equivalently,

$$\frac{\partial x^i}{\partial z^k}\,\mathbf{g}_i = \frac{\partial x^i}{\partial z^k}\frac{\partial z^j}{\partial x^i}\,\mathbf{e}_j = \frac{\partial z^j}{\partial z^k}\,\mathbf{e}_j = \mathbf{e}_k \,, \tag{A2}$$

where we have invoked the chain rule of differentiation.
We define the metric tensor

$$g_{ij} = \mathbf{g}_i \cdot \mathbf{g}_j = \frac{\partial z^\ell}{\partial x^i}\,\frac{\partial z^\ell}{\partial x^j} \tag{A3}$$

and note that it is symmetric in its two indices.
Taking the dot product of both sides of (A2) with $\mathbf{g}_j$, we obtain

$$\frac{\partial x^i}{\partial z^k}\,g_{ij} = \mathbf{e}_k \cdot \mathbf{g}_j = \mathbf{e}_k \cdot \frac{\partial z^r}{\partial x^j}\,\mathbf{e}_r = \frac{\partial z^k}{\partial x^j} \tag{A4}$$

We define reciprocal base vectors $\mathbf{g}^j$ by the relation

$$\mathbf{g}^j \cdot \mathbf{g}_i = \delta^j_i \tag{A5}$$

where δ^j_i is the Kronecker delta, and observe that

$$\frac{\partial x^j}{\partial z^\ell}\,\mathbf{e}_\ell \cdot \mathbf{g}_i = \frac{\partial x^j}{\partial z^\ell}\,\mathbf{e}_\ell \cdot \frac{\partial z^r}{\partial x^i}\,\mathbf{e}_r$$

$$= \frac{\partial x^j}{\partial z^\ell}\,\frac{\partial z}{\partial x^i} = \frac{\partial x^j}{\partial x^i} = \delta^j_i \,.$$

Hence,

$$\underset{\sim}{g}^j = \frac{\partial x^j}{\partial z^\ell} \underset{\sim}{e}_\ell \qquad \text{(A6)}$$

Substituting (A2) into the above, we obtain

$$\underset{\sim}{g}^j = \frac{\partial x^j}{\partial z^\ell} \frac{\partial x^i}{\partial z^\ell} \underset{\sim}{g}_i = \underset{\sim}{g}_i g^{ij} \qquad \text{(A7)}$$

where we have introduced the reciprocal metric tensor,

$$g^{ij} = \underset{\sim}{g}^i \cdot \underset{\sim}{g}^j = \frac{\partial x^i}{\partial z^\ell} \frac{\partial x^j}{\partial z^\ell} \qquad \text{(A8)}$$

Note that it is also symmetric. Invoking now (A5) and (A7), we deduce that

$$g_{ik} g^{ij} = \underset{\sim}{g}_k \cdot \underset{\sim}{g}_i g^{ij} = \underset{\sim}{g}_k \cdot \underset{\sim}{g}^j = \delta_k^j \qquad \text{(A9)}$$

If we multiply through the above by g, where

$$g = \det(g_{ik}) , \qquad \text{(A10)}$$

we obtain

$$g_{ki}[g^{ij} g] = \delta_k^j g$$

or

$$g_{k1}[g^{1k} g] + g_{k2}[g^{2k} g] + g_{k3}[g^{3k} g] = g ,$$

where there is no summation over the index k.

We can regard the above as the expansion of a determinant in terms of cofactors, where $[g^{1k} g]$ is the cofactor of g_{k1}, and so forth. Recalling that the cofactor of a matrix element a_{ij} contains no terms involving elements from either the i^{th}

row or the jth column, we realize that none of the cofactors in the last equation depend functionally upon g_{k1}, g_{k2}, or g_{k3}. Accordingly, we obtain by partial differentiation

$$\frac{\partial g}{\partial g_{ki}} = g^{ik} g$$

It follows then by the chain rule of differentiation that

$$\frac{\partial g}{\partial x^j} = \frac{\partial g}{\partial g_{ki}} \frac{\partial g_{ki}}{\partial x^j} = g\, g^{ik} \frac{\partial g_{ki}}{\partial x^j} \tag{A 11}$$

Let us now find tensor representations for the familiar operator ∇. We know that the gradient of a scalar,

$$\begin{aligned} \nabla A &= \underset{\sim}{e}_i \frac{\partial A}{\partial z^i} = \underset{\sim}{e}_i \frac{\partial x^j}{\partial z^i} \frac{\partial A}{\partial x^j} \\ &= \underset{\sim}{g}^j \frac{\partial A}{\partial x^j} = \underset{\sim}{g}_i\, g^{ij} \frac{\partial A}{\partial x^j} \end{aligned} \tag{A 12}$$

where we have made use of (A 6) and (A 7) in the last two steps, respectively. We can similarly obtain expressions for the divergence of a vector:

$$\begin{aligned} \nabla \cdot \underset{\sim}{B} &= \underset{\sim}{e}_k \frac{\partial}{\partial z^k} \cdot \underset{\sim}{B} = \underset{\sim}{e}_k \frac{\partial x^j}{\partial z^k} \frac{\partial}{\partial x^j} \cdot \underset{\sim}{B} \\ &= \underset{\sim}{g}^j \frac{\partial}{\partial x^j} \cdot \underset{\sim}{B} = \underset{\sim}{g}^j \cdot \left(\frac{\partial B^i}{\partial x^j} \underset{\sim}{g}_i + B^i \frac{\partial \underset{\sim}{g}_i}{\partial x^j}\right) \end{aligned} \tag{A 13}$$

where we have set $\underset{\sim}{B} = B^i \underset{\sim}{g}_i$. Now, invoking (A 1) and then (A 2), we obtain

$$\frac{\partial \underset{\sim}{g}_i}{\partial x^j} = \frac{\partial}{\partial x^j} \left(\frac{\partial z^k}{\partial x^i} \underset{\sim}{e}_k\right) = \frac{\partial^2 z^k}{\partial x^j \partial x^i} \underset{\sim}{e}_k = \frac{\partial^2 z^k}{\partial x^j \partial x^i} \frac{\partial x^m}{\partial z^k} \underset{\sim}{g}_m$$

The system of quantities $\frac{\partial^2 z^k}{\partial x^j \partial x^i} \frac{\partial x^m}{\partial z^k}$ is customarily denoted

by $\left\{ {m \atop j\ i} \right\}$,

the Christoffel symbol of the second kind.

Substituting the relation

$$\frac{\partial g_i}{\partial x^j} = \left\{ {m \atop j\ i} \right\} g_m \quad , \quad \text{where } \left\{ {m \atop j\ i} \right\} = \frac{\partial^2 z^k}{\partial x^j \partial x^i} \frac{\partial x^m}{\partial z^k} \qquad \text{(A 14)}$$

into (A 13) and using (A 5), we obtain

$$\nabla \cdot B^i g_i = \frac{\partial B^i}{\partial x^i} + B^i \left\{ {j \atop j\ i} \right\} \qquad \text{(A15)}$$

We seek, now, a more convenient expression for $\nabla . B^i g_i$

Invoking (A 4) and (A 14), we obtain

$$\left\{ {m \atop j\ i} \right\} g_{mn} = \frac{\partial^2 z^k}{\partial x^j \partial x^i} \frac{\partial z^k}{\partial x^n} \ .$$

Using (A 3) it may readily be verified that

$$\left\{ {m \atop j\ i} \right\} g_{mn} = \frac{1}{2}\left(\frac{\partial g_{jn}}{\partial x^i} + \frac{\partial g_{in}}{\partial x^j} - \frac{\partial g_{ji}}{\partial x^n}\right) \ ,$$

so that, with the use of (A 9), we can infer that

$$\left\{ {k \atop j\ i} \right\} = \frac{1}{2}\left(\frac{\partial g_{jn}}{\partial x^i} + \frac{\partial g_{in}}{\partial x^j} - \frac{\partial g_{ji}}{\partial x^n}\right) g^{nk}$$

Hence

$$\begin{aligned} \left\{ {j \atop j\ i} \right\} &= \frac{1}{2} \frac{\partial g_{jn}}{\partial x^i} g^{nj} \\ &= \frac{1}{2g} \frac{\partial g}{\partial x^i} \\ &= \frac{1}{2g} \frac{\partial g}{\partial \sqrt{g}} \frac{\partial \sqrt{g}}{\partial x^i} \\ &= \frac{1}{\sqrt{g}} \frac{\partial \sqrt{g}}{\partial x^i} \end{aligned}$$

where we have used the symmetry of g_{ij} and g^{ij} in the first step and have invoked (A 11) in the second. We now note that

$$\begin{aligned}\frac{1}{\sqrt{g}}\frac{\partial}{\partial x^i}(\sqrt{g}\;B^i) &= \frac{\partial B^i}{\partial x^i} + \frac{1}{\sqrt{g}}\frac{\partial\sqrt{g}}{\partial x^i}B^i \\ &= \frac{\partial B^i}{\partial x^i} + \left\{ {j \atop j\;i} \right\} B^i \;;\end{aligned}$$

hence, in view of (A 15),

$$\bar{\nabla} \cdot B^i \underset{\sim}{g}_i = \frac{1}{\sqrt{g}}\frac{\partial}{\partial x^i}(\sqrt{g}\;B^i) \;.$$

As a particular case of the above, we can set B equal to the gradient of a scalar and, using (A 12), obtain an expression for the Laplacian:

$$\nabla^2 A = \bar{\nabla} \cdot \bar{\nabla} A = \frac{1}{\sqrt{g}}\frac{\partial}{\partial x^i}\left(\sqrt{g}\;\; g^{ij}\frac{\partial A}{\partial x^j}\right) \tag{A 16}$$

A.2 Calculation of Distributed Force and Moment

With these preliminaries at our disposal we can now tackle the problem we set out to investigate, that of finding the force and moment acting along a spheroid as it undergoes plane motion. We begin by describing the three coordinate systems which figure in the subsequent derivations. It is convenient, first of all, to introduce a Cartesian system (z^1, z^2, z^3) which is fixed in space, that is to say, which has the property that an observer at rest in it measuring fluid velocities would find that they tend to zero far away from the moving spheroid.

This is the frame of reference in which Bernoulli's equation applies in its most familiar form:

$$\frac{p - p_\infty}{\rho} = -\frac{\partial\phi}{\partial t} - \frac{1}{2}\nabla\phi.\nabla\phi \tag{A 17}$$

Here, p is the ambient pressure, ρ is the fluid density, which is considered to be constant, and ϕ is a scalar function whose gradient equals the fluid velocity at each point. In order to find ϕ for a translating and rotating ellipsoid of revolution, it is necessary to work in terms of coordinates which move with the body. We introduce, therefore, a second Cartesian system (z^1, z^2, z^3) whose origin coincides at all times with the spheroid's centroid, the z^1- axis pointing along the axis of the body. We assume, without loss of generality, that the two coordinate systems were initially coincident and take the translational and angular velocities of the spheroid, as measured in the fixed frame, to be $\underset{\sim}{V}(t)$ and $\underset{\sim}{\omega}(t)$ respectively. Accordingly, for an arbitrary particle moving through space, the position vectors corresponding to the fixed and moving coordinate systems, $\underset{\sim}{R}$ and $\underset{\sim}{r}$ respectively, must be related as follows:

$$\underset{\sim}{R}(t) = \int_0^t \underset{\sim}{V}(\tau)d\tau + \underset{\sim}{r}(t) \quad ;$$

$$\dot{\underset{\sim}{R}}(t) = \underset{\sim}{V}(t) + \dot{\underset{\sim}{r}}(t) + \underset{\sim}{\omega}(t) \times \underset{\sim}{r}(t) \; . \tag{A 18}$$

We are obliged to consider also a set of spheroidal coordinates (x^1, x^2, x^3) which are defined by the relations below and interpreted in Figure 5b :

$$z^1 = a\, e\, x^1\, x^2$$

$$z^2 = a\, e \sqrt{[x^1]^2 - 1}\, \sqrt{1 - [x^2]^2}\, \cos x^3$$

$$z^3 = a\, e \sqrt{[x^1]^2 - 1}\, \sqrt{1 - [x^3]^2}\, \sin x^3 \tag{A 19}$$

where $x^1 > 1$, $-1 < x^2 < 1$, and $0 < x^3 < 2\pi$

It should be noted that the locus of points satisfying $x^1 = \frac{1}{e}$ is a prolate spheroid whose length is 2a and whose maximum radius is

$$b = a\sqrt{1 - e^2} \tag{A 20}$$

We shall take the relation

$$F(x^i) = x^1 - \frac{1}{e} = 0 \tag{A 21}$$

to define the surface of the ellipsoid whose motion we wish to study.

We shall throughout the course of the argument which follows observe the moving ellipsoid and measure the fluid velocity $\nabla\phi$ from a frame of reference fixed in the Z^i coordinate system. Now, within the context of incompressible, ideal-fluid flow, the equation of continuity takes on the particularly simple form,

$$\nabla^2 \phi = 0. \qquad \text{(A 22a)}$$

In order to obtain boundary conditions we note that along the interface between the spheroid and the fluid the normal component of velocity of the body's surface must equal the normal component of fluid velocity. Hence,

$$\nabla\phi . \underset{\sim}{n} = \dot{\underset{\sim}{R}} . \underset{\sim}{n} \quad \text{on} \quad F(Z^i, t) = 0 , \qquad \text{(A 22b)}$$

where $\underset{\sim}{n}$ denotes a unit vector normal to the surface of the moving spheroid and $\underset{\sim}{R}$ is understood to be a displacement vector which follows some point on this surface. We also require $\nabla\phi$ to approach zero at distances far from the body

While continuing to regard $\nabla\phi$ as the fluid velocity as measured from a vantage point fixed in space, we now set out to express it as a function of the z^i's. Since the Z^i and z^i coordinate systems differ only in that they are in relative motion, gradients and Laplacians should be the same whether evaluated in terms of one system or of the other. Using, then, (A 18) we can rewrite equations (A 22) in terms of the z^i:

$$\nabla^2 \phi = 0$$

$$\nabla\phi . \underset{\sim}{n} = (\underset{\sim}{V}(t) + \underset{\sim}{\omega}(t) \times \underset{\sim}{r}) . \underset{\sim}{n} \quad \text{on} \quad F(z^i) = 0 \qquad \text{(A 23)}$$

In this last step we have recognized that since the z^i co-ordinate system moves with the spheroid, the equation of its surface F = 0 does not involve time explicitly and, furthermore, the position vector $\underset{\sim}{r}$ of a representative point on this surface does not depend functionally upon time.

Before we can expand equations (A 23) in terms of spheroidal coordinates, we must evaluate a number of tensor quantities. Applying the relations (A 1), (A 3), (A 9) and (A 10) to (A 19) we obtain:

$$\underset{\sim}{g}_1 = aex^2\, \underset{\sim}{e}_1 + ae\frac{x^1}{\sqrt{[x^1]^2-1}}\sqrt{1-[x^2]^2}\cos x^3\, \underset{\sim}{e}_2 + ae\frac{x^1}{\sqrt{[x^1]^2-1}}\sqrt{1-[x^2]^2}\sin x^3\, \underset{\sim}{e}_3 \;;$$

$$\underset{\sim}{g}_2 = aex^1\, \underset{\sim}{e}_1 - ae\sqrt{[x^1]^2-1}\,\frac{x^2}{\sqrt{1-[x^2]^2}}\cos x^3\, \underset{\sim}{e}_2 - ae\sqrt{[x^1]^2-1}\,\frac{x^2}{\sqrt{1-[x^2]^2}}\sin x^3\, \underset{\sim}{e}_3 \;;$$

$$\underset{\sim}{g}_3 = -ae\sqrt{[x^1]^2-1}\,\sqrt{1-[x^2]^2}\sin x^3\, \underset{\sim}{e}_2 + ae\sqrt{[x^1]^2-1}\,\sqrt{1-[x^1]^2}\cos x^3\, \underset{\sim}{e}_3 \;;$$

$$g_{11} = a^2e^2\left\{\frac{[x^1]^2 - [x^2]^2}{[x^1]^2 - 1}\right\} \;;$$

$$g_{22} = a^2e^2\left\{\frac{[x^1]^2 - [x^3]^2}{1 - [x^2]^2}\right\} \;;$$

$$g_{33} = a^2e^2\{[x^1]^2-1\}\{1-[x^2]^2\} \quad ;$$

$$g_{ij} = 0 \qquad \text{if} \quad i \neq j \quad ;$$

$$g^{ij} = \frac{1}{g_{ij}} \qquad \text{if} \quad i = j$$

$$\qquad 0 \qquad \text{if} \quad i \neq j \quad ;$$

$$g = a^6e^6\,([x^1]^2 - [x^2]^2)^2 \;. \tag{A 24}$$

Substituting from the above into (A 16), we can write out the first of equations (A 23) in spheroidal co-ordinates:

$$\frac{\partial}{\partial x^1}\left\{([x^1]^2-1)\frac{\partial\phi}{\partial x^1}\right\} + \frac{\partial}{\partial x^2}\left\{(1-[x^2]^2)\,\frac{\partial\phi}{\partial x^2}\right\}$$
$$+ \frac{\partial}{\partial x^3}\left\{\frac{[x^1]^2-[x^2]^2}{([x^1]^2-1)(1-[x^2]^2)}\,\frac{\partial\phi}{\partial x^3}\right\} = 0 \tag{A 25a}$$

In order to deal with the boundary conditions we must obtain an expression for the unit normal $\underset{\sim}{n}$. Recalling that, in general, $\overline{\nabla}F$ points in a direction perpendiculur to the surface $F = 0$, we set

$$\underset{\sim}{n} = \frac{\overline{\nabla}F}{|\overline{\nabla}F|} = \frac{\underset{\sim}{g}_1\, g^{11}}{|\underset{\sim}{g}_1\, g^{11}|}\Bigg|_{x^1 = \frac{1}{e}} = \frac{\underset{\sim}{g}_1}{\sqrt{g_{11}}}\Bigg|_{x^1 = \frac{1}{e}}$$
$$= \sqrt{1-e^2}\,\frac{x^2}{\sqrt{1-e^2[x^2]^2}}\,\underset{\sim}{e}_1 + \frac{\sqrt{1-[x^2]^2}}{\sqrt{1-e^2[x^2]^2}}\cos x^3\,\underset{\sim}{e}_2 \tag{A 26}$$
$$+ \frac{\sqrt{1-[x^2]^2}}{\sqrt{1-e^2[x^2]^2}}\sin x^3\,\underset{\sim}{e}_3 \;,$$

where we have applied (A 12) to (A 21) in the second step and make use of relations (A 24) in the last. We note by inspection that $\underset{\sim}{n}$ is, in fact, an <u>outward</u> normal. If we specialize, now, to the case of general plane motion,

$$\begin{aligned} \underset{\sim}{v} &= v^1(t)\ \underset{\sim}{e}_1 + v^2(t)\ \underset{\sim}{e}_2 \\ \underset{\sim}{\omega} &= \omega^3(t)\ \underset{\sim}{e}_3 \quad , \end{aligned} \tag{A 27}$$

and substitute from (A 12), (A 24), and (A 26) into the second of equations (A 23), we obtain as our boundary condition

$$\left(\underset{\sim}{g}_1\, g^{11} \frac{\partial\phi}{\partial x^1} + \underset{\sim}{g}_2\, g^{22} \frac{\partial\phi}{\partial x^2} + \underset{\sim}{g}_3\, g^{33} \frac{\partial\phi}{\partial x^3}\right) \cdot \frac{\underset{\sim}{g}_1}{\sqrt{g_{11}}}$$

$$= \left([v^1 - \omega^3 z^2]\ \underset{\sim}{e}_1 + [v^2 + \omega^3 z^1]\ \underset{\sim}{e}_2\right) \cdot \frac{\underset{\sim}{g}_1}{\sqrt{g_{11}}}$$

$$\text{on } F = x^1 - \frac{1}{e} = 0 \ ;$$

$$\left.\frac{\partial\phi}{\partial x^1}\right|_{x^1=\frac{1}{e}} = v^1 a e x^2 + v^2 a \frac{e}{\sqrt{1-e^2}} \sqrt{1-[x^2]^2}\ \cos x^3$$

$$+ \omega^3 a^2 \frac{e^3}{\sqrt{1-e^2}}\ x^2 \sqrt{1-[x^2]^2}\ \cos x^3 \ , \tag{A 25b}$$

where we have made use of (A 19) in the last step.

The general problem of finding solutions to equation (A 25a) has been tackled systematically by Lamb [35] . It will suffice for our purposes to note that the following function does indeed satisfy (A 25a) and meet the boundary condition (A 25b):

$$\phi = \frac{v^1\, ae}{\frac{1}{2}\log\frac{1+e}{1-e} - \frac{e}{1-e^2}} \left\{\frac{1}{2}\, x^1 \log\frac{x^1+1}{x^1-1} - 1\right\} x^2$$

$$+ \frac{v^2\, ae}{\frac{1}{2}\log\frac{1+e}{1-e} - \frac{e-2e^3}{1-e^2}} \sqrt{[x^1]^2-1} \left\{\frac{1}{2}\log\frac{x^1+1}{x^1-1} - \frac{x^1}{[x^1]^2-1}\right\}$$

$$\cdot \sqrt{1-[x^2]^2} \cos x^3$$

$$+ \frac{\omega^3\, a^2 e^3}{\frac{3}{2}\left(\frac{2-e^2}{e}\right)\log\frac{1+e}{1-e} - 6 + \frac{e^2}{1-e^2}} \qquad \text{(A 28)}$$

$$\cdot \sqrt{[x^1]^2-1} \left\{\frac{3}{2}\, x^1 \log\frac{x^1+1}{x^1-1} - 3 - \frac{1}{[x^1]^2-1}\right\} x^2 \sqrt{1-[x^2]^2} \cos x^3$$

Having found the hydrodynamic potential ϕ, we can now invoke Bernoulli's equation (A 17) to obtain the distribution of pressures about the spheroid. We must bear in mind that this relation holds only if the fluid velocity field $\bar{\nabla}\phi$ is measured from a frame of reference which is inertial and in which fluid velocities tend to zero at points far away from the moving spheroid. This requirement poses no direct problem for us since we have consistently defined $\bar{\nabla}\phi$ in just this way. It is important to realize also that the term $\frac{\partial\phi}{\partial t}$ in (A 17) refers to the time rate at which ϕ is changing <u>at a point fixed in this same reference frame</u>. This can be appreciated by noting that in the derivation of Bernoulli's equation it is necessary to set the material derivative.

$$\frac{D}{Dt} = \frac{\partial}{\partial t} + \bar{\nabla}\phi \cdot \bar{\nabla}$$

Since $\nabla\phi$ is the fluid velocity as measured from a fixed point in space, $\frac{\partial\phi}{\partial t}$ must also be evaluated at a position fixed relative to the z^i coordinate system.

As a preliminary to finding $\frac{\partial\phi}{\partial t}$ in the sense of (A 17), we consider what would be seen by an observer whose position in space is given by an arbitrary time-dependent position vector $\underset{\sim}{r} = z^i \underset{\sim}{e}_i$. For him, ϕ would appear to fluctuate at a rate

$$\frac{d\phi}{dt} = \left.\frac{\partial\phi}{\partial t}\right|_{\underset{\sim}{r} = \text{constant}} + \frac{\partial z^i}{\partial t}\frac{\partial\phi}{\partial z^i}$$

$$= \left.\frac{\partial\phi}{\partial t}\right|_{\underset{\sim}{r} = \text{constant}} + \dot{\underset{\sim}{r}} \cdot \nabla\phi \quad ;$$

$$\frac{d\phi}{dt} = \left.\frac{\partial\phi}{\partial t}\right|_{\underset{\sim}{r} = \text{constant}} + (\dot{\underset{\sim}{R}}(t) - \underset{\sim}{v}(t) - \underset{\sim}{\omega}(t) x \underset{\sim}{r}) \cdot \nabla\phi \, ,$$

in view of (A 18). Now to obtain the rate of change of ϕ as seen by an observer fixed in space, we need simply set $\dot{R}(t)=0$ in the above equation. Bernoulli's equation (A 17) can, therefore, be written equivalently as follows:

$$\frac{P-P_\infty}{\rho} = -\left.\frac{\partial\phi}{\partial t}\right|_{\underset{\sim}{r} = \text{constant}} + (\underset{\sim}{V}+\underset{\sim}{\omega} \times \underset{\sim}{r}) \cdot \nabla\phi - \frac{1}{2}\nabla\phi\cdot\nabla\phi \qquad \text{(A 29)}$$

We are interested in finding the pressure distribution only over the surface of the spheroid and shall accordingly set $x^1 = \frac{1}{e}$ as we proceed in evaluating the terms on the right hand side of (A 29). We can readily deduce from (A 28) that

$$- \frac{\partial \phi}{\partial t}_{\underset{\sim}{r} = \text{constant}} = \dot{v}^1 a\, k_1\, x^2 + \dot{v}^2 b\, k_2 \sqrt{1-[x^2]^2} \cos x^3 + \dot{\omega}^3 ab\, \ell_3\, x^2 \sqrt{1-[x^2]^2} \cos x^3 , \qquad \text{(A 30)}$$

where we have made use of (A 20) and have introduced the constants

$$- k_1 = \frac{e\{\frac{1}{2e} \log \frac{1+e}{1-e} - 1\}}{\frac{1}{2}\log \frac{1+e}{1-e} - \frac{e}{1-e^2}} ,$$

$$- k_2 = \frac{\{\frac{1}{2} \log \frac{1+e}{1-e} - \frac{e}{1-e^2}\}}{\frac{1}{2}\log \frac{1+e}{1-e} - \frac{e-2e^3}{1-e^2}} , \qquad \text{(A 31)}$$

$$- \ell_3 = \frac{e^2\{\frac{3}{2e} \log \frac{1+e}{1-e} - 3 - \frac{e^2}{1-e^2}\}}{\frac{3}{2}\left(\frac{2-e^2}{e}\right) \log \frac{1+e}{1-e} - b + \frac{e^2}{1-e^2}}$$

We obtain an expression for $\nabla\phi$ on the surface $x^1 = \frac{1}{e}$ by applying (A 12) to (A 28), making use of (A25b) and (A 20), and recalling that $g^{ij} = 0$ for $i \neq j$:

$$\nabla\phi = \underset{\sim}{g}_1 g^{11} \{v^1 aex^2 + v^2 a \frac{e}{\sqrt{1-e^2}} \sqrt{1-[x^2]^2} \cos x^3 + \omega^3 a^2 \frac{e^3}{\sqrt{1-e^2}} x^2 \sqrt{1-[x^2]^2} \cos x^3\}$$

$$+ \underset{\sim}{g}_2 g^{22} \{-v^1 ak_1 + v^2 bk_2 \frac{x^2}{\sqrt{1-[x^2]^2}} \cos x^3$$

$$- \omega^3 ab\ell_3 \frac{(1-2[x^2]^2)}{\sqrt{1-[x^2]^2}} \cos x^3 \} \qquad \text{(A 32)}$$

$$+ \underset{\sim}{g}_3 g^{33} \{ v^2 bk_2 \sqrt{1-[x^2]^2} \sin x^3 + \omega^3 ab\ell_3 x^2 \sqrt{1-[x^2]^2} \sin x^3 \}$$

Using (A 27), (A 19), (A 20), and (A 24) in conjunction with the above, we can evaluate the second term on the right-hand side of (A 29):

$$(\underset{\sim}{V} + \underset{\sim}{\omega} \times \underset{\sim}{r})\{ . \overline{\nabla}\phi = (v^1-\omega^3 z^2)\underset{\sim}{e}_1 + (v^2+\omega^3 z^1)\underset{\sim}{e}_2 \;.\; \nabla\phi \}$$

$$= (v^1-\omega^3 b\sqrt{1-[x^2]^2} \cos x^3) \{ aex^2 . \frac{1}{a^2e^2} \frac{1-e^2}{1-e^2[x^2]^2}$$

$$.(v^1 aex^2 + v^2 a \frac{e}{\sqrt{1-e^2}} \sqrt{1-[x^2]^2} \cos x^3$$

$$+ \omega^3 a^2 \frac{e^3}{\sqrt{1-e^2}} x^2 \sqrt{1-[x^2]^2} \cos x^3)$$

$$+ a \;.\; \frac{1}{a^2} \frac{1-[x^2]^2}{1-e^2[x^2]^2}$$

$$.(-v^1 ak_1 + v^2 bk_2 \frac{x^2}{\sqrt{1-[x^2]^2}} \cos x^3$$

$$- \omega^3 ab\ell_3 \frac{(1-2[x^2]^2)}{\sqrt{1-[x^2]^2}} \cos x^3)\}$$

$$+(v^2 + \omega^3 a\, x^2) \{ a \frac{e}{\sqrt{1-e^2}} \sqrt{1-[x^2]^2} \cos x^3 . \frac{1}{a^2e^2} . \frac{1-e^2}{1-e^2[x^2]^2}$$

$$.(v^1 ae\, x^2 + v^2 a \frac{e}{\sqrt{1-e^2}} \sqrt{1-[x^2]^2} \cos x^3$$

$$+ \omega^3 a^2 \frac{e^3}{\sqrt{1-e^2}} x^2 \sqrt{1-[x^2]^2} \cos x^3)$$

$$- b \frac{x^2}{\sqrt{1-[x^2]^2}} \cos x^3 . \frac{1}{a^2} \frac{1-[x^2]^2}{1-e^2[x^2]^2}$$

$$\cdot \left(-v^1 a k_1 + v^2 b k_2 \frac{x^2}{\sqrt{1-[x^2]^2}} \cos x^3 - \omega^3\, ab\ell_3 \frac{(1-2[x^2]^2)}{\sqrt{1-[x^2]^2}} \cos x^3\right)$$

$$- b\sqrt{1-[x^2]^2} \sin x^3 \; \frac{1}{a^2} \frac{1}{(1-e^2)(1-[x^2]^2)}$$

$$\cdot \left(v^2 b k_2 \sqrt{1-[x^2]^2} \sin x^3 + \omega^3 ab\ell_3\, x^2 \sqrt{1-[x^2]^2} \sin x^3\right)\} \qquad \text{(A 33)}$$

We can evaluate the last term on the right-hand side of Bernoulli's equation (A 29) with the use of (A 32), (A 24), and (A 21):

$$- \frac{1}{2} \nabla\phi . \nabla\phi$$

$$= -\frac{1}{2} \frac{1}{a^2 e^2} \frac{1-e^2}{1-e^2[x^2]^2} \{v^1 a e x^2 + v^2 a \frac{e}{\sqrt{1-e^2}} \sqrt{1-[x^2]^2} \cos x^3 + \omega^3 a^2 \frac{e^3}{\sqrt{1-e^2}} x^2 \sqrt{1-[x^2]^2} \cos x^3\}^2$$

$$-\frac{1}{2} \frac{1}{a^2} \frac{1-[x^2]^2}{1-e^2[x^2]^2} \{-v^1 a k_1 + v^2 b k_2 \frac{x^2}{\sqrt{1-[x^2]^2}} \cos x^3 - \omega^3 ab\ell_3 \frac{(1-2[x^2]^2)}{\sqrt{1-[x^2]^2}} \cos x^3\}^2$$

$$-\frac{1}{2} \frac{1}{a^2} \frac{1}{(1-e^2)(1-[x^2]^2)} \cdot \{v^2 b k_2 \sqrt{1-[x^2]^2} \sin x^3 + \omega^3 ab\ell_3\, x^2 \sqrt{1-[x^2]^2} \sin x^3\}^2 \qquad \text{(A 34)}$$

Substituting, now, (A 31), (A 33), and (A 34) into Bernoulli's equation (A 29) and regrouping terms, we obtain an expression for the pressure distribution on the surface of the moving spheroid.

$$\frac{P-P_\infty}{\rho} = c_o + c_1 \cos x^3 + c_2 \cos^2 x^3 + c_3 \sin^2 x^3,$$

where

$$c_o = \dot{v}^1 a k_1 x^2 + \frac{1}{2}[v^1]^2 \left(1 - \frac{(1+k_1)^2(1-[x^2]^2)}{1-e^2[x^2]^2}\right);$$

$$c_1 = \dot{v}^2 b k_2 \sqrt{1-[x^2]^2} + v^1 v^2 \left(\frac{b}{a}\right)(1+k_1)1+k_2) \frac{x^2\sqrt{1-[x^2]^2}}{1-e^2[x^2]^2}$$

$$+ \dot{\omega}^3 \; a b \ell_3 \, x^2\sqrt{1-[x^2]^2}$$

$$+ \omega^3 v^1 b\left\{\frac{(1+k_1)(1+\ell_3(2[x^2]^2-1)}{1-e^2[x^2]^2} - 1\right\}\sqrt{1-[x^2]^2};$$

$$c_2 = \frac{1}{2}[v^2]^2\left\{1 - \frac{\left(\frac{b}{a}\right)^2 (1+k_2)^2[x^2]^2}{1-e^2[x^2]^2}\right\}$$

$$+ \omega^3 v^2 a x^2\left\{1 - \frac{\left(\frac{b}{a}\right)^2 (1+k_2)(1+\ell_3(2[x^2]^2-1)}{1-e^2[x^2]^2}\right\}$$

$$+ \frac{1}{2}[\omega^3]^2 \left\{a^2[x^2]^2 + b^2(1-[x^2]^2) - \frac{b^2(1+\ell_3(2[x^2]^2-1))^2}{1-e^2[x^2]^2}\right\};$$

$$c_3 = \frac{1}{2}[v^2]^2\{1-(1+k_2)^2\} + \omega^3 v^2 a x^2\{1-(1+k_2)(1+\ell_3)\}$$

$$+ \frac{1}{2}[\omega^3]^2 a^2[x^2]^2\{1-(1+\ell_3)^2\} \qquad \text{(A 35)}$$

Having determined the distribution of pressure about a moving spheroid, we can now investigate the force to which this pressure gives rise. As a preliminary we recall the well-known result, discussed at some length in Franklin that the area of an orientable surface is given unambiguously by

$$A = \int dA = \iint_{P_{z^1 z^2}} \frac{1}{|\cos\gamma|} dz^1 dz^2 ,$$

where the integration is carried out over the projection of the surface onto the (z^1, z^2) plane. It is implicitly assumed here that no two regions of the surface project onto the same part of $P_{z^1 z^2}$, since γ is the angle between the normal to the surface and the z^3- direction; hence

$$\cos\gamma = \underset{\sim}{n} \cdot \underset{\sim}{e}_3$$

More generally, the surface integral of a function f whose domain is the surface under consideration,

$$\int f \, dA = \iint_{P_{z^1 z^2}} \frac{f}{|\underset{\sim}{n} \cdot \underset{\sim}{e}_3|} dz^1 dz^2 .$$

Remembering that the unit normal $\underset{\sim}{n}$ points in the outward direction, we can readily see that the force acting on an element dA of the spheroid's surface is equal to -pndA. Accordingly, if we let f be the vector function $-p\underset{\sim}{n}$ and apply the above equation first to the portion of the ellipsoid above the (z^1,z^2) plane and then to the part below, we determine that the total force acting over the body,

$$\underset{\sim}{F} = \int_{-a}^{a} \int_{-b\sqrt{1-[\frac{z^1}{a}]^2}}^{b\sqrt{1-[\frac{z^1}{a}]^2}} \frac{-P\underset{\sim}{n}}{|\underset{\sim}{n}\cdot\underset{\sim}{e}_3|}\, dz^2 dz^1 \qquad \text{(upper sector)}$$

$$+ \int_{-a}^{a} \int_{+b\sqrt{1-[\frac{z^1}{a}]^2}}^{-b\sqrt{1-[\frac{z^1}{a}]^2}} \frac{-P\underset{\sim}{n}}{|\underset{\sim}{n}\cdot\underset{\sim}{e}_3|}\, dz^2 dz^1 . \qquad \text{(lower sector)}$$

Actually, we have no interest in evaluating the above integrals; expressions for $\underset{\sim}{F}$ can be obtained by more direct means. What we do wish to find is the force per unit length along the spheroid's axis,

$$\frac{\partial \underset{\sim}{F}}{\partial z^1} = \int_{-b\sqrt{1-[\frac{z^1}{a}]^2}}^{b\sqrt{1-[\frac{z^1}{a}]^2}} \frac{-P\underset{\sim}{n}}{|\underset{\sim}{n}\cdot\underset{\sim}{e}_3|}\, dz^2 \qquad \text{(upper sector)}$$

$$+ \int_{+b\sqrt{1-[\frac{z^1}{a}]^2}}^{-b\sqrt{1-[\frac{z^1}{a}]^2}} \frac{-P\underset{\sim}{n}}{|\underset{\sim}{n}\cdot\underset{\sim}{e}_3|}\, dz^2 \qquad \text{(lower sector)}$$

In performing these integrations we must hold constant $z^1 = ax^2$. (Recall that $x^1 = \frac{1}{e}$ on the spheroid.) It follows, in view of (A 19), that

$$dZ^2 = -b\sqrt{1-[x^2]^2}\ \sin x^3\ dx^3 \quad ;$$

hence

$$\frac{\partial \underset{\sim}{F}}{\partial Z^1} = \int_{\pi}^{0} \frac{-P\underset{\sim}{n}}{|\underset{\sim}{n}\cdot\underset{\sim}{e}_3|}\left(-b\sqrt{1-[x^2]^2}\ \sin x^3\right) dx^3 \qquad \text{(upper sector)}$$

$$+ \int_{2\pi}^{\pi} \frac{-P\underset{\sim}{n}}{|\underset{\sim}{n}\cdot\underset{\sim}{e}_3|}\left(-b\sqrt{1-[x^2]^2}\ \sin x^3\right) dx^3 \qquad \text{(lower sector)}$$

$$= \int_{0}^{2\pi} \frac{-P\underset{\sim}{n}}{|\underset{\sim}{n}\cdot\underset{\sim}{e}_3|}\ b\sqrt{1-[x^2]^2}\ \sin x^3\ dx^3 \tag{A 36}$$

$$= -\underset{\sim}{e}_1 \frac{b^2}{a} x^2 \int_0^{2\pi} P\ dx^3 - \underset{\sim}{e}_2\ b\sqrt{1-[x^2]^2} \int_0^{2\pi} P \cos x^3\ dx^3$$

$$- \underset{\sim}{e}_3\ b\sqrt{1-[x^2]^2} \int_0^{2\pi} P \sin x^3\ dx^3$$

$$= -\underset{\sim}{e}_1\ \rho \frac{b^2}{a} x^2 (2\pi c_0 + \pi c_2 + \pi c_3)$$

$$-\underset{\sim}{e}_2\ \rho b\sqrt{1-[x^2]^2}\ \pi c_1 \quad ,$$

where we have used (A 26) in next to the last step and have made reference to (A 35) in the last. It should be noted that in this final step we have neglected a term involving P_∞, which is not spatially dependent and cannot therefore

$$\frac{\partial \tilde{F}}{\partial z^1} \cdot \underset{\sim}{e}_1 = -\rho\pi \frac{b^2}{a} x^2\{2\dot{v}^1 ak_1x^2$$

$$+ [v^1]^2 (1 - \frac{(1+k_1)^2(1-[x^2]^2)}{1-e^2[x^2]^2})$$

$$+ \frac{1}{2}[v^2]^2(1 - \frac{(\frac{b}{a})^2(1+k_2)^2[x^2]^2}{1-e^2[x^2]^2})$$

$$+ \dot{\omega}^3v^2 ax^2(1 - \frac{(\frac{b}{a})^2(1+k_2)(1+\ell_3(2[x^2]^2-1)}{1-e^2[x^2]^2})$$

$$+ \frac{1}{2}[\omega^3]^2(a^2[x^2]^2 + b^2(1-[x^2]^2) - \frac{b^2(1+\ell_3(2[x^2]^2-1))^2}{1-e^2[x^2]^2})$$

$$+ \frac{1}{2}[v^2]^2(1-(1-k_2)^2) + \omega^3v^2 ax^2(1-(1+k_2)(1+\ell_3))$$

$$+ \frac{1}{2}[\omega^3]^2 a^2 [x^2]^2 (1-(1+\ell_3)^2\} \quad , \qquad \text{(A37a)}$$

and to a component in the transverse direction,

$$\frac{\partial \tilde{F}}{\partial z^1} \cdot \underset{\sim}{e}_2 = -\rho\pi b^2(1-[x^2]^2) \{\dot{v}^2k_2$$

$$+ v^1v^2(\frac{1}{a})(1+k_1)(1+k_2)\frac{x^2}{1-e^2[x^2]^2} + \dot{\omega}^3a\ell_3x^2$$

$$+ \omega^3v^1(\frac{(1+k_1)(1+\ell_3(2[x^2]^2-1))}{1-e^2[x^2]^2} - 1)\} \quad , \qquad \text{(A37b)}$$

where we have made use of (A 35).

By reasoning analogous to that leading to (A 36), we find that the moment exerted by the fluid on a transverse section of the spheroid,

$$\frac{\partial \underset{\sim}{M}}{\partial z^1} = \int_0^{2\pi} \frac{\underset{\sim}{r} \times (-P)\underset{\sim}{n}}{|\underset{\sim}{n} \cdot \underset{\sim}{e}_3|} \cdot b\sqrt{1-[x^2]^2} \sin x^3 \, dx^3$$

$$= -\underset{\sim}{e}_3 \{ z^1 \cdot b\sqrt{1-[x^2]^2} \int_0^{2\pi} P \cos x^3 \, dx^3$$

$$- \frac{b^2}{a} x^2 \cdot b\sqrt{1-[x^2]^2} \int_0^{2\pi} P \cos x^3 \, dx^3 \}$$

$$= \underset{\sim}{e}_3 \left(z^1 - \frac{b^2}{a} x^2\right) \frac{\partial \underset{\sim}{F}}{\partial z^1} \cdot \underset{\sim}{e}_2 \, , \qquad \text{(A 38)}$$

where we have made use of (A 19), (A 26), and the statement following (A 37)

APPENDIX B: NON-DIMENSIONAL INTEGRALS

$$i_{11m} = \frac{D_{max}}{S_{max}} \int_{-\frac{1}{2}-\lambda_1}^{-\frac{1}{2}} \frac{S(\xi)}{D(\xi)} (\xi+\tfrac{1}{2})^m d\xi$$

$$i_{12m} = \frac{D_{max}}{S_{max}} \int_{\frac{1}{2}}^{\frac{1}{2}+\lambda_2} \frac{S(\xi)}{D(\xi)} (\xi-\tfrac{1}{2})^m d\xi$$

$$i_{21m} = \frac{1}{S_{max}} \int_{-\frac{1}{2}-\lambda_1}^{-\frac{1}{2}} S(\xi)(\xi+\tfrac{1}{2})^m d\xi$$

$$i_{22m} = \frac{1}{S_{max}} \int_{\frac{1}{2}}^{\frac{1}{2}+\lambda_2} S(\xi)(\xi-\tfrac{1}{2})^m d\xi$$

$$i_{31m} = \frac{1}{S_{max}} \int_{-\frac{1}{2}-\lambda_1}^{-\frac{1}{2}} S(\xi)k_2(\xi+\tfrac{1}{2})^m d\xi$$

$$i_{32m} = \frac{1}{S_{max}} \int_{\frac{1}{2}}^{\frac{1}{2}+\lambda_2} S(\xi)k_2(\xi-\tfrac{1}{2})^m d\xi$$

$$i_{41m} = \frac{1}{S_{max}} \int_{-\frac{1}{2}-\lambda_1}^{-\frac{1}{2}} S(\xi)\frac{L}{a}(1+k_1)(1+k_2)\frac{x^2}{1-e^2[x^2[^2}(\xi+\tfrac{1}{2})^m d\xi$$

$$i_{42m} = \frac{1}{S_{max}} \int_{\frac{1}{2}}^{\frac{1}{2}+\lambda_2} S(\xi)\frac{L}{a}(1+k_1)(1+k_2)\frac{x^2}{1-e^2[x^2]^2}(\xi-\tfrac{1}{2})^m d\xi$$

$$i_{51m} = \frac{1}{S_{max}} \int_{-\frac{1}{2}-\lambda_1}^{-\frac{1}{2}} S(\xi)\frac{a}{L}\ell_3 x^2 (\xi+\tfrac{1}{2})^m d\xi$$

$$i_{52m} = \frac{1}{S_{max}} \int_{\frac{1}{2}}^{\frac{1}{2}+\lambda_2} S(\xi)\frac{a}{L}\ell_3 x^2 (\xi-\tfrac{1}{2})^m d\xi$$

$$i_{61m} = \frac{1}{S_{max}} \int_{-\frac{1}{2}-\lambda_1}^{-\frac{1}{2}} S(\xi)\left[\frac{(1+k_1)\{1+\ell_3(2[x^2]^2-1)\}}{1-e^2[x^2]^2}-1\right](\xi+\tfrac{1}{2})^m d\xi$$

$$i_{62m} = \frac{1}{S_{max}} \int_{\frac{1}{2}}^{\frac{1}{2}+\lambda_2} S(\xi)\left[\frac{(1+k_1)\{1+\ell_3(2[x^2]^2-1)\}}{1-e^2[x^2]^2}-1\right](\xi-\tfrac{1}{2})^m d\xi$$

$$i_{71m} = \int_{-\frac{1}{2}-\lambda_1}^{-\frac{1}{2}} \frac{L}{a} x^2 \left\{\frac{(1+k_1)^2(1-[x^2]^2)}{1-e^2[x^2]^2} - 1\right\}(\xi+\tfrac{1}{2})^m d\xi$$

$$i_{72m} = \int_{\frac{1}{2}}^{\frac{1}{2}+\lambda_2} \frac{L}{a} x^2 \left\{\frac{(1+k_1)^2(1-[x^2]^2)}{1-e^2[x^2]^2} - 1\right\}(\xi-\tfrac{1}{2})^m d\xi$$

It should be noted that the quantities x^2, a, e, k_1, k_2 and ℓ_3 are all functions of ξ and any of the integrals listed above becomes a small quantity, if $m > 1$.

The nose and tail sections consist of half ellipsoids, whose major axis is $2\lambda_1$ and minor axis $\frac{1}{\varepsilon}$. The tail may be less than a half ellipsoid since its end may have been cut off to make it blunter; in such cases $\lambda_2 = \alpha\lambda_1$.

The integrals above are easily evaluated by hand, after suppressing the common $\frac{1}{2}$ or $-\frac{1}{2}$ from the limits of integration.

APPENDIX C: COEFFICIENTS OF DIFFERENTIAL EQUATIONS OF THE PRESENT THEORY

$$g_o = 1 + \nu(i\omega)$$

$$g_1 = u^2[1-\tfrac{1}{2}\{\varepsilon c_f(\tfrac{1}{2}+i_{120}) + 2\, i_{720} \quad \frac{S_{Base}}{S} C_{DB}\}]$$

$$g_2 = \tfrac{1}{2}u^2\varepsilon c_f$$

$$g_3 = \tfrac{1}{2}u^2\{\varepsilon(c_o+c_f)\} + 2\beta^{\frac{1}{2}}u(i\omega)$$

$$g_4 = \tfrac{1}{2}\beta^{\frac{1}{2}}u\varepsilon c_f(i\omega) - \omega^2$$

$$g_5 = u^2[-\tfrac{1}{2}(\frac{\lambda_{1+\Lambda}}{\Lambda}) \{\varepsilon c_f(1+i_{110}+i_{120}) + 2(i_{710}+i_{720})$$

$$+ \frac{S_{Base}}{S} C_{DB}\} + \tfrac{1}{2}\, \varepsilon i_{110}(c_o+c_f)$$

$$+ i_{410}] + \beta^{\frac{1}{2}}u(-i_{310}+i_{610})(i\omega)$$

$$+ \beta i_{510} \ \omega^2$$

$$g_6 = u^2[\frac{1}{2\Lambda} \{\varepsilon c_f(1+i_{110}+i_{120}) + 2(i_{710}+i_{720})$$

$$+ \frac{S_{Base}}{S} C_{DB}\}] + \beta^{\frac{1}{2}}u\{\tfrac{1}{2}\varepsilon c_f\, i_{110}+i_{410} (i\omega) -$$

$$- \beta(i_{210}-i_{310})\omega^2$$

$$g_7 = -\frac{\lambda l}{2} u^2 [\varepsilon c_f(1+i_{110}+i_{120}) + 2(i_{710}+i_{720}) + \frac{S_{Base}}{S} C_{DB}] \{\frac{\lambda_1+\Lambda}{\Lambda}\}$$

$$g_8 = \frac{\lambda l}{2\Lambda} u^2 [\varepsilon c_f(1+i_{110}+i_{120}) + 2(i_{710}+i_{720}) + \frac{S_{Base}}{S} C_{DB}]$$

$$g_9 = -u^2 [\tfrac{1}{2}\varepsilon(c_o+c_f)i_{120} - i_{420}] - \beta^{\frac{1}{2}}u(i_{320}-i_{620})(i\omega) + \beta i_{520}\omega^2$$

$$g_{10} = -\beta^{\frac{1}{2}}u(\tfrac{1}{2}\varepsilon c_f i_{120}-i_{420}) + \beta(i_{320} + i_{220})\omega^2$$

Note that in the computer program of Appendix E the coefficients g_i are denoted C_i and that C_5 to C_{10} have apposite sign to g_5 to g_{10}.

APPENDIX D: COEFFICIENTS OF DIFFERENTIAL EQUATIONS OF THE MODIFIED OLD THEORY

$$h_0 = 1 + \nu(i\omega)$$

$$h_1 = u^2\{1 - \tfrac{1}{2}(\tfrac{1}{2}\varepsilon c_f + \frac{S_{Base}}{S} C_2)\}$$

$$h_2 = \tfrac{1}{2}u^2 \varepsilon c_f$$

$$h_3 = \tfrac{1}{2}u^2 \varepsilon c_f + 2\beta^{\frac{1}{2}} u(i\omega)$$

$$h_4 = \tfrac{1}{2}\beta^{\frac{1}{2}} u\varepsilon c_f (i\omega) - \omega^2$$

$$h_5 = u^2\{f_1 - \tfrac{1}{2}(\frac{\lambda_1 + \Lambda}{\Lambda})(C_1 + C_2 + \varepsilon c_f)\}$$

$$h_6 = \frac{u^2}{2\Lambda}(C_1 + C_2 + \varepsilon c_f) + f_1\beta^{\frac{1}{2}} u(i\omega) - \beta i_{210}(1+f_1)\omega^2$$

$$h_7 = -\frac{\lambda_1}{2}(\frac{\lambda_1 + \Lambda}{\Lambda})(C_1 + C_2 + \varepsilon c_f)u^2$$

$$h_8 = \frac{\lambda_1}{2\Lambda}(C_1 + C_2 + \varepsilon c_f)u^2$$

$$h_9 = f_2 u^2$$

$$h_{10} = f_2\beta^{\frac{1}{2}} u(i\omega) + \beta(1+f_2)i_{220}\,\omega^2$$

APPENDIX E: THE COMPUTER PROGRAM USED TO OBTAIN THE CURVES OF FIGURES 6 AND 8 TO 15

```
      $WATFIV ,TIME=999,PAGES=999
            IMPLICIT COMPLEX*16(O,A,C,Y),REAL*8(B,D-H,P-X,Z)
            COMMON Q1,Q2,QE,QA,XCN,XCT
            COMMON F1,F2,XC1,XC2
      C    PARAMETERS
            Q1=0.015D0
            Q2=1.D0
            QA=1.D0
            QE=40.D0
            F1=1.D0
            F2=0.8D0
            XCN=0.025D0
            XCT=0.025D0
      C     XCN IS THE NORMAL COMPONENT OF THE DRAG COEFFUCIENT
      C     XCT IS THE LONGITUDINAL COMPONENT OF DRAG COEFFUCIENT
            XC1=0.D0
            XC2=1.D0-F2
      C    PARAMETERS
            N=4
            MODE=2
            IAX=1
            IUPAX=1
            KM=12
            KEY=1
            IFEND=100
            DM=2.D-4
            UM=14.D0
      C     UM IS THE MAXIMUM DIMENSIONLESS VELOCITY GIVEN
            U=0.D0
            DU=0.5D0
            OM=(62.D0,0.D0)
            OM1=(59.D0,0.D0)
            OD1=(-1.D0,0.05D0)
            WRITE(6,100) MODE,N,DM
        100 FORMAT('1*MODE=',I1,'**N=',I2,'**DM=',1PD7.1///)
            DO1IN=1,IFEND
            CALL PREDIC(OM1,OM,OD1,OD2,U,DU,DM,IN,N,K2,K1,K,IAX,IUPAX,KM,KEY)
            EIGIM=(0.D0,-1.D0)*OM1
            EIGIM=DSIGN(DSQRT(DABS(EIGIM)),EIGIM)
            EIGRE=OM1
            EIGRE=DSQRT(DABS(EIGRE))
            WRITE(6,10)U,OM1,EIGRE,EIGIM,K
         10 FORMAT(' ',F10.7,4X,'OMEGA=',1P2D14.6,11X,'SQRT(OMEGA)=',0P2F9.6,13X,I3,'
           *3X,I3,'ITERATIONS'/)
            EI=EIGIM*EIGIM
            IF((K.GE.KM+1).OR.((U-UM)*DU.GT.0.D0).OR.(EI.GT.1.D2))GOTO1000
          1 CONTINUE
       1000 CONTINUE
            STOP
            END

            SUBROUTINE MATRIX(A,U,OMEGA,M)
            IMPLICIT COMPLEX*16(O,A,B,C,Z),REAL*8(D-H,P-Y)
            COMMON Q1,Q2,QE,QA,XCN,XCT
            COMMON F1,F2,XC1,XC2
            DIMENSION A(10,10),B(85,10),C(85,10)
            O=(0.D0,1.D0)
            Z=OMEGA
            Z2=Z*Z
```

```
      BETA=DSQRT(2.D0)
      PI=3.14159265350D0
      Q11=Q1*Q1
      QEE=QE*QE
      QAA=QA*QA
C
C     Q1 IS THE RATIO OF LENGTH OF NOSE SECTION/LENGTH OF MAIN BODY
C     Q2 IS THE RATIO OF LENGTH OF TOW-ROPE/LENGTH OF MAIN BODY
C     QA IS THE RATIO OF LENGTH OF TAIL SECTION/LENGTH OF NOSE SECTION
C     QE IS THE RATIO OF LENGTH OF MAIN BODY/DIAMETER OF CYLINDER
      YE=DSQRT(1.D0-1.D0/(4.D0*Q11*QEE))
C     YE IS THE ECCENTRICITY OF THE ELLIPSOID
      YEE=YE*YE
      YEI=1.D0/YE
      YEL=DLOG((1.D0+YE)/(1.D0-YE))
      YEX=YE/(1.D0-YEE)
      YEXX=YEE/(1.D0-YEE)
      YEEE=YEE*YE
      YEEI=1.D0/YEE
      XK1=-YE*(0.5D0*YEI*YEL-1.D0)/(0.5D0*YEL-YEX)
      XK2=-(0.5D0*YEL-YEX)/(0.5D0*YEL-YEX*(1.D0-2.D0*YEE))
      XL3=-YEE*(1.5D0*YEI*YEL-3.D0-YEXX)/(1.5D0*(2.D0*YEI-YE)*YEL-6.D0+
     *YEXX)
C
C     DIMENSIONLESS PARAMETERS OF I.S
      Y110=PI*Q1/4.D0
      Y120=0.5D0*Q1*(QA*DSQRT(1.D0-QAA)+DARSIN(QA))
      Y210=2.D0*Q1/3.D0
      Y220=QA*Q1*(1.D0-QAA/3.D0)
      Y310=2.D0*Q1*XK2/3.D0
      Y320=QA*Q1*(1.D0-QAA/3.D0)*XK2
      XXK1=1.D0+XK1
      XXK2=1.D0+XK2
      XXK12=XXK1*XXK2
      XXK11=XXK1*XXK1
      XXK22=XXK2*XXK2
      XYAE=YE*QA
      XXA=XK1-(1.D0+XK1)*XL3
      XXB=YEE+2.D0*XXK1*XL3
      YEEZ=(1.D0-YEE)/YEE
      TE1=DLOG(1.D0-YEE)
      TE2=DLOG(1.D0-YEE*QAA)
      TT1=(XXA-XXB)*YEEI
      Y410=XXK12*YEEI*(1.D0+YEEZ*TE1)/2.D0
      Y420=XXK12*YEEI*(QAA+YEEZ*TE2)/2.D0
      Y510=Q11*XL3/4.D0
      Y520=Q11*QAA*XL3*(2.D0-QAA)/4.D0
      Y610=Q1*(XXA-2.D0*XXB/3.D0+XXB*YEEI+(XXA-TT1-XXB*YEEI*YEEI)*0.5D0*
     *YE*YEL)*YEEI
      Y620=Q1*(XXB*QAA*QA/3.D0+(XXA-XXB+XXB*YEEI)*QA+(XXA-TT1-XXB*YEEI*
     5YEEI)*0.5D0*YE*DLOG((1.D0+XYAE)/(1.D0-XYAE)))*YEEI
      Y710=0.5D0*YEEI*(XXK11-YEE+YEEZ*XXK11*TE1)
      Y720=0.5D0*YEEI*(QAA*(XXK11-YEE)+YEEZ*XXK11*TE2)
      SMAX=PI/(4.D0*QEE)
      SBASE=PI*(1.D0-QAA)/(4.D0*QEE)
      XCDF=QE*XCT*(1.D0+Y110+Y120)+2.D0*(Y710+Y720)
      XCD=0.029D0*(1.D0-QAA)**1.5/DSQRT(XCDF)
      U2=U*U
      UX1=U*DSQRT(2.D0)
      UX2=U/DSQRT(2.D0)
```

```
      X1=0.01D0
      X2=X1
      DRR=XC1+XC2+QE*XCT
C
C     COEFFICIENTS OF DIFFERENTIAL EQUATIONS C'S
      C1=U2*(1.D0-0.5D0*(QE*XCT*(0.5D0+Y120)+2.D0*Y720+SBASE*XCD/SMAX))
      C2=U2*0.5D0*QE*XCT
      C3=0.5D0*QE*XCN*U2+UX1*D*Z
      C4=-Z2+0.5D0*UX2*QE*XCN*D*Z
      P2=Q2
      C5=U2*0.5D0*((Q1+P2)*(QE*XCT*(1.D0+Y110+Y120)+2.D0*(Y710+Y720)+
     1SBASE*XCD/SMAX)/Q2-QE*XCN*Y110-2.D0*Y410)+UX2*(-Y610+Y310)*D*Z-
     20.5D0*Y510*Z2
      C6=-0.5D0*U2*(QE*XCT*(1.D0+Y110+Y120)+2.D0*(Y710+Y720)+SBASE*XCD
     3/SMAX)/Q2+UX2*(-0.5D0*QE*XCN*Y110-Y410)*D*Z+0.5D0*(Y210-Y310)*Z2
      C7=U2*0.5D0*Q1*(QE*XCT*(1.D0+Y110+Y120)+2.D0*(Y710+Y720)+SBASE*XCD
     4/SMAX)*(Q1+P2)/Q2
      C8=-U2*0.5D0*Q1*(QE*XCT*(1.D0+Y110+Y120)+2.D0*(Y710+Y720)+SBASE*
     5XCD/SMAX)/Q2
      C9=U2*(0.5D0*QE*XCN*Y120-Y420)+UX2*(Y320-Y620)*D*Z-0.5D0*Y520*Z2
      C10=UX2*(0.5D0*QE*XCN*Y120-Y420)*D*Z-0.5D0*(Y220+Y320)*Z2
      DO 91 I=1,4
      DO 92 J=1,4
   92 C(I,J)=(0.D0,0.D0)
   91 C(I,I)=(1.D0,0.D0)
C     MM IS THE ORDER  OF POWER SERIES
      MM=70
      DO 93 N=5,MM
      J=N-1
      CX1=-(C1-0.5D0*C2)/(J*(J-1))
      CX2=-(C2*(J-4)+C3)/(J*(J-1)*(J-2))
      CX3=-C4/(J*(J-1)*(J-2)*(J-3))
      DO 94 I=1,4
      C(N,I)=CX1*C(N-2,I)+CX2*C(N-3,I)+CX3*C(N-4,I)
   94 CONTINUE
   93 CONTINUE
      A(1,1)=C6
      A(1,2)=C5
      A(1,3)=(0.D0,0.D0)
      A(1,4)=(-6.D0,0.D0)
      A(2,1)=C8
      A(2,2)=C7
      A(2,3)=(-2.D0,0.D0)
      A(2,4)=(0.D0,0.D0)
      A(3,1)=(0.D0,0.D0)
      A(3,2)=(0.D0,0.D0)
      A(3,3)=(2.D0,0.D0)
      A(3,4)=(6.D0,0.D0)
      A(4,1)=C10
      A(4,2)=C9+C10
      A(4,3)=2.D0*C9+C10
      A(4,4)=3.D0*C9+C10-6.D0
      DO 81 N=5,MM
      B(N,1)=(N-1)*(N-2)*C(N,1)
   81 A(3,1)=A(3,1)+B(N,1)
      DO 99 N=5,MM
      B(N,2)=(N-1)*(N-2)*C(N,2)
   99 A(3,2)=A(3,2)+B(N,2)
      DO 96 N=5,MM
      B(N,3)=(N-1)*(N-2)*C(N,3)
```

```
   96 A(3,3)=A(3,3)+B(N,3)
      DO 71 N=5,MM
      B(N,4)=(N-1)*(N-2)*C(N,4)
   71 A(3,4)=A(3,4)+B(N,4)
      DO 72 N=5,MM
      B(N,1)=((N-1)*(N-2)*(N-3)-C9*(N-1)-C10)*C(N,1)
   72 A(4,1)=A(4,1)-B(N,1)
      DO 73 N=5,MM
      B(N,2)=((N-1)*(N-2)*(N-3)-C9*(N-1)-C10)*C(N,2)
   73 A(4,2)=A(4,2)-B(N,2)
      DO 74 N=5,MM
      B(N,3)=((N-1)*(N-2)*(N-3)-C9*(N-1)-C10)*C(N,3)
   74 A(4,3)=A(4,3)-B(N,3)
      DO 75 N=5,MM
      B(N,4)=((N-1)*(N-2)*(N-3)-C9*(N-1)-C10)*C(N,4)
   75 A(4,4)=A(4,4)-B(N,4)
      RETURN
      END


      COMPLEX FUNCTION CDET*16(A,N)
      COMPLEX*16 A,PIVOT,HOLD
      INTEGER END, ROW, COL, PIVROW, PIVCOL
      DIMENSION A(10,10),L(10),M(10)
C     DETERMINANT OF THE BOUNDARY CONDITIONS
C
    1 END =N-1
      CDET=(1.D0,0.D0)
      DO 10 I=1,N
      L(I)=I
   10 M(I)=I
      DO 100 LMNT=1,END
      PIVOT=(0.D0,0.D0)
      DO 20 I=LMNT,N
      ROW=L(I)
      DO 20 J=LMNT,N
      COL=M(J)
      IF(CDABS(PIVOT).GE.CDABS(A(ROW,COL))) GO TO 20
      PIVROW=I
      PIVCOL=J
      PIVOT=A(ROW,COL)
   20 CONTINUE
      IF(PIVROW.EQ.LMNT)  GO TO 22
      CDET=-CDET
      KEEP=L(PIVROW)
      L(PIVROW)=L(LMNT)
      L(LMNT)=KEEP
   22 IF(PIVCOL.EQ.LMNT)  GO TO 26
      CDET=-CDET
      KEEP=M(PIVCOL)
      M(PIVCOL)=M(LMNT)
      M(LMNT)=KEEP
   26 CDET=CDET*PIVOT
      IF(CDABS(PIVOT).EQ.0.D0)  GO TO 333
      JAUG=LMNT+1
      PIVROW=L(LMNT)
      PIVCOL=M(LMNT)
      DO 100 I=JAUG,N
      ROW=L(I)
      HOLD=A(ROW,PIVCOL)/PIVOT
```

```
      D1=(5*D1+3*D)/32+(I/IM)*(D1-D)/8.D0
      OM1=OM+D1
      I1=4
      I2=2
      GO TO 80
C  SPECIAL PROCEDURE TO FACE TOO QUICK VARIATIONS OF FREQUENCY.
4     IF(KEY.LT.0) GO TO 6
      IF(IN.EQ.4) GO TO 64
      IF(IAX.EQ.0) GO TO 5
      F=(OM1-OM)/D
      IF((ABS(F).LT.0.5).AND.(I.LE.2)) J=-1
      I=I-J
      IF(IAX.GT.4) GO TO 5
C  SECOND , THIRD, FOURTH POINTS ON OR OFF IM-AXIS.
      D=(D+OM1-OM)/2.D0
      I=MIN0(I,2)
      GO TO 6
5     IF(I.GE.3) GO TO 6
      IF( I*I1*I2.LE.8) GO TO 64
      IF(I.EQ.1) GO TO 65
      GO TO 6
64    KU=(U+RM/5.D0)/DU
      IF(KEY.EQ.0) KU=0
      IF(KU-(KU/2)*2 .EQ. 0 ) GO TO 66
65    J=I-2-(4/IN)*MIN0(I-3,2)
      GO TO 67
66    J=I/2 - (I/4)*(IN/4)
      IF((I*I1.EQ.1).AND.(KU-(KU/4)*4 .EQ. 0) ) J=1
67    I=I-J
C  PREDICTED STEP FACTOR . NEW CHARACTERISTICS.
6     DDB=2.D0**(2-I)
      IDUM=DABS(DU/(101*RM))
      IF((IDUM+1)*DDB.LT.0.9D0)  DDB=2.D0**(2/(IDUM+1) - 2)
      DU=DU*DDB
      F=(OM1-OM)/D1
      IF(F.GT.0.) J1=-1
      DD1=(OM1-OM-D1)/2.D0
      D1 =(3*(OM1-OM)-D + (OM1-OM-D)*DDB)*DDB/2.D0
      D  =(3*(OM1-OM)-D - (OM1-OM-D)*DDB)*DDB/2.D0
      DD1=DD1*D1/D
      I2=I1-1+1/I1
      I1=I+J
7     U=U+DU
      OM1=OM1+D1+DD1
      IF(IAX.NE.0) IAX=IAX+1
      GO TO 80
C  FIRST POINT OFF RE-AXIS (TO BE RECALCULATED)
10    IAX=1
      H1=D1
      IF(((RO+3.D0*H1).GT.0.D0) .AND. (I.EQ.IM)) GO TO 11
      D1  =GI*CDABS(D)*IUP
      OM1=OM-RO
      GO TO 51
C  FIRST POINT OFF IM-AXIS (TO BE RECALCULATED)
11    IAX=-4
      D1=(CDABS(D) + D1/2.D0)*1.5D0
      IF(RO.GT.10.D0*RM) D1=(GI*CDABS(D)*IUP+H1)*0.75D0
      OM1=OM
      GO TO 52
C  SECOND POINT OFF IM-AXIS (TO BE PREDICTED)
```

```
      DO 100 J=JAUG,N
      COL=M(J)
  100 A(ROW,COL)=A(ROW,COL)-HOLD*A(PIVROW,COL)
      CDET=CDET*A(ROW,COL)
  333 RETURN
      END
C   REQUIRED SUBROUTINE SECANT(A,XI,XO,U,DN,KM,L,M,N,K,KEY) AND N<20 ***
C   OM1 = (IN-1)-TH FREQUENCY (REQUIRED INITIALLY (IN=1)) --> (IN)-TH
C   OM  = (IN-2)-TH FREQUENCY . AT IN=1,CHOSEN CLOSE TO EXPECTED ROOT
C            GENERALLY BECOMES THE (IN-1)-TH EXEPT NEAR DISCONTINUITIES.
C   D1  = (IN-1)-TH FREQUENCY INCREMENT PREDICTED (REQUIRED INITIALLY)
C   D   = (IN-2)-TH REAL FREQUENCY INCREMENT (NOT REQUIRED INITIALLY).
C   DU  = (IN-1)-TH VELOCITY INCREMENT , BECOMES THE IN-TH.
C   U   = (IN-1)-TH VELOCITY ,BECOMING THE IN-TH (REQUIRED INITIALLY).
C   RM  = GENERAL ACCURACY (MINIMUM DU = 100*RM).
C   IN  = NUMBER OF POINTS CALCULATED SO FAR  (LOOP IN MAIN PROGRAM).
C   I2  = (IN-3)-TH SECANT ITERATIONS (NOT REQUIRED AT IN=1).
C   I1  = (IN-2)-TH SECANT ITERATIONS (NOT REQUIRED AT IN=1).
C   I   = (IN-1)-TH SECANT ITERATIONS (NOT REQUIRED AT IN=1).
C   IAX = NUMBER OF POINTS INVESTIGTED ON IM-AXIS (INITIALLY 0 OR 1).
C   IUP = 1 FOR UPWARDS ANALYSIS OF IMAGINARY BRANCH (-1 DOWNWARDS).
C   IM  = MAXIMUM SECANT ITERATIONS (I=IM+1 IN CASE OF DIVERGENCE).
C   KEY = 1,0,-1 IF INTERMEDIATE CALCULATIONS ARE TO BE PRINTED OUT,OR
C         > 0 IF REGULAR VARIABLE STEPS IN VELOCITY ARE RNQURRED (DU MAY
C            BE DOUBLED IF U IS AN INTEGER MULTIPLE OF 2*DU AND I*I1*I2<9),
C         = 0 FOR NON NECESSARY REGULAR INTEGER STEPPED VALUES OF U.
C         < 0 IF DU IS TO REMAIN CONSTANT. (ALMOST ACHIEVED BY I=2,I1>4)

      SUBROUTINE PREDIC(OM1,OM,D1,D,U,DU,RM,IN,N,I2,I1,I,IAX,IUP,IM,KEY)
      DIMENSION A(10,10),L(10),M(10)
      COMPLEX*16 A,OM1,OMO,OM,D1,D,GI
      REAL*8 U,DU,RM,DDB,RO,R1,HI
      DD1=0
      J1=1 + (1/IN)*(IM-1)
C  INITIAL VELOCITY . INITIAL CHARACTERISTICS KEPT FOR NEXT STEP.
      IF(IN .EQ. 1) GO TO 81
      GI=(0.D0,1.D0)
      J=0
 1000 RO=OM
      IF(I.LT.IM) GO TO 1
C  SPECIAL CASES OF DIVERGENCE.
      IF(IN.LE.3) GO TO 101
      IF((I1.EQ.1) .AND. (I2.EQ.1)) GO TO 3
      IF(IAX) 101,10,11
C  SPECIAL CASES OF CONVERGENCE.
    1 IF( KEY.LT.0 ) I=2
      IF(IN.LE.3) GO TO 50
      JAX=IAX+5
      GO TO (12,4,4,4,2,7,4,4,4,4),JAX
    2 R1=OM1
      IF((R1.GT.RM*10. ).AND.(RO.LT.RM*10. )) GO TO 12
      IF((R1.LT.RM*10. ).AND.(RO.GT.RM*10. )) GO TO 10
      IF( (R1+ RM .LT.  RO/2.) .AND. (I1.GT.1) ) I=MINO(I,4)
      IF(R1+RM .LT. RO/4.) I=MAXO(2,I-I1)
      IF((I.LE.4+4/IN).OR.(DABS(DU/4.D0).LT.100*RM)) GO TO 4
C  SLOW CONVERGENCE . DIVISION OF STEP BY 4.
    3 U=U-0.75D0*DU
      DU=DU/4.D0
      D =(5*D+3*D1)/3
```

```
 12     IAX=-3
        D1=CDABS(OM1-OM)
 50     U=U+DU
        IF(IN.NE.3) GO TO 52
        IAX=5*IAX
        D1=OM1-OM
 51     D=D1
 52     OM1=OM1+D1
        I2=2
        I1=2
        IF(IN.GT.3) J1=1+IABS(IAX+1)
        DD1=0
 80     OM=OM1-D1-DD1
        R1=OM1
        RO=OM
C  INVESTIGATION OF A NEGATIVE PREDICTION BEYOND IM-AXIS.
        IF((R1.LT.10.D0*RM) .AND. (IAX .EQ.0)) GO TO 10
 81     OMO=OM +D1+DD1-J1*D1/IM
        IF(IN.GT.1) J1=I
        CALL SECANT(A,OM1,OMO,U,RM,IM,N,I,KEY)
        IF(I*J1 .GE. IM*IM) I=IM+1
        IF((I.LT.IM) .OR. (DABS(DU).LT.199*RM) .OR. (IN.LT.4)) GO TO 100
        IF((IAX-1)*(IAX+4)) 91,90,100
 90     D1=(D*(1-IAX)+H1*(4+IAX))/5
        D=D1
        IAX=-IAX+1
 91     IF(IAX.EQ.0) GO TO 100,
        WRITE(6,99) U
 99     FORMAT(' -PREDIC- VELOCITY SET BACK TO',F9.6,'-3/4*DU & DU=DU/4'/)
        GO TO 3
 101    I=IM+1
 100    IF(I.EQ.IM) GO TO 1000
        RETURN
        END

        SUBROUTINE SECANT(A,X1,X0,UE,DM,KM,N,K,KEY) .
        DIMENSION A(10,10)
        COMPLEX*16 A,X0,X1,X2,Y1,Y0,CDET,X
        REAL*8 UE,UI,DM,RX,CX
        X=X1
        K=0
        IF(CDABS(X0).LT.DM .OR. CDABS(X1-X0).LT.DM) X0=X0+(1.D0,1.D0)*DM
 4      CALL MATRIX(A,UE,X0,N)
        M=N
        Y0=CDET(A,M)
        Z0=CDABS(Y0)
 1      K=K+1
        CALL MATRIX(A,UE,X1,N)
        Y1=CDET(A,M)
        WRITE(6,100)Y0,Y1
  100   FORMAT(10X,1P2D15.6,1P2D15.6)
        Z1=CDABS(Y1)
        X2=(X1*Y0-X0*Y1)/(Y0-Y1)
        RX=X2
        YRO=Y0
        W0=YRO*Y1
        W1=(YRO-Y0)*Y1/DM
        IF((W0.LE.0.) .AND. (W1.LT.-W0)) Z0=10.*Z0
        IF(((1-1/K)*Z1.GT.Z0) .OR. (K.GE.KM)) GO TO 3
```

```
      IF(IABS(KEY).NE.1) GO TO 5
      WRITE(6,10) UE,X0,Y0,X1,Y1,X2
10    FORMAT(' V=',F9.6,2('   X=',1P2D10.3,' Y=',2D8.1),'   X2=',2D11.4)
5     CX=(0.D0,-1.D0)*X2
      IF(DABS(CX).LT.DM) X2=RX
      IF((CDABS(1.D0-X1/X2).LT.DM).OR.(CDABS(X2-X1).LT.DM)) GO TO 2
      IF(RX+DM) 6,6,7
6     Z0=X1-X0
      X0=X2-RX
      X1=X0-(0,D0,1.D0)*RX
      IF(Z0.GT.2.*DM) X0=X0-RX
      GO TO 4
7     X0=X1
      X1=X2
      IF(DABS(RX).LT.DM) X1=X1-RX
      Z0=Z1
      Y0=Y1
      GO TO 1
3     WRITE(6,11) K,KM,UE,X0,Y0,X1,Y1,X2
11    FORMAT('0-SECANT- INTERRUPTED BECAUSE OF DIVERGENCE OF FREQUENCY A
     1FTER K=',I2,' ITERATIONS IF K<KMAX=',I2,'  .LAST ITERATION TRACEBA
     1CK :'/' V=',F9.6,2('   X=',1P2D10.3,' Y=',2D8.1),'   X2=',2D11.4/)
      K=KM
2     X0=X
      X1=X2
      RETURN
      END
```

APPENDIX F: THE COMPUTER PROGRAM USED TO OBTAIN THE CURVES OF FIGURE 16

```
$WATFIV ,TIME=999,PAGES=999
        IMPLICIT REAL*8(A-H,O-Z)
        DIMENSION A(20),XR(30),XXR(30),XI(30),XXI(30)
        DIMENSION B(30),C(30),X1(30),X2(30),XE(30),XA(30)
        Q1=0.05D0
        Q2=10.D0
        QE=40.D0
        QAX=0.02D0
        DO 100 IX=1,50
        QA=QAX*IX
        PI=3.1415926D0
        XCN=0.025D0
        XCT=0.025D0
C
C       Q1 IS THE RATIO OF LENGTH OF NOSE SECTION/LENGTH OF MAIN BODY
C       Q2 IS THE RATIO OF LENGTH OF TOW-ROPE/LENGTH OF MAIN BODY
C       QE IS THE RATIO OF LENGTH OF MAIN BODY/DIAMETER OF CYLINDER
C       XCT IS THE LONGITUDINAL COMPONENT OF DRAG COEFFUCIENT
C       XCN IS THE NORMAL COMPONENT OF THE DRAG COEFFUCIENT
        Q11=Q1*Q1
        QEE=QE*QE
        QAA=QA*QA
        YE=DSQRT(1.D0-1.D0/(4.D0*Q11*QEE))
C       YE IS THE ECCENTRICITY OF THE ELLIPSOID
        YEE=YE*YE
        YEI=1.D0/YE
        YEL=DLOG((1.D0+YE)/(1.D0-YE))
        YEX=YE/(1.D0-YEE)
        YEXX=YEE/(1.D0-YEE)
        YEEE=YEE*YE
        YEEI=1.D0/YEE
        XK1=-YE*(0.5D0*YEI*YEL-1.D0)/(0.5D0*YEL-YEX)
        XK2=-(0.5D0*YEL-YEX)/(0.5D0*YEL-YEX*(1.D0-2.D0*YEE))
        XL3=-YEE*(1.5D0*YEI*YEL-3.D0-YEXX)/(1.5D0*(2.D0*YEI-YE)*YEL-6.D0+
     *YEXX)
C       DIMENSIONLESS PARAMETERS OF I'S
        Y110=PI*Q1/4.D0
        Y120=0.5D0*Q1*(QA*DSQRT(1.D0-QAA)+DARSIN(QA))
        Y210=2.D0*Q1/3.D0
        Y220=QA*Q1*(1.D0-QAA/3.D0)
        Y310=2.D0*Q1*XK2/3.D0
        Y320=QA*Q1*(1.D0-QAA/3.D0)*XK2
        XXK1=1.D0+XK1
        XXK2=1.D0+XK2
        XXK12=XXK1*XXK2
        XXK11=XXK1*XXK1
        XXK22=XXK2*XXK2
        XYAE=YE*QA
        XXA=XK1-(1.D0+XK1)*XL3
        XXB=YEE+2.D0*XXK1*XL3
        YEEZ=(1.D0-YEE)/YEE
        ZE1=DLOG(1.D0-YEE)
        ZE2=DLOG(1.D0-YEE*QAA)
        ZZ1=(XXA-XXB)*YEEI
        P2=Q2
        Y410=XXK12*YEEI*(1.D0+YEEZ*ZE1)/2.D0
        Y420=XXK12*YEEI*(QAA+YEEZ*ZE2)/2.D0
        Y510=Q11*XL3/4.D0
        Y520=Q11*QAA*XL3*(2.D0-QAA)/4.D0
        Y610=Q1*(XXA-2.D0*XXB/3.D0+XXB*YEEI+(XXA-ZZ1-XXB*YEEI*YEEI)*0.5D0*
```

```
     *YE*YEL)*YEEI
      Y620=Q1*(XXB*QAA*QA/3.D0+(XXA-XXB+XXB*YEEI)*QA+(XXA-ZZ1-XXB*YEEI*
     5YEEI)*0.5D0*YE*DLOG((1.D0+XYAE)/(1.D0-XYAE)))*YEEI
      Y710=0.5D0*YEEI*(XXK11-YEE+YEEZ*XXK11*ZE1)
      Y720=0.5D0*YEEI*(QAA*(XXK11-YEE)+YEEZ*XXK11*ZE2)
      SMAX=PI/(4.D0*QEE)
      SBASE=PI*(1.D0-QAA)/(4.D0*QEE)
      CDFB=QE*XCT*(1.D0+Y110+Y120)+2.D0*(Y710+Y720)
      CDB=0.029D0*(1.D0-QAA)**1.5/DSQRT(CDFB)
      A1=2.D0+Y210+Y220-Y310+Y320
      A2=0.5D0*QE*XCN*(1.D0+Y110+Y120)+Y410-Y420
      A3=0.5D0*(QE*XCT*(1.D0+Y110+Y120)+2.D0*(Y710+Y720)+SBASE*CDB/SMAX)
     2/Q2
      B1=0.5D0*(-Y210+Y220+Y310+Y320)-Y510+Y520
      B2=2.D0-Y310+Y320+Y610-Y620-0.5D0*(Y410+Y420)+0.25D0*QE*XCN*(-Y110
     *+Y120)
      B3=0.5D0*QE*XCN*(1.D0+Y110+Y120)+Y410-Y420-0.5D0*(QE*XCT*(1.D0+
     3Y110+Y120)+2.D0*(Y710+Y720)+SBASE*CDB/SMAX)*(0.5D0+Q1+P2)/Q2
      C1=0.5D0*(-Y210+Y220+Y310+Y320)
      C2=-.5D0*(Y410+Y420)+0.25D0*QE*XCN*(-Y110+Y120)
      C3=0.5D0*(QE*XCT*(1.D0+Y110+Y120)+2.D0*(Y710+Y720)+SBASE*CDB/SMAX)
     4*(-0.5D0-Q1)/Q2
      D1=1.D0/6.D0+0.25D0*(Y210+Y220-Y310+Y320)+0.5D0*(+Y510+Y520)
      D2=0.5D0*(+Y310+Y320-Y610-Y620)+0.25D0*(Y410-Y420)+0.125D0*QE*XCN*
     5(1.D0/3.D0+Y110+Y120)
      D3=0.25D0*QE*XCN*(-Y110+Y120)-0.5D0*(Y410+Y420)+0.5D0*(QE*XCT*
     7(1.D0+Y110+Y120)+2.D0*(Y710+Y720)+SBASE*CDB/SMAX)*(0.5D0+Q1*P2)*
     8(0.5D0+Q1)/Q2
      QQ=A1*D1-B1*C1
C     THE COEFFICIENT OF A QUARTIC EQUATION
      A(1)=1.D0
      A(2)=(A1*D2+A2*D1-B1*C2-B2*C1)/QQ
      A(3)=(A1*D3+A2*D2+A3*D1-B1*C3-B2*C2-B3*C1)/QQ
      A(4)=(A2*D3+A3*D2-B2*C3-B3*C2)/QQ
      A(5)=(A3*D3-B3*C3)/QQ
C     BAIRSTOW METHOD
      DATA N,EPS,P,Q/4,1.D-07,1.D0,1.D0/
      NN =  N + 1
      M = 0
   10 J = N-2*M
      M = M + 1
      JJ = J +1
      IF(J-2) 20, 25, 30
   20 XR(N) = -A(2)/A(1)
      XI(N)=0.D0
      GO TO 60
   25 AA = A(1)
      BB = A(2)
      CC = A(3)
      GO TO 51
   30 NL = 1
   35 B(1) = A(1)
      B(2) = A(2)-P*B(1)
      DO 36 I= 3,JJ
   36 B(I) = A(I)-P*B(I-1)-Q*B(I-2)
      C(1) = B(1)
      C(2) = B(2)-P*C(1)
      DO 37 I=3,J
   37 C(I) = B(I)-P*C(I-1)-Q*C(I-2)
      CX = C(J)-B(J)
```

```
      CY = C(J-1)**2-CX*C(J-2)
      DP = (B(JJ)*C(J-1)-B(J)*C(J-2))/CY
      DQ = (B(JJ)*C(J-1)-B(J)*CX)/CY
      P = P + DP
      Q = Q +DQ
      IF(DABS(DP).GT.EPS) GO TO 40
      IF(DABS(DQ).LT.EPS) GO TO 45
   40 IF(NL.GE.1000) GO TO 45
      NL=NL+1
      GO TO 35
   45 DO 50 I = 1,JJ
   50 A(I)=B(I)
      AA = 1.D0
      BB = P
      CC = Q
   51 D=BB*BB-4.D0*AA*CC
      IF(D.GE.0.D0) GO TO 52
      X1J=-BB/(2.D0*AA)
      X2J = X1J
      X1K=DSQRT(-D)/(2.D0*AA)
      X2K = -X1K
      GO TO 55
   52 DD = DSQRT(D)
      X1J=(-BB+DD)/(2.D0*AA)
      X2J=(-BB-DD)/(2.D0*AA)
      X1K=0.D0
      X2K=0.D0
   55 XR(2*M-1) = X1J
      XR(2*M) = X2J
      XI(2*M-1) = X1K
      XI(2*M) = X2K
      IF(J.GT.2) GO TO 10
   60 WRITE(6,300)
  300 FORMAT(' ','ROOT',9X,'REAL PART',7X,'IMAGINARY PART')
      DO 64 I=1,N
      XXR(I)=XI(I)
      XXI(I)=-XR(I)
      IF((DABS(XXR(I)).LT.1.D-5).AND.(XXI(I).LT.0.D0)) GO TO 1000
   64 CONTINUE
  100 CONTINUE
 1000 WRITE(6,200) Q1,QA,Q2,QE
  200 FORMAT(2X,4F15.3///)
      STOP
      END
```